THE
PHYSICAL REVIEW
A journal of experimental and theoretical physics established by E. L. Nichols in 1893

SECOND SERIES, VOL. 69, NOS. 1 AND 2 JANUARY 1 AND 15, 1946

Fast Neutron Energy Absorption in Gases, Walls, and Tissue

PAUL C. AEBERSOLD,* *Radiation Laboratory, Department of Physics, University of California, Berkeley, California*
AND
GLADYS A. ANSLOW,** *Department of Physics, Smith College, Northampton, Massachusetts*
(Received August 12, 1945)

The ionization produced by a collimated beam of fast neutrons, filtered for gamma-rays, resulting from neutron collisions in various hydrogenous and non-hydrogenous gases at pressures ranging from 3 mm to 3 atmospheres or resulting from collisions in various hydrogenous and non-hydrogenous wall materials has been measured in ionization chambers of various types. In large wire-defined gas-walled chambers the ionizing particles are the recoiling gas nuclei. The long range protons of hydrogenous gases expend part of their energy in the walls of the container at ordinary pressures; hence their ionization-pressure curves are quasi-parabolic, becoming linear at higher pressures in accordance with theoretical predictions. The ionization-pressure curves for non-hydrogenous gases are linear except at low pressures. The limiting pressures at which linearity sets in lead to maximum values of the range and energy of the recoiling nuclei and indicate that in the beam of the 37-inch Berkeley cyclotron 5-Mev neutrons predominate. The slopes of the linear portions of the $i-p$ curves permit the calculation of the rate, E_i, at which energy is transferred from the neutron beam to nuclear constituents of the gas. The component of the ionization resulting from gamma-rays, produced in the target and in the walls of the collimator and chamber, was found less than 1 percent in hydrogenous gases and only 2–6 percent in other gases. From the rate of energy transfer and the neutron energy flux an approximate mean value of the $n-p$ cross section for neutron energy distribution of the beam was calculated; also the lower limits of similar cross sections for other nuclei have been estimated, these values containing both the scattering cross sections and those due to neutron absorption followed by disintegrations. In thimble chambers with 1-cm and in cylindrical chambers with 2-mm wall separations, the ionization results in large part from the recoiling wall nuclei. Ranges and energies of the heavier recoiling wall nuclei are indicated by the limiting pressures revealed in $i-p$ curves. The gamma-ray percentage is greater than in large volumed chambers. Neutron responses from most non-hydrogenous walls are practically independent of wall material. The excess response from hydrogenous walls is proportional to proton content. From the E_i values measured in large chambers the energies absorbed per g of various biological substances and of hydrogenous and non-hydrogenous wall materials have been calculated, and (1) predict the respective responses measured in thimble chambers and (2) indicate that the energy absorption per g of tissue must be similar to that for a wall material like amber. Finally, analysis of the relative x-ray and neutron energy absorptions in such materials yields a factor $k_n>2$, which must be applied to reduce neutron exposures measured in certain hydrogenous-walled chambers to tissue doses.

INTRODUCTION

IN a review[1] of the physiological effects of neutron rays on various types of biological media Aebersold and Lawrence included a discussion of the ionization measurements utilized in dosimetry and referred to an extended study of the ionization effects obtained in gas-filled chambers under varied operating conditions, i.e., with an assortment of sizes, wall materials, and gases at pressures ranging from 3 mm of Hg to 3 atmospheres, when exposed to a collimated beam

* At present with Manhattan Engineer District Project, Los Alamos, New Mexico.
** At University of California during sabbatical leave from Smith College.
[1] P. C. Aebersold and J. H. Lawrence, Ann. Rev. Physiol. 4, 25 (1942).

of fast neutrons produced under standard operating conditions in the 37-inch Berkeley cyclotron. The results of this investigation permitted the calibration of the thimble chambers commonly employed in biological experiments at this laboratory, giving a measure of the energy absorbed per gram of biological material, and hence an estimate of the relative effectiveness of neutron and x-ray irradiation of these materials.

The theoretical analysis of the ionization measurements is of considerable importance in pure nuclear physics, since average values of fast neutron cross sections for the nuclei of the various gases employed may be calculated from the ionization measurements taken in large gas-walled chambers, and the ranges and hence the energies of the various recoil nuclei released from the wall materials are revealed in the results obtained with small chambers. Preliminary descriptions of these experiments, which were performed at the University of California in 1938–1939, have been presented before the American Physical Society.[2] Publication of complete details has been delayed by the pressure of the activities of at least one of the authors in war research.

Three groups of experiments were undertaken. In the first a large ionization chamber (Type I) was used with gas-like walls and with dimensions so chosen that at normal pressures the ranges of recoil nuclei scattered in elastic collisions were less than the chamber dimensions. Numerous gases at wide ranges of pressures were employed. At the higher pressures all recoiling nuclei responsible for the measured ionization were released from the gas itself. In the second group very small chambers (Type II) with walls of hydrogeneous and of non-hydrogenous materials were employed, such that at normal pressures most of the neutron ionization was effected by nuclei released from the walls, the ranges of the recoil protons far exceeding the chamber dimensions. In the third group of chambers (Type III) intermediate sizes with solid walls were filled with selected gases under varying pressure conditions and the results used to interpret the measurements obtained with large and small chambers. The ionization occurring in the first type of chamber may be characterized as resulting from the "gas effect," with the second type as from the "wall effect," and with the third as from combined gas and wall effects.

[2] P. C. Aebersold and G. A. Anslow, Phys. Rev. **55**, 680, 1134 (1939).

THEORETICAL CONSIDERATIONS

Fast Neutron Energy Spent in Ionization

In all chambers ionizing particles are released from the walls and the contained gas either by elastic or inelastic scattering of nuclei in neutron collisions, by nuclear disintegrations following neutron absorption, or by electron emission consequent to gamma-ray absorption in the walls. Since biologically important light nuclei, with the exception of nitrogen, have very small cross sections for neutron absorption, in the following treatment this effect may be neglected and only introduced in particular problems involving nitrogen. Moreover, since inelastic collisions cannot occur with protons and are not considered very probable for other biologically important nuclei, most of the neutron energy must be spent during elastic scattering processes.

The Gas Effect

The energy transferred to the gas may be evaluated by considering the effects within a small test volume situated within a large volume of a gas undergoing irradiation, the distances of the surface of the test volume from the outside boundary being greater than the range of any of the ionizing particles. A condition of secondary particle equilibrium exists within such a volume, even though the ranges of the ionizing particles exceed its dimensions, for the energy expended outside the test volume by particles originating within it is compensated by the energy expended within the volume by those particles which originate outside but traverse it.

In general a neutron beam, particularly that from a D−Be source, is complex in its energy distribution. The evaluation of the transferred energy is correspondingly involved. To accomplish this, consider the effect in such a test volume of a homogeneous beam of $N(k)$ neutron with energy $E(k)$ on the $\sum_j N_{T,p} n_j$ nuclei in unit volume of the gas, k being the wave number of the neutrons and $N_{T,p}$ the number of molecules per cc at temperature T and pressure p, each

containing n_j atoms of type j. Both the neutron elastic collision cross section per unit solid angle, $\sigma_j(k, \theta)$, and the fraction of the neutron energy, $f_j(\theta)$, transferred during collisions depend on the scattering angle, θ; hence, the mean fraction of energy transferred per atomic nucleus per incident neutron is given by an energy conversion coefficient

$$K_j(k)=\langle 4\pi\sigma_j(k,\theta)f_j(\theta)\rangle_{Av}$$
$$=16\pi\frac{m_n m_j}{(m_n+m_j)^2}\langle\sigma_j(k,\theta)\sin^2\tfrac{1}{2}\theta\rangle_{Av}, \quad (1)$$

since

$$f_j(\theta)=\frac{4m_n m_j}{(m_n+m_j)^2}\sin^2\tfrac{1}{2}\theta. \quad (2)$$

The neutron energy transferred to the ionizing gas particles which produce $I_{G,G}(k)$‡ ions per cc of gas G with a mean expenditure of energy, W_G, per ion pair is, writing $Q(k)=N(k)\cdot E(k)$ for the energy flux of the $N(k)$ neutrons,

$$W_G I_{G,G}(k)=N_{T,p}Q(k)\sum_j n_j K_j(k), \quad (3)$$

an expression differing from that stated by Gray and Read[3] only through the recognition of the varying asymmetrical character of the scattering cross sections with neutron energy. Since $N_{T,p}=N_{T,760}p/760$, it is obvious that in such a test volume the ionization density is a linear function of the pressure p.

The "gas-walled" chamber utilized in these experiments realized these ideal conditions when filled with non-hydrogenous gases, but in most hydrogenous gases the recoil protons have ranges in excess of the dimensions of the outside shield, as do the faster nuclei in non-hydrogenous gases at low pressures. Under these conditions only a portion of the energy of the recoil particles is utilized in producing ions in the gas, the rest being expended in the walls, the fraction utilized being approximately the mean ratio, $\bar{r}_j(g, k, \theta)p$, of the path lengths within the confining chamber to the corresponding ranges of particles at that gas pressure, this ratio being a function of the geometry, g, of the chamber, the neutron energy and scattering angle, and of the pressure. Under these conditions the energy spent in ionization per cc of the gas

$$W_G I_{G,G}(k)=N_{T,760}(p/760)^2Q(k)$$
$$\times\sum_j n_j K_j(k)\bar{r}_j(g,k,\theta) \quad (4)$$

is a quadratic function of the pressure and consequently ionization-pressure curves are parabolic.

Because of the distribution in energy of the neutron beam and the various scattering angles, the range of the recoil nuclei must vary widely. For each energy of recoil particles of type j there is a transition pressure $p_{G(j)}$ of the gas G, at which the limiting dimension of the solid container equals the range R_j. At higher pressures the ionization-pressure curve is linear and the energy expenditure equation is

$$W_G I_{G,G}(k)=\frac{N_{T,760}}{760}Q(k)\sum_j n_j K_j(k)$$
$$\times[(p^2_{G(j)}/760)(R_j)\bar{r}_j+\{p-p_{G(j)}(R_j)\}], \quad (5)$$

and the slope of the ionization-pressure curve

$$\frac{d}{dp}[W_G I_{G,G}(k)]=\frac{N_{T,760}}{760}Q(k)\sum_j n_j K_j(k),$$
$$p>p_{G(j)} \quad (6)$$

has the same magnitude as the corresponding expression obtainable from Eq. (3), which expresses the ideal conditions. This correspondence is achieved at pressures of a few cm of Hg in non-hydrogenous gases, since the ranges of the recoil particles in these gases seldom exceed a few mm at atmospheric pressure. In hydrogenous gases, on the other hand, the long ranges of recoil protons at normal pressures necessitate the use of several atmospheres of pressure before this condition is realized.

Finally, the complexity in the energy distribution of the neutron beam demands that all these expressions, (2)–(6), be summed for neutrons of various wave numbers, k. For example,

$$\frac{d}{dp}[W_G\sum_k I_{G,G}(k)]=\frac{N_{T,760}}{760}\sum_k\sum_j$$
$$\times Q(k)n_j K_j(k), \quad p>p_{G(j)}, \quad (6')$$

which indicates for the rate E_m, at which the

‡ $I_{G,G}$ represents the ionization in gas G surrounded by a wall of G. $I_{A,G}$ represents the ionization in gas G surrounded by a wall of material A.

[3] L. H. Gray and J. Read, Nature **144**, 439 (1939).

neutron energy is transferred per molecule of the gas

$$E_m=\frac{d}{dN}[W_G\sum_k I_{G,G}(k)]$$
$$=\frac{760}{N_{T,760}}\frac{d}{dp}[W_G\sum_k I_{G,G}(k)],\ p>p_{G(j)}$$
$$=\sum_k\sum_j Q(k)n_jK_j(k), \quad (7)$$

a corresponding expression holding for E_j, the rate of energy absorption per atom. The evaluation of these latter quantities, E_m and E_j, make possible the interpretation of the effect of fast neutron irradiation on organic material.

Fast Neutron Cross Sections

The determination of E_j and hence of the energy conversion coefficient, $K_j(k)$, leads under particular conditions to the evaluation of the mean value over all scattering angles of fast neutron cross sections. To accomplish this the energy content of the beam must be known and a theoretical expression for $\sigma_j(k,\theta)$, such as that given by Placzek and Bethe[4] in their development of the continuum theory of the complex nucleus, must be employed. If the scattering angular distributions are symmetrical in space in the center of mass system, as is nearly true for $n-p$ cross sections except at very high energies,

$$\bar{\sigma}_j=4\pi\langle\sigma_j(k,\theta)\rangle_{Av}=\frac{(m_n+m_j)^2}{2m_nm_j}K_j(k), \quad (8)$$

$\bar{\sigma}_j$ being the mean cross section weighted for the energy distribution of the neutron beam. However, angular distributions are usually distinctly asymmetrical,[5] mainly in the forward direction at high energies, and (8) will give values greater than the mean cross sections averaged over all scattering angles as well as neutron energies, since

$$\langle\sigma_j(k,\theta)\sin^2\tfrac{1}{2}\theta\rangle_{Av}<\langle\sigma_j(k,\theta)\rangle_{Av}. \quad (9)$$

The Wall Effects

As already stated, the energy released by ionizing particles from the chamber walls results from neutron collisions and gamma-ray absorption. The neutron energy transferred during elastic collisions decreases with increasing mass of the nucleus, (Eq. (2)); hence the effect of the recoil nuclei must be treated in two categories: (1) those with ranges in excess of the chamber dimensions, such as protons and C, O, and N nuclei at low pressures in small chambers and (2) those with ranges less than the chamber dimensions, the heavier nuclei at normal gas pressures. Although the ionization resulting from the latter group is small, it is a sensible portion of that produced in small chambers and cannot be neglected. It is difficult to evaluate accurately since the nuclei released at different levels within the chamber walls travel correspondingly different distances within the chamber. In chambers with wall separation of about a cm, as the experiments to be described indicate, the effect may be neglected at normal pressures since the energy lost by C, O, and other heavy recoil particles to the gas is nearly compensated by the energy lost in the walls by recoiling gas nuclei.

Gamma-radiation of quite high energy is created in the target with the production of fast neutrons or arises from scattering and absorption of fast and slow neutrons by surrounding materials. The secondary electrons released from the walls hence have much longer ranges than those of the recoil nuclei. It is possible to differentiate the resulting ionization in Type I chambers, and thus to evaluate it for the other chambers, since the neutron ionization varies parabolically with pressure at low pressures but linearly at high pressures and the gamma-ray ionization varies linearly at all pressures.

As Gray[6] has shown, the kinetic energy Q_A of all fast moving particles released from unit volume of a medium A, which cross a cavity filled with gas G, producing $I_{A,G}$ ions per cc, is given by the equation

$$Q_A=I_{A,G}W_G(S_A/S_G), \quad (10)$$

or

$$Q_A=I_{A,G}W_G(N_As_A/N_Gs_G), \quad (11)$$

S_A, S_G, and s_A, s_G representing the stopping powers of the wall and of the gas per cc and per molecule, respectively. The dependence of the magnitudes of these stopping powers and also of

[4] G. Placzek and H. A. Bethe, Phys. Rev. **57**, 1075 (1941).

[5] H. Aoki, Phys. Rev. **55**, 795 (1939); S. Kikuchi, H. Aoki, and I. Wakatuki, Phys. Rev. **55**, 1264 (1939); T. Wakatuki and S. Kikuchi, Proc. Phys. Math. Soc. Jap. **21**, 656 (1939).

[6] L. H. Gray, Proc. Roy. Soc. **A156**, 578 (1936).

W_G upon the mass and speed of the ionizing particle have been discussed in detail by Gray.[7]

Writing $I_{A(p),G}$, $I_{A(c),G}$, and $I_{A(e),G}$ for the components of the ionization effected by recoil protons, by heavier recoil nuclei, such as carbon, nitrogen, and oxygen, and by extra-nuclear electrons, respectively, the total ionization which results from the absorption in the wall of neutron energies, $Q_{A(p)}$ and $Q_{A(c)}$, and of gamma-ray ernergy $Q_{A(e)}$, is

$$I_{A,G}=I_{A(p),G}+I_{A(c),G}+I_{A(e),G}$$
$$=\frac{N_{T,p}}{N_A}\left[\frac{Q_{A(p)}}{W_{G(p)}}\frac{s_{G(p)}}{s_{A(p)}}+\frac{Q_{A(c)}}{W_{G(c)}}\frac{s_{G(c)}}{s_{A(c)}}+\frac{Q_{A(e)}}{W_{G(e)}}\frac{s_{G(e)}}{s_{A(e)}}\right];\quad p<p_{G(c)\min} \tag{12}$$

or

$$=\frac{Q_{A(c)}}{W_{G(c)}}+\frac{N_{T,p}}{N_A}\left[\frac{Q_{A(p)}}{W_{G(p)}}\frac{s_{G(p)}}{s_{A(p)}}+\frac{Q_{A(e)}}{W_{G(e)}}\frac{s_{G(e)}}{s_{A(e)}}\right].\quad p>p_{G(c)\max}. \tag{12'}$$

The corresponding ionization-pressure curves will inflect in the region of the pressures $p_{G(c)}$, for which the limiting chamber dimension is the range of some of the heavier recoil nuclei. Since there are usually several types of such nuclei in wall materials and there is wide scattering, the energies and hence the ranges of the nuclei must vary widely. Consequently, the slope of the ionization-pressure curve will start to decrease at a pressure $p_{G(c)\min}$, corresponding to short ranges and continue to decrease up to $p_{G(c)\max}$ defining long ranges.

Since the measured ionization I_G is the sum of that produced by the wall particles and the recoiling gas nuclei, $I_{A,G}+\sum I_{G,G}(k)$, there will be inflections of this curve for each of the transition pressures, $p_{G(j)}$. From these the ranges of the gas nuclei may be calculated.

Identification of the Gamma-Ray and Neutron Components

Several series of measurements are necessary to separate gamma-ray from the various neutron components of the ionization measured. In the experiments of Type I, chambers with non-hydrogenous walls are filled with hydrogen at low pressures. The measured ionization may be written

$$I_{A,G}=a+bp+cp^2, \tag{13}$$

where

$$a=\frac{Q_{A(c)}}{W_{G(c)}};\quad b=\frac{N_{T,760}}{760}\frac{Q_{A(e)}}{W_{G(e)}}\frac{s_{G(e)}}{N_A s_{A(e)}},$$

and

$$c=\frac{N_{T,760}}{(760)^2}\sum_k\sum_j\frac{Q(k)n_j}{W_{G(j)}}K_j(k)\bar{r}_j(g,k,\theta).$$

Accordingly, observations taken at various low pressures permit the evaluation of the constants, a, b, and c, identifying the gamma-ray (b) and neutron components of the gas (c) and wall (a) effects.

Since the gamma-ray ionization produced from the same wall in different gases at the same pressures are related as

$$\frac{I_{A,G}}{I_{A,G'}}=\frac{b}{b'}=\frac{s_{G(e)}}{s_{G'(e)}}\times\frac{W_{G'}}{W_G}, \tag{14}$$

the gamma-ray component in other gases may be calculated from the hydrogen determination. Values of stopping powers for gamma-ray produced electrons, not those in the literature for alpha-rays, must be used. This necessitated measurements of these stopping powers in various gases which were irradiated by a pure gamma-ray source with an energy content similar to that encountered in the neutron experiments.

At higher pressures, $p_{G(j)}$, in any gas, both the gamma-ray and the neutron "gas-effect" increase linearly with pressure, and the neutron component of the non-hydrogenous "wall effect" does not appear in the equation

$$\frac{dI_G}{dp}=\frac{d}{dp}[I_{A,G(e)}]+\frac{d}{dp}[\textstyle\sum_k I_{G,G}(k)]. \tag{15}$$

By using in this equation values obtained for gamma-ray components through the preceding equation, neutron "gas effects" are finally derived, the quantities desired for the interpretation of biological measurements and for the calculation of fast neutron cross sections.

If the chamber walls contain hydrogen, an auxiliary measurement must be made, for the method above does not differentiate between proton and gamma-ray components in the "wall

[7] L. H. Gray, Proc. Camb. Phil. Soc. **40**, 72 (1944).

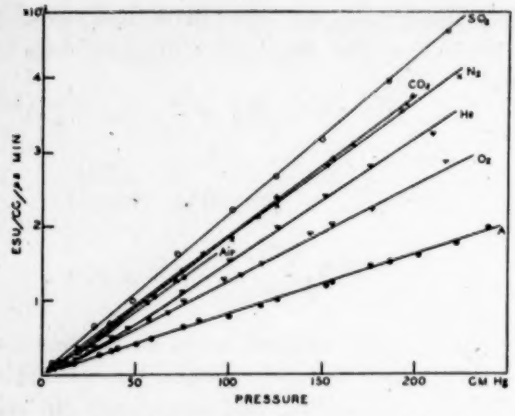

FIG. 1. Ionization-pressure curves for non-hydrogenous gases in gas-walled chamber, linear at normal pressures. Ranges of recoil particles < chamber dimensions.

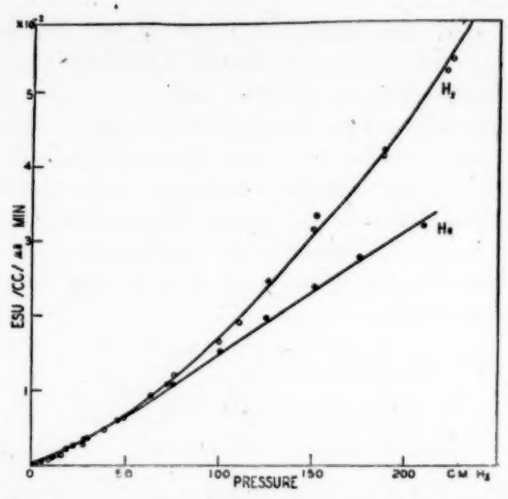

FIG. 2. Ionization in hydrogen and in helium. Ranges of recoil protons > chamber dimensions at all pressures employed. Ranges of alpha-particles < chamber dimensions at pressures > 70 cm.

effect." An extensive study[8] of the relative gamma-ray ionizations resulting in various hydrogenous and non-hydrogenous walled chambers filled with the same gas has shown that the gamma-ray effect in light wall materials, such as carbon, bakelite, and amber, are practically the same. Hence comparative measurements with a carbon chamber may be used to separate gamma-ray and neutron ionization effects in chambers with hydrogenous walls.

EXPERIMENTAL PROCEDURE

The Neutron Source

The neutron source used in the early biological experiments of this laboratory[8] was employed. A beryllium target in the 37-inch cyclotron of Lawrence and Cooksey[9] was bombarded by 8-Mev deuterons and the measurements were made at the exit of the collimating arrangement described by Aebersold,[8] which gives a neutron beam in the forward direction of the deuteron beam. This arrangement localizes the effect of the fast neutrons to a sharply defined region and quite well suppresses gamma-ray effects. It does not absorb slow neutrons other than by the large masses of the material of the collimator.

The Ionization Chambers

A gas-walled chamber (Group I) was formed of fine (No. 30) copper wires spaced approximately 7 mm apart to define a cylindrical surface, 3.3 cm long and 4 cm in diameter, the ends being formed by meshing wires with the same spacing, thus forming a volume of about 66 cc with a 96 percent gas-walled surface. The collecting electrode, 3 mm in diam. and 4.5 cm long was mounted along the axis of the cylinder, and the lead to this electrode was protected against the collection of ions in the space between the shield and the chamber by a cylindrical brass guard which surrounded the amber insulating plug and was in contact with the outer shield. This chamber was housed in a large brass cylindrical shield, leaving 10 cm between the front faces of the shield and the chamber, 5 cm between their rear faces, and 5 cm between their cylindrical surfaces, distances adequate to provide inside the chamber the conditions of secondary particle equilibrium discussed earlier in this paper. The front face of the shield was placed in contact with the aperture of the neutron collimating cones, so that the neutron beam was directed along the length of the ionization chamber. The center of the chamber was approximately 85 cm from the neutron source.

TABLE I. Magnitudes of Jaffé constant "c."

Gas	O_2, CH_4, C_2H_4, C_2H_6, C_3H_8, C_4H_{10}, H_2S, NH_3	SO_2, C_2H_2	CO_2
c	10^{-4}	10^{-5}	3×10^{-6}

[8] P. C. Aebersold, Phys. Rev. 56, 714 (1939).
[9] E. O. Lawrence and D. Cooksey, Phys. Rev. 50, 1131 (1936).

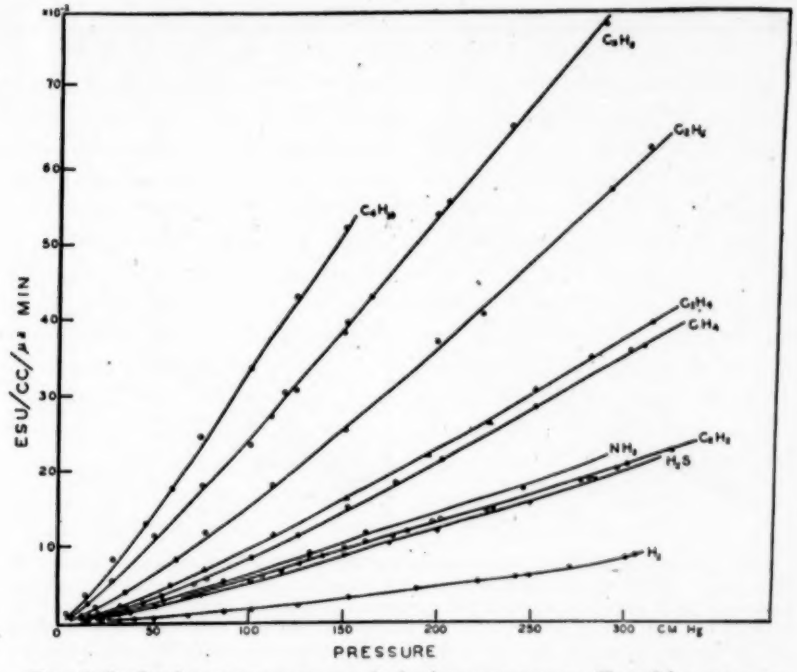

FIG. 3. Ionization-pressure curves in hydrogenous gases. Transition pressures occur in H_2S, C_2H_2, CH_4, C_2H_4, C_2H_6, C_3H_8, C_4H_{10} at 240, 240, 275, 200, 190, 130, and 100 cm, respectively.

Type II chambers were of two kinds, the thimble chambers, described by Aebersold[8] with C, brass, Cd, Sn, Pb, Bakelite, and Amber walls, and "cylindrical" chambers with C and celluloid walls.[10] The latter consist of an inner cylindrical electrode of the material, 1.22 cm in diam. and 5.0 cm long, held concentrically inside a tube of the same material of 1.43 cm inside diam. of an amber plug. To protect the brass lead of the center electrode from the collection of ions, it is mounted inside a concentric brass shielding tube. The effective volume of the chamber is 2.15 cc. To render the celluloid surfaces conductive they were sparsely covered with powdered graphite. Neutron beams were directed across the Type II chambers, normal to their axes. In the thimble chambers the longest path available to recoil wall particles is the 1-cm diameter, and in the cylindrical chambers this limiting distance is 0.74 cm, the width of the plane which is tangent to the outer surface of the inner electrode and is bounded by its intersections with the outer cylinder.

[10] Chambers of various other wall materials were constructed, but the measurements taken are too limited in extent to report at this time. The Bakelite material was that used in the manufacture of Victoreen chambers.

The Measurements

Ionization currents were measured by a null method with an FP54 electrometer tube amplifier, the tube and high resistors being housed in an evacuated chamber. To avoid any effect from the strong magnetic field of the cyclotron, the tube was magnetically shielded by a concentric iron cylinder, also housed inside the chamber, which was located about 60 cm from the ionization chamber, practically outside of the magnetic field. Connection between the control grid and the collecting electrode of the ionization chamber was made by a fine wire strung through amber insulators supported in an evacuated shielding tube. To protect the observer from harmful biological effects the measuring circuit was placed outside the 30-inch water walls which surround the cyclotron. To eliminate radio frequency effects the entire circuit assembly with its leads was housed in a continuous copper shield, using a common ground; to dampen out this pick-up on the high voltage lead to the ionization chamber a filter was introduced just outside the chamber. Finally, all zero readings were taken with the oscillators in operation, the test of

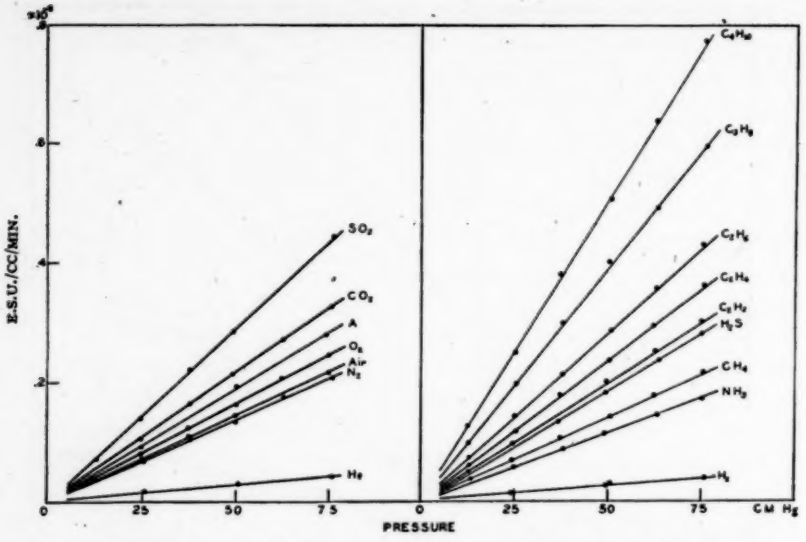

FIG. 4. Gamma-ray ionization curves for 100-cc chamber, showing validity of Bragg-Gray relation (ionization linear with pressure and proportional to stopping power of gas). Relative gamma-ray responses compared with those for neutron ionization (Figs. 1 and 3) indicate the distinctly different relative magnitudes of the energy absorbed by the ionizing particles, electrons or nuclei, respectively.

adequate shielding being identical circuit calibrations with or without oscillator operation.

With the large chambers ionization currents were measured in sixteen gases, including air, at pressures ranging from 3 mm of Hg to 4 atmospheres in hydrogenous gases and to only 2 atmospheres in non-hydrogenous gases. The complete results for only the "gas-walled" chamber will be quoted, those with the 100-cc and 500-cc brass chambers being used for interpretative purposes. With the small chambers currents were read in a few of these two types of gases, the maximum pressures being one or two atmospheres.

The neutron output for a particular deuteron current, maintained between 25 and 30 μamp., was kept steady during measurements, its constancy being checked at frequent intervals by using as monitor the ionization produced in the 100-cc brass chamber when filled with air at atmospheric pressure. All ionization values were reduced to the number of electrostatic units of charge associated with ions of one kind produced per cc per μamp. min. of deuteron charge. It was found that if any of the principal operating conditions of the cyclotron varied, such as the strength of the magnetic field or the deflector voltage, a simultaneous variation occurred in the neutron output. Hence, all sets of readings reported in this paper were taken within short intervals of time during which the operating conditions remained nearly constant, several independent sets of readings being taken for each gas, results agreeing within 2–3 percent.

Since the ionization produced by recoil nuclei is columnar and very dense, ionic recombinations occurred, particularly at high pressures; accordingly corrections were made to the measured values of the ionization at various voltages according to the theory of Jaffé,[11] using the method of Zanstra.[12] These corrections were not made in the earlier reported results, nor was recombination taken into account in the similar early measurements of Bonner.[13] With the large chambers a voltage-supply which gave 3250 volts with 400-volt intervals was employed for all but the lower pressures, for which batteries were substituted, since they permitted smaller voltage intervals. With the small chambers batteries were adequate except for the highest pressures. In the application of the Jaffé-Zanstra formula to the results obtained with the gas-walled chamber the average field intensity in a region within one cm of the cylindrical walls of

[11] G. Jaffé, Ann. de Physique **42**, 303 (1913).
[12] H. Zanstra, Physica **2**, 817 (1935).
[13] T. W. Bonner, Phys. Rev. **45**, 101 (1934).

the chamber was used, since calculations indicate that the field varies only slightly in this region and that the volume of the region is such that about ¾ of the ions are produced within it. With 3250 volts between the walls and the collecting electrode the field in this region was about 1000 volts per cm in the wire chamber and about ¼ this value in the 500-cm solid-walled chamber. Closer to the central collecting electrode the fields were naturally much larger.

The value of the Hankel function employed in a reduction was obtained from coefficient c, itself determined by the Zanstra method. This coefficient has been determined previously for a limited number of gases, for air by Zanstra[12] and for He, N, Ar, and Ne by Clay and Kwieser,[14] the present observations demanding the same values of c for their reduction. The approximate values of c obtained for other gases are listed in Table I. Collection was so nearly complete in hydrogen, even at the highest pressure, no value of c was obtained. The smaller the value of c, the more likely are recombinations under identical pressure and electric field conditions.

DISCUSSION OF RESULTS

The gases studied with the "gas-walled" chamber fall into two groups: non-hydrogenous gases, in which recoil nuclei have relatively short ranges; and hydrogenous gases, in which the recoil protons have relatively long ranges, H_2, CH_4, C_2H_4, C_2H_6, C_3H_8, C_4H_{10}, C_2H_2, H_2S, and NH_3. In Fig. 1 are shown the ionization-pressure curves, corrected for ionic recombinations, of the non-hydrogenous group, which except for that of He are linear beyond 5 cm mercury pressure, indicating that at all but very low pressures the conditions necessary for secondary particle equilibrium exist. Because of the longer range of He nuclei and the smaller stopping power of the gas, this equilibrium condition is not fulfilled in He at pressures less than 70 cm, the ionization-pressure curve being quasi-parabolic at lower pressures, as is evident in Fig. 2. The diagram also depicts the parabolic $i-p$ conditions in H_2, in which gas the proton ranges are so long that the equilibrium condition was not attained even at the maximum pressure employed.

The corresponding $i-p$ curves obtained with the hydrogenous gases are shown in Fig. 3. At the lower pressures all these curves are quasi-parabolic. For the gases with the greater stopping powers the curves become linear at approximately one atmosphere pressure; as the stopping powers decrease the transition pressures increase, occurring at about 3 atmospheres for CH_4. The mean value of the normal range in air (24.0 ± 0.95 cm) of these long range protons, obtained from the curves for H_2S, C_2H_2, CH_4, C_2H_4, C_2H_6, and C_3H_8, indicates that these protons and hence many of the neutrons have energies of about 5.0 Mev (estimated from the Livingston and

TABLE II. Molecular stopping powers for fast electrons released from brass by gamma-rays from Ra.

Gas	Ionization per cc relative to air	Total ionization relative to air (quoted from alpha-particle measurements)	Molecular stopping powers relative to air for fast electrons	alpha-particles (quoted)
H_2	0.170	0.99 (1, 2)	0.17	0.21 (5)
He	0.192	1.148 (3)	0.16	0.175 (6)
N_2	0.94	0.98 (3)	0.96	0.990 (5)
O_2	1.13	1.10 (4)	1.03	1.060 (5)
CO_2	1.49	0.996 (4)	1.50	1.53 (7)
SO_2	2.00	1.03 (1)	1.93	1.87 (8)
A	1.31	1.38 (3)	0.96	0.97 (6)
CH_4	0.97	1.173 (1)	0.82	0.88 (11)
C_2H_2	1.37	1.265(1)	1.08	1.12 (11)
C_2H_4	1.62	1.22 (1)	1.33	1.34 (11)
C_2H_6	1.93	1.30) (1)	1.47	1.53 (11)
C_3H_8	2.58	(1.31)	2.01	(2.09) (11) (13)
C_4H_{10}	3.47	(1.33)	2.61	(2.72) (11) (13)
H_2S	1.29	(1.27) (9, 10)	1.01	(1.12) (11) (13)
NH_3	0.80	0.90 (1)	0.89	0.82 (11) (12)

TABLE III. Total ionization and the gamma-ray component; fast neutron energy expended per μ amp. min. of deuteron charge.

Gas	Total ionization in e.s.u. per cc per cm pressure (dI_G/dp)	Gamma-ray component in e.s.u. per cc per cm pressure ($dI_{G(\gamma),G}/dp$)	Percentage due to gamma-radiation	Energy in Mev expended by fast neutrons per molecule (E_m)
H_2	$>4.05\times10^{-4}$	0.70×10^{-6}	<0.17	——
He	1.760	0.79	0.45	3.48×10^{-17}
N_2	1.882	4.09	2.2	4.54
O_2	1.325	4.27	3.6	2.82
CO_2	1.893	7.09	3.7	4.37
SO_2	2.172	8.26	3.9	5.06
A	0.772	3.98	5.8	1.33
CH_4	13.61	3.98	0.29	26.90
C_2H_2	8.33	5.65	0.68	15.50
C_2H_4	13.30	6.93	0.45	28.56
C_2H_6	23.20	8.06	0.35	41.19
C_3H_8	30.53	10.38	0.34	54.82
C_4H_{10}	37.83	14.29	0.38	68.11
H_2S	7.98	5.83	0.73	14.62
NH_3	8.12	3.29	0.40	21.01
Air	1.669	4.16	2.5	3.96

[14] J. Clay and M. Kwieser, Physica 5, 724 (1938).

TABLE IV. Effect of chamber dimensions on total ionization and on percentage due to gamma-rays.

Chamber Type	Chamber Wall	Ratio surface area to volume	Distance from target	Gamma-ray percentage in air	CO_2	A	CH_4	Ionization in normal air in e.s.u./cc/μ amp. min. $\times 10^2$ (a) measured	(b) neutron component at 74 cm from target
wire	gas	0.36	85 cm	2.5	3.5	5.8	0.29	1.30	1.66
100-cc	brass	0.81	80	3.9	5.4		0.50	1.51	1.68
500-cc	brass	1.42	80	8.0	11.0	21.2	3.7	1.58	1.69
thimble	brass	5.0	74	20?	30?			2.04	1.64
thimble	carbon	5.0	74	20?	30?			1.96*	1.57

Bethe range curves).[15] The helium results discussed above indicate neutron energies of at least 4.5 Mev.

Separation of the Gamma-Ray and Neutron Components

Since 8-Mev deuterons on beryllium may release 12 Mev of energy, these 5-Mev neutrons must be accompanied by strong gamma-radiation, much of which was suppressed from the beam by the lead filter. Before estimating the portion of the response of the different gases in the various chambers caused by gamma-radiation, the applicability of the Bragg-Gray relationship (Eqs. (10) and (14)) was tested by use of the 100-cc and the 500-cc brass chambers and a 1.07-mc Ra standard with a 1-mm Pb filter. In each gas the resulting ionization, Fig. 4, appeared to be linear with gas pressure, indicating that even in the gases with the greatest stopping powers the high energy electrons liberated from the brass walls completely crossed the chamber. Gamma-ray stopping powers were calculated from the slopes of the ionization-pressure curves and are of the same order of magnitude as, though not equal to, the values measured in alpha-particle stopping, in agreement with the theory that stopping powers for fast electrons are relativity functions of their velocity and for heavy particles are effected by the difficulty they experience in producing K-electron ionization.[16]

For the calculations, values of W_G, or of relative ionizations W_G/W_{air}, produced by high energy electrons, protons, and other recoil nuclei, were required. As Gray[7] has pointed out, the mean energy expended in ionization varies not only with the nature of the ionizing particle, i.e., with its mass and cross section, but also with its velocity. At low energies magnitudes of W_G increase rapidly as the energy of the ionizing particle decreases; at high energies magnitudes are practically constant, in air being approximately 35.1 ev for 6–8-Mev alpha-particles, 36.0 ev for 1–8 Mev protons, and 32.5 ev for high energy electrons. Moreover, at these high energies relative ionization magnitudes appear to be nearly independent of the nature of the ionizing particle, though at low energies values are functions of the velocity of the particle and also of the gas concerned. At high energies the ionization relative to air for H_2, N_2, D_2, CO_2, and SO_2 is practically unity, a value frequently employed in energy-loss calculations, but lies between 1.2 and 1.3 for the hydrocarbon and monatomic gases. No investigations are recorded giving values of W_G for the C, N, O, S, and A recoil nuclei, which were ionizing agents in some of the gases concerned, but since C, O, and N particles take from the neutrons about one-quarter of the energy imparted to recoil protons, and S and A particles less than one-eighth, corresponding W values must be fairly large, certainly as large as

TABLE V. Percentage decrease caused by magnetic field on ionization produced by gamma-radiation.

Chamber	Diameter	Percentage decrease with chamber located (a) at collimator exit	(b) adjacent to magnet pole
Shield of wire mesh	14.0 cm	30	50
500-cc	7.6	5	32
100-cc	3.3	1	4
Thimble	1.0	none	1

[15] M. S. Livingston and H. A. Bethe, Rev. Mod. Phys. 9, 245 (1937).
[16] M. S. Livingston and H. A. Bethe, Rev. Mod. Phys. 9, 263–265 (1937).

that obtained with 1–2-Mev alpha-particles, namely 38.0 ev in air. This value was used in the calculations which involved ionizations by the heavier recoil nuclei, introducing uncertainties of 2–3 percent in resulting magnitudes, smaller uncertainties being introduced by using 32.5 ev for the electron, 36.0 ev for proton, and 35.6 ev for alpha-particle ionizations. In addition relative ionizations in the various gases were assumed the same for all these particles, for their energies were sufficiently high to warrant the assumption. The resulting values of fast electron stopping powers are listed in Table II together with the quantities used in their calculation and with mean values of alpha-particle stopping powers.[17]

The ionization produced by the neutron source in hydrogen at low pressures with "gas-walled" chambers was carefully measured and from the values obtained at pressures less than 3 cm mercury the value of "a" in Eq. (13) was determined as 0.678×10^{-6} e.s.u./cc/μ amp. min. per cm pressure. From these measurements and the values of W_G obtained from Table II the gamma-ray component of the ionization produced in the other gases was calculated through Eq. (14), the resulting values of $dI_{G(\epsilon)}/dp$, accurate to 20–30 percent, being listed in Table III.

The table also includes the experimental values of dI_G/dp (total) (with less than 2 percent probable error in the measurements), and the percentages of the total ionization attributable to gamma-rays at pressures in excess of the respective limiting pressures. It is apparent that the gamma-ray component of the measured ionization varies from less than 1 percent of the total in gases containing hydrogen and helium to 2–6 percent in gases containing only heavier particles.

Similar calculations from low pressure hydrogen curves in the solid-walled brass chambers indicate larger gamma-ray contributions (Table IV), ranging from about 1 percent in hydrogeneous gases to nearly 10 percent in O_2, N_2, and CO_2, and nearly 20 percent in A. But the neutron component, i.e., the "gas effect," is nearly independent of chamber characteristics. The larger gamma-ray contribution in these chambers with smaller dimensions, with a larger ratio of surface area to volume, can be largely attributed to the relatively greater contribution to the ionization from the electrons released from the surfaces. An equally effective cause of the difference may be the deflection of the paths of the light electrons by the magnetic field of the cyclotron, causing a certain percentage of these particles to return to the wall from which they were ejected without passing through the small wire mesh chamber. This hypothesis was tested by measuring the ionization produced by gamma-rays from the Ra standard with the magnetic field on and off. In Table V are tabulated the results obtained with the chambers discussed and also with the small thimble chambers (Type II) used for the study of the wall effect and for neutron dosimetry. In the 100-cc and thimble chambers, in which the walls are fairly close together, the recoiling electrons apparently travel nearly equivalent distances within the chambers on the curved paths imposed by the magnetic field and on the

TABLE VI. Neutron energy transferred per μamp. min. of D charge per atomic nucleus.

Element	Gases used	E_A in Mev per nucleus per μamp. min. of D charge $\times10^{17}$	E_A/E_H
H	CH_4, C_2H_2, C_2H_4, C_2H_6, C_3H_8	6.20±0.07	1.000
He	He	3.48±0.04	0.551
C	CO_2, O_2, C_2H_4, CH_4	1.58±0.02	0.252
N	N_2	2.27±0.03	0.368
O	O_2	1.41±0.02	0.227
S	SO_2, O_2	2.24±0.02	0.360
A	A	1.33±0.02	0.213

[17] Quoted values are from the following sources: (1) A. F. Kovarik and L. W. McKeehan, Bull. Nat. Research Council (1925) No. 51, 72; (2) R. W. Gurney, Proc. Roy. Soc. **A107**, 332 (1925); (3) R. Naidu, Ann. Chim. Phys. **1**, 72 (1934); (4) C. E. Gibson and H. Eyring, Phys. Rev. **30**, 553 (1927); (5) G. I. Harper and E. Solomon, Proc. Roy. Soc. **A127**, 175 (1930); (6) G. Mano, J. Phys. Radium [7] **5**, 628 (1934); (7) C. E. Gibson and E. W. Gardner, Phys. Rev. **30**, 543 (1927); (8) L. F. Bates, Proc. Roy. Soc. **A106**, 622 (1924); (9) W. C. Price, J. Chem. Phys. **4**, 147 (1936); (10) J. C. Morris, Phys. Rev. **32**, 456 (1928); (11) K. Schnieder, Ann. d. Physik **35**, 445 (1939); (12) H. von Trauenberg and K. Phillip, Zeits. f. Physik **5**, 404 (1921); (13) W. H. Bragg, Phil. Mag. **13**, 333 (1907). Values in parentheses are estimated in the absence of experimental determinations; those for relative total ionization by assuming the value of H_2S to be similar to that of C_2H_2 (their ionization potentials are similar); and those of C_3H_8 and C_4H_{10} as intermediate between those of C_2H_6 and C_5H_{12}, quoted in (1). Estimated values of relative stopping powers were obtained by using the Bragg rule that stopping powers are additive.

linear paths followed in the absence of the field, and the gamma-ray ionization is little affected by the magnetic field. But in larger diameter chambers, particularly those constructed with an inner wire collecting chamber, the deflection of the ionizing beta particles materially reduces the gamma-ray ionization.

No tests were made of the effect of the field on the paths of the recoil nuclei released from the walls and gas by neutron irradiation, but the deflecting force on such particles moving in a magnetic field can be only 0.3–2 percent of that on beta-particles of the same energy; hence the effect of the field on neutron ionization must be negligible. This conclusion is confirmed by cloud-chamber photographs taken close to the magnet of the cyclotron.[9]

Rate of Conversion of Neutron Energy by Various Nuclei

From the values listed in the first two columns of Table IV and from Eq. (11) the neutron energy expended in the various gases was calculated by using the W_G values characteristic of the ionizing particle and recalling that in compound gases the neutron energy made available for ionization is distributed between the particles in accordance with Eq. (2), the resulting values being listed in the last column of that table, expressed in terms of E_m, Eq. (7), the rate of absorption of neutron energy per μamp. min. of deuteron charge. In Table VI are given the corresponding values of E_A, the rate of absorption of neutron energy per atomic nucleus, calculated, with the exception of the proton value, either directly from the E_m value of the corresponding gas or as the difference of these values for two gases. From E_C, the weighted mean of the two indicated calculations for carbon, and from the E_m values of the stated hydrocarbons, values of E_H have been calculated, their unweighted mean being quoted. The probable errors of the E_A values result from the errors of the E_m values, themselves propagated from those of WdI_{exp}/dp and the correction for the gamma-ray component of the ionization. From the E_m values of C_4H_{10}, H_2S, and NH_3 together with the E_A values of C, S, and N, respectively, values of E_H, 5.89, 6.04, and 6.13 were obtained but not included in the determination of its probable value because of the uncertainty in the W values of these gases and their relatively large ionic recombinations. Relative values of E_A are also those of the atomic energy conversion coefficients, K_{jk} (Eq. (1)), provided the neutron energy is monochromatic.

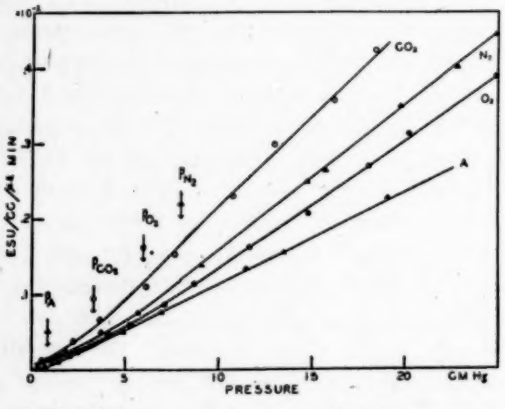

FIG. 5. Transition gas pressures revealed in i–p curves for 100-cc (3.3-cm diam.) brass chamber.

N–p Cross Section (Weighted Mean Value)

As already stated the mean value of the n–p cross section, weighted for the energy distribution of the neutron beam, can be calculated from these values (Eq. (8)), provided the neutron energy flux is known. Lacking a direct measurement of the neutron flux in the beam employed, an approximate value has been calculated by comparing the ionization produced by these D-Be neutrons with that produced by Rn-Be neutrons, measured by Dunning and quoted by Aebersold[8] as 1500 ion pairs per cc of air per sec. at 30 cm from a 1-curie radon beryllium source. In the present experiment 4.28×10^5 ion pairs per μamp. deuteron current were formed per cc of air per sec. at 85 cm from the target; hence the neutron beam created in the 37-inch cyclotron per μamp. min. of 8-Mev deuterons may be considered equivalent to that from a 2.38×10^3 curie Rn-Be source. According to Amaldi, Hafstad, and Tuve[18] 25,000 neutrons per sec. are emitted from the latter source per mc of radon, hence at 85 cm from the source the neutron energy flux per sq. cm is equivalent to that of

[18] E. Amaldi, L. R. Hafstad, and M. A. Tuve, Phys. Rev. 51, 896 (1937).

TABLE VII. Transition gas pressures, and mean ranges and recoil energies.

Transition pressures in cm mercury at 25°C						Ranges and energies at 760 mm and 15°C				
	Chamber and limiting dimension						Range in			
Gas	100-cc brass 3.3 cm	500-cc brass 7.6 cm	Gas-walls 10 cm	Thimble 1.05 cm (calc.)	Cylindrical 2.1 mm (calc.)	Principal recoiling nuclei	gas	air	Energy in Mev of nucleus	neutron
							in mm			
air	7.5	3.5	3	24.8	118	*N*, O	3.2	3.2		
N_2	8.0	4.0		26	124	N	3.3	3.3	1.27	5.07
O_2	6.0	3.0		20	95	O	2.5	2.7	1.10	5.00
CO_2	4.3	2.0		13.5	68	*C*, O	1.89	2.9	1.44	5.14
A	0.5			1.6	8.4	A	0.21	0.20	0.5	5
He		100	70	9 atmos	43 atmos	He	9.2 cm	1.62 cm	2.9	4.55
CH_4			275	36 atmos	172 atmos	H	36 cm	32 cm		
C_2H_4			200	26 atmos	125 atmos	H	26 cm	30 cm		
Mean of C_2H_2, CH_4, C_2H_4, C_2H_6, C_3H_8, and H_2S transition gas pressures lead to H								34 cm		5.0

3.72×10^7 Rn-Be neutrons per μamp. of direct-current. The mean energy of these neutrons, estimated from Dunning's graph[19] for the distribution in range of the forward projected protons and from the energy-range values of Livingston and Bethe, is about 2.5 Mev. Hence the neutron energy flux per μamp. of deuteron current in the beam employed was, approximately, 9.1×10^7 Mev per min.

The resulting $n-p$ cross section is approximately 1.3×10^{-24} cm². From this quantity and the values given in Table VI lower limits of the cross sections of He, C, N, O, S, and A are obtained as 1.1, 1.2, 1.9, 1.4, 4.1, and 3.0×10^{-24} cm², respectively. These calculations neglect the effects of asymmetry, but nevertheless indicate that most of the neutron ionization effected by He, C, and O reactions result from elastic collisions, and that 30–40 percent of the N effects must result from disintegrations. The magnitudes obtained for the heavier nuclei may be relatively small since the 38-ev value used for W_G in the E_m calculations may have been too low. Since the ionization curves indicated that many 5-Mev neutrons as well as neutrons with lower energies and possibly some with higher energies were in the beam, the weighted mean cross sections must be quite different from values measured for monoenergetic neutrons. This is indeed the case for hydrogen and carbon, which have been calculated as 0.61 and 1.31×10^{-24} cm², respectively, for 15-Mev neutrons by Salant and Ramsay,[20] and as 2.40 and 1.96×10^{-24} cm² for 2.88-Mev neutrons by Zinn, Seely, and Cohen.[21] The values stated above for N, O, and S are higher than those obtained by the latter group, namely, 1.38, 1.25, and 3.12×10^{-24} cm².

Transition Gas Pressures

The dimensions of the large ionization chambers were chosen so that in at least one the transition pressure, $p_{G(j)}$, of the type j nuclei of the gas G, lies within the pressure range available for use. For the short range C, O, N, and A recoils in CO_2, O_2, N_2, and A the 3.3-cm diameter brass chamber was most useful, yielding the curves in Fig. 5, which clearly indicate the $p_{G(j)}$ regions. Since these pressures vary with the ranges of the particles, many of which are less than the maximum, the pressures stated in Table VII are approximate values. The table also includes the pressures measured with the 7.6-cm brass chamber or with the 10-cm gas-walled chamber for alpha-particles in He, Fig. 2, and for protons in CH_4 and C_2H_4, Fig. 3, and the resulting calculated transition pressures for small chambers with dimensions those of the thimble and cylindrical chambers. With He, CH_4, and C_2H_4 in the small chambers these pressures are greater than those employed; hence the parabolic shape of the gas ionization curve impresses a continuous curvature on the resultant experimental curve (Figs. 6b and 7b). The argon recoils have such short ranges that even with the smallest chamber ionization-

[19] J. R. Dunning, Phys. Rev. **45**, 586 (1934).
[20] E. O. Salant and N. Ramsay, Phys. Rev. **57**, 1985 (1940).
[21] W. H. Zinn, S. Seely, and W. V. Cohen, Phys. Rev. **56**, 260 (1939).

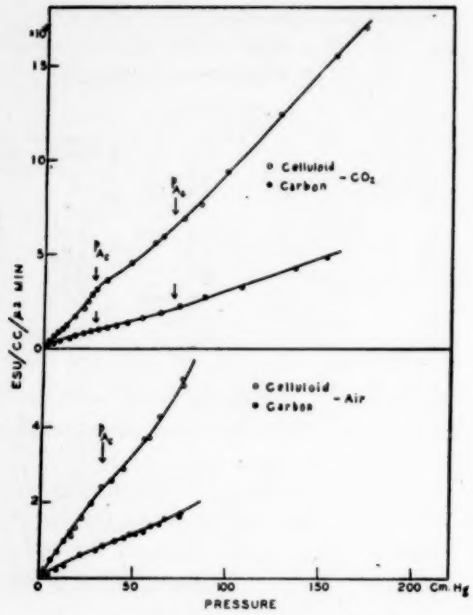

FIG. 6a. Cylindrical chamber curves showing transition pressures for wall and gas nuclei in air and in carbon dioxide.

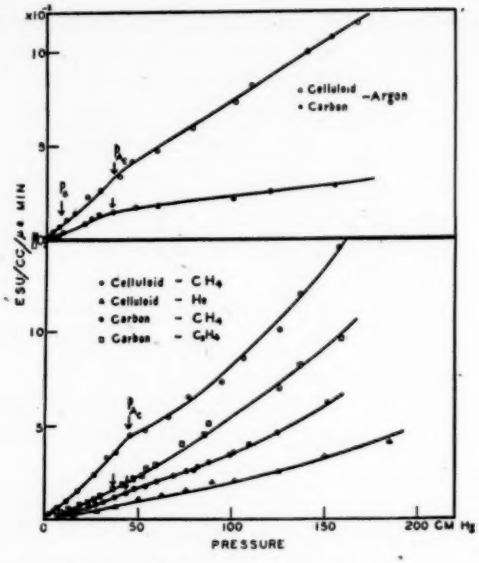

FIG. 6b. Cylindrical chamber responses in argon and in methane, ethylene, and helium.

pressure curves are practically linear throughout. With air and CO_2 the onset of linearity at the predicted pressures is easily identified in the thimble chamber curves (Fig. 7); with CO_2 and A it is observable in the cylindrical chamber results (Fig. 6).

Ranges and Energies of Recoiling Nuclei

From the transition pressures, the limiting dimensions of the containers, and the stopping powers of the gas for heavy particles, the maximum ranges of the various recoiling nuclei in their respective gases and the corresponding ranges in air have been calculated (Table VII). From the range-energy curves of Blackett and Lees[22] and Feather[23] for N, O, and C nuclei recoiling in alpha-particle collisions, the energies of these particles have been estimated. The range found for the A nuclei is considerably less than any studied by Blackett and Lees, hardly justifying an extrapolation for range. Since in elastic collisions (Eq. (2)), the maximum energy of C, N, O, and A recoiling nuclei is 0.28, 0.25, 0.22, and 0.10, respectively, of the incident neutron energy, a large portion of the neutrons entering the chambers must have energies of at least 5 Mev, the value mentioned earlier in this paper as calculated from the proton and alpha-particle ranges in hydrogenous gases and in helium, respectively.

Wall Effects in Small Chambers

For the wall effect analysis, thimble chambers with carbon, Bakelite, amber, brass, tin, or lead walls and cylindrical chambers with carbon or celluloid walls were irradiated. Short range heavy

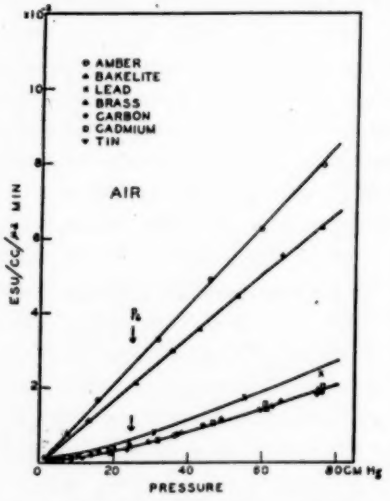

FIG. 7a. Thimble chamber responses in air.

[22] P. M. S. Blackett and D. S. Lees, Proc. Roy. Soc. **A134**, 658 (1931); **A136**, 325, 338 (1932).
[23] N. Feather, Proc. Roy. Soc. **A141**, 194 (1933).

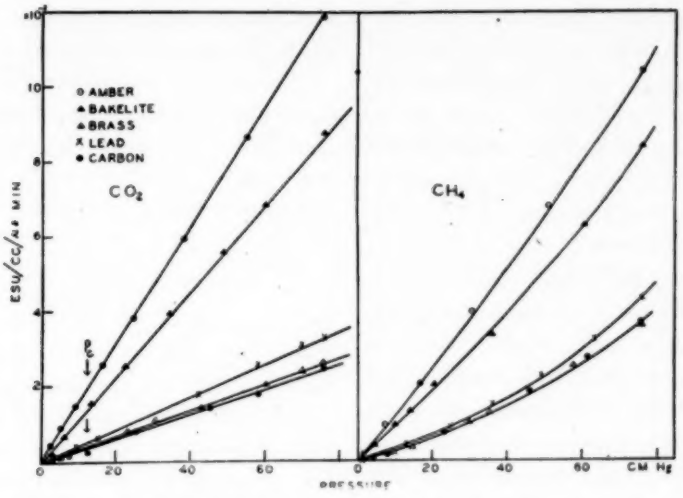

FIG. 7b. Thimble chamber responses in carbon dioxide and in methane.

nuclei are present in all these materials; protons are also present in amber, Bakelite, and celluloid walls. The ionizing effects of the C, N, and O wall particles are not easily separable from the effects of the gas nuclei, when measurements are made in gases containing these nuclei, but are strikingly separable in argon, since the ranges of the latter are less than a tenth of the C, N, and O ranges. The $i-p$ curves obtained when this gas is used in cylindrical chambers, particularly in the carbon chamber, Fig. 6b, indicate that at pressures exceeding 10 cm (at which the gas effect becomes linear), the curves are practically linear to about 35 cm, the slope then decreasing to about 50 cm, becoming linear again at higher pressures. At 35-cm pressure the longest range carbon particles are just able to cross the 0.74-cm limiting dimension obliquely to the tangent plane just across the chamber. At still higher pressures the energy of all is completely utilized in the chamber, producing $Q_{A(c)}/W_G$ ions.

The results obtained when these cylindrical chambers were filled with air, CO_2, or C_2H_4 (Fig. 6) also indicate the pressures $p_{A(c)}$, since the directions of the C, O, and N gas particles are much more at random than those emitted by the walls, so that the gas components of the $i-p$ curves remain parabolic to higher pressures determined by the 0.2-mm distance between the chamber walls. The resulting values of the ranges of the C and O wall nuclei agree, with these reservations, very well with those obtained directly from the "gas effect."

In thimble chambers transition pressures for heavy wall particles in the gases studied, air, CO_2, CH_4, and A are, with the exception of CH_4, about the same as those for the gas recoils; hence ionizing energy lost in the walls by gas recoils is very nearly compensated by that gained from recoiling wall particles. Ionization curves are linear except at the lowest pressures, the error introduced by assuming complete compensation being not more than 3 percent. Hence in the case of many non-hydrogenous-walled chambers the analysis $I_{A(c),G}+\sum I_{G,G}(k)$ may be replaced by the expression $I_{G,G}=Q_G/W_G$, where $Q_G=\sum_k Q_k$. That is, $I_{G,G}$ is the ionization which occurs in the gas when there is secondary particle equilibrium, its magnitude being proportional to the gas pressure, as are the other two components of the ionization caused by wall protons and by gamma-rays.

Consequently the fast neutron responses of thimble chambers with non-hydrogenous walls are practically the same (Fig. 7), the excess ionization in chambers with heavy walls such as lead being attributable to additional gamma-ray absorption. The relative gamma-ray responses of these chambers at atmospheric pressure have already been reported by Aebersold. They are shown at various pressures in Fig. 8. The ionization is linear with pressure, approximately four

times as dense as in 100-cc chambers (Fig. 4), the same in carbon, Bakelite, amber, brass, and cadmium-walled chambers, and is approximately 40 or 70 percent higher in chambers with tin or lead walls. The greater intensity undoubtedly results from the large ratio of the surface area to the volume of these small chambers. Similar relative gamma-ray effects must occur in neutron bombardment. Recalling that the ionizing electrons are not able through magnetic deflection to escape from the chambers before complete transit, it is reasonable to assume that in air in a carbon chamber the gamma-ray component is approximately 20 percent of the total response, and to calculate the component in the other chambers from the relative gamma-ray sensitivities revealed in Fig. 8. Since the stopping power of CO_2 is 50 percent higher than that of air, gamma-ray components in this gas must be correspondingly greater (Table VIII). The validity of an assumption of such high percentage of gamma-ray effects is shown both by the similar values calculated for $I_{G,G}$ in the various chambers for the two gases and by their relative values, shown in the same table, the CO_2/air ratio being 1.10, a quantity agreeably close to that obtained from alpha-particle measurements of the absorption of energy by the gas, namely, 1.113. Since under corresponding conditions the magnitudes of the gamma-ray responses of amber, Bakelite, and carbon must be practically the same (Fig. 8), only 5–6 percent of the total ionization measured in the amber and Bakelite chambers can be attributed to gamma-ray effects.

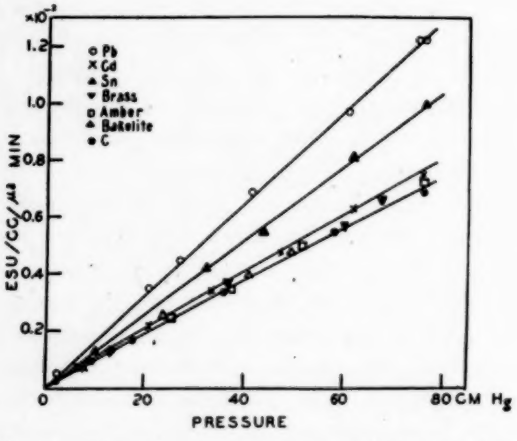

FIG. 8. Gamma-ray responses of air-filled thimble chambers. Ionization densities are nearly four times the densities obtained with 100-cc chamber (Fig. 4).

The excess response of chambers with hydrogenous walls over that of carbon-walled chambers must result from protons in the walls, the ratio of this proton component to the gas component being determined by

$$\frac{I_{A(p),G}}{I_{G,G}}=\frac{Q_{A_p}N_{T,p}S_{G(p)}}{Q_GN_AS_{A(p)}}=\frac{E_{A(p)}S_{G(p)}}{E_GS_{A(p)}},$$

where the E's represent the energies absorbed per molecule of the respective media. To test this relation, values of the energy absorbed by the protons per molecule were calculated from the values of E_m listed in Table IX and from the stopping powers per molecule relative to air calculated from the stopping powers of the atomic constituents, those of H and C being the values given by Livingston and Bethe for 3.26-Mev protons and that of O, the alpha-particle value. The molecular formulae and physical constants employed in this and further calculations are listed in Table X. The values of the ratios of the proton and gas recoil components of the ionization in amber and Bakelite chambers in air and CO_2 thus obtained are in excellent agreement, considering the possible contributing errors, those of the estimation of the gamma-ray component and of the uncertainties in the molecular formulae of the materials and in their stopping powers for high energy protons and heavy particles.

Finally, the energy absorbed by protons per cc of these wall materials, the quantity needed for the interpretation of biological experiments, has been calculated in three ways, directly through Eq. (11) from the proton component of the ionization (Table VII), indirectly from the product of the ratio of the proton and gas recoil components of the ionization (same table) and the energy E_G absorbed per gas molecule calculated from the values of E_j measured in the gas effect (Table VI) through the equation

$$Q_{A(p)}=E_G\frac{I_{A(p),G}}{I_{G,G}}N_A\frac{S_{A(p)}}{S_{G(p)}},$$

and directly from the product of the energy $E_{A(p)}$ absorbed by the protons per molecule calculated from the E_j's, and the number of mole-

TABLE VIII. The components of the ionization in thimble chambers (ionization expressed in e.s.u./cc/μamp. min. per cm pressure $\times 10^{-4}$).

Chamber wall	Total ionization in air	Total ionization in CO_2	Gamma-ray percentage air	Gamma-ray percentage CO_2	Gas-wall component air	Gas-wall component CO_2	Neutron effects: Proton component air	Neutron effects: Proton component CO_2	Proton/gas ratio air exp.	Proton/gas ratio air calc.	Proton/gas ratio CO_2 exp.	Proton/gas ratio CO_2 calc.
Carbon	2.64	3.40	20	30	2.12	2.38						
Brass	2.88	3.60	22	33	2.15	2.40						
Cadmium	2.76		22	33	2.11							
Lead	3.26	4.64	34	51	2.15	2.28						
Amber	10.80	16.04	5	8	10.28	15.02	8.16	12.64	3.85	3.95	5.32	5.39
Bakelite	8.24	11.72	6	9	7.72	10.70	5.60	8.32	2.66	2.63	3.50	3.61

cules, N_A per cc. The excellent agreement in the results so obtained (Table IX) indicates that any one of the three methods may be used for calculation of the energy absorbed by the protons of hydrogenous material.

NEUTRON EFFECTS IN TISSUE

Energy Calculations

The last described method has been used to calculate the energy absorbed per g of various "tissues" and tissue-like materials frequently used for the walls of small ionization chambers. A molecular formula for tissue, stated in Table X, has been derived on the assumption that tissue is 85 percent water and 15 percent protein, the formula for protein being the average of those indicated from the analyses[24] of several tissue proteins. The energies absorbed per gram in such substances and in the tissue represented by the formulae proposed by Gray and Read[3] and by Zimmer[25] are given in the table, together with values for several gases, whose suitability for use in such chambers is discussed in this paper.

The calculations indicate that the response of amber to fast neutrons is very nearly that of tissue A, surpassing the responses of Bakelite and Aerion, materials most frequently used for the walls of the small chambers employed in dosimetry. The response of celluloid is similar to that of the protein molecule. It is obvious that if Aerion is used as a chamber wall, the ionization response will be much less than for a tissue wall and a large correction factor will be necessary in calculating the energy absorption in tissue.

Amber and Bakelite are not electrically conducting whereas Aerion is; consequently the conducting layer with which amber and Bakelite chambers must be lined causes some loss of energy of the protons emerging from the hydrogenous walls and the layer itself will contribute no protons. The graphite conducting layers used in these chambers have been varied from thicknesses quite translucent to light to those opaque with a resultant variation of the ionization response of only a few percent. Very thin layers were sufficient to form the conducting layer. The average path length of a proton in crossing the chambers must have been of the order of 0.5 cm, the range of a recoil proton of energy 0.3 Mev. To penetrate a carbon lining opaque to light and to cross the chamber the proton must have 0.4 Mev of energy, a negligible fraction of the predominant energy (5 Mev) indicated by transition pressures.

The advantage of the hydrocarbons as wall materials results both from the relative fractions of the energy absorbed by the nuclei involved and from the relative collision cross sections. Since the latter are energy dependent, varying widely between the 2- and 16-Mev regions commonly studied, it follows that the relative energies absorbed per gram by tissue-like substances

TABLE IX. Energy in ergs absorbed by protons per cc of hydrogenous material per μamp. min. of deuteron charge at 85 cm from target.

Material	Source of calculation: Proton component in "wall effect" air	Proton component in "wall effect" CO_2	Proton/gas ratio air	Proton/gas ratio CO_2	"Gas effect" (Table X)
Amber	6.80	6.82	6.86	6.87	6.64
Bakelite	4.16	4.03	4.26	4.18	4.00

[24] H. S. Sherman, *Chemistry of Food and Nutrition* (The Macmillan Company, New York, 1937), fifth edition, pp. 57–66.

[25] N. W. Timozeeff-Ressovsky and K. G. Zimmer, Naturwiss. **26**, 362 (1938).

TABLE X. Neutron energy absorbed per μamp. min. of 8-Mev deuterons on Be.

Material	Formula[a]	M	Number of molecular groups per cc[b]	Stopping power per molecular group	Energy absorbed in "ϵ" units[c]	Percent absorbed by protons
Amber	$C_5H_8O_{0.5}$	76.0	8.24×10^{21}	3.35	7.35	88
Bakelite	$C_7H_8O_2$	124.0	6.44	5.05	4.98	80
Celluloid	$C_{5.2}H_8O_{2.4}N_{0.7}$	129.2	6.35	5.29	4.53	80
Aerion	$C_{10.9}H_8O_{2.7}$	100.4	4.81	7.46	3.73	77
Tissue[d] *A*	$C_{0.5}H_8O_{0.8}N_{0.14}$	75.0	7.80	3.13	7.11	90
Tissue *B*	$C_{0.6}H_8O_4$	71.6	7.40	3.67	6.68	88
Tissue *C*	$C_{5.2}H_8$	70.4	8.60	3.18	7.96	87
Water	$4(H_2O)$	72	8.42	3.16	7.40	88
Paraffin	$4(CH_2)$	56	9.72	2.64	9.55	89
Air	$O_{0.4}N_{1.6}$	28.8	0.027	1.00	1.38	0
Oxygen	O_2	32	0.027	0.99	0.84	0
Carbon dioxide	CO_2	44	0.027	1.50	0.96	0
Ethylene	$2(C_2H_4)$	56	0.013	2.64	9.55	89

[a] Formulae for hydrogenous materials adjusted to give equivalent proton constituents.
[b] Calculated from density and molecular formula. Density of tissue taken as unity.
[c] Authors propose use of unit "ϵ," 1 erg of energy absorbed per g of material.
[d] Tissue *A* taken as 15 percent protein and 85 percent water. Approximate protein formula was calculated from analyses of beef muscle tissue, egg albumin, casein, and gelatin, quoted by Shermann (see reference 24). Tissue *B* is formula given by Gray and Read (see reference 3). Tissue *C* is formula given by Zimmer (see reference 25).

must vary, as is indicated in Table XI by the ratios of the energy absorbed by tissue molecules and by air and oxygen, calculated from selected values of cross sections appearing in the literature. The observations of Salent and Ramsay[22] are for H and C alone, the proton value being a fraction of that quoted by Kichuchi and Aoki[26] for the same energy range; hence, if the former values are combined with the O and N values of the latter, much lower absorbed energies are indicated. According to the calculations the protons from less energetic neutrons, 2–3 Mev, are relatively more effective than those from higher energy neutrons. Neutrons with the lower energies as well as soft neutrons must be abundant in the beams used in neutron therapy, particularly after penetration of the skin and tissue to the depth of the section under treatment. Lacking direct knowledge of the energy distribution of the beam, measurements such as those herein described should be conducted for the various operating conditions.

Calculation of Energy Absorbed in Tissue from Ionization Measurements

For the dosimetry measurements incidental to the interpretation of the effects of neutron irradiation of biological specimens the energy absorbed from the beam must be calculated directly from simultaneous ionization measurements utilizing either "gas-effect" large chambers or "wall-effect" small chambers. In the former case the energy is calculated by first correcting the gas ionization for its gamma-ray component and then calculating the neutron energy absorbed per gram of the gas and multiplying this by the tissue/gas ratio given in Table XI. It is often suggested that the gas employed might well have atomic constituents equivalent to those of the tissue, such as C_2H_4 or some composition gas. But the recoil protons of such gases have long ranges, the limiting pressures at which secondary particle equilibrium sets in is several atmospheres, and because of the parabolic $i-p$ relationship below this pressure the assumption of proportionality between responses and densities of the gas is erroneous. For example, with C_2H_4 at atmospheric pressure in the large wire chamber used in the experiments reported in this paper the response is 51 percent of that calculated from $p(W_G dI_G/dp)$; in a chamber of about 1-cm dimensions the response would be less than 10 percent of the theoretical value. In non-hydrogenous gases, on the other hand, the range of the recoil nuclei is short and the gas response is very nearly proportional to its density. Although air is commonly used, oxygen is a more suitable gas, since in nitrogen-containing gases a considerable proportion of the ionizing particles released by neutron irradiation are nuclear

[26] S. Kichuchi and A. Aoki, Proc. Phys. Math. Soc. Japan 21, 75 (1939).

TABLE XI. Energies absorbed per g of tissue-like substances relative to air and O_2, calculated from cross sections obtained at various neutron energies.

Neutron source and energy	Observers	Ratios of energies absorbed calculated for relative to	amber	Bakelite	tissue A[a]
D—Be 5 Mev	Aebersold and Anslow	air	5.3	3.6	5.2
		O_2	8.8	5.9	8.4
D—D	Zinn, Seely, and Cohen (see reference 21)	air	12.7	8.0	12.3
		O_2	16.5	10.9	16.0
D—D	Kichuchi and Aoki (see reference 26)	air	10.4	6.8	10.2
		O_2	13.9	9.0	13.4
D—Li	Kichuchi and Aoki (see reference 26)	air	6.3	4.2	6.2
		O_2	10.8	7.2	10.6
D—Li[b]	Salant and Ramsay (see reference 20) with Kichuchi and Aoki	air	3.0	2.2	3.1
		O_2	5.2	3.6	5.3

[a] See note with Table VI.
[b] The H and C cross sections of Salant and Ramsay are combined with the N and O cross sections of Kichuchi and Aoki.

disintegration products, whereas in both oxygen and tissue practically all are recoil nuclei.

When small chambers are utilized for the calculation, the energy may be estimated quite simply from the response of a chamber with hydrogenous walls, such as a Victoreen thimble chamber with Bakelite walls, through an extension of the Bragg-Gray law to relate the energies absorbed by tissue and by chamber walls to the ionizations produced in the two media.

Since a high percentage of the ionization effected in tissue is produced by recoil protons the energies absorbed by the protons in the respective walls may be used for the calculations. The proportionality existing between these energies and the respective proton densities is expressed by

$$Q_{T(p)}/Q_{A(p)} = p_T N_T / p_A N_A, \tag{16}$$

where subscripts T refer to tissue and A to chamber walls, and p represents the number of protons per molecule, N being the number of molecules per cc.

The Bragg-Gray relationship states that for tissue

$$Q_{T(p)\text{per cc}} = W_{T(p)} I_{T(p),\, T\text{per cc}}, \tag{17}$$

and that for the chamber walls

$$Q_{A(p)\text{per cc}} = W_{G(p)} \frac{N_A S_A}{N_G S_G} I_{A(p),\, G\text{per cc}}. \tag{11}$$

Combining Eqs. (11) and (16) and reducing unit volume to unit mass measurements, we obtain

$$Q_{T(p)\text{per gram}} = k_n W_{G(p)} I_{A(p),\, G\text{per gram}} = k_n E_{A(p),\, G\text{per gram}}. \tag{18}$$

Here $E_{A(p),G\text{per gram}}$ is the energy transferred to a gram of the gas by the ionizing protons released from a gram of the wall material and

$$k_n = p_T M_G S_A / p_A M_T S_G, \tag{19}$$

i.e., the product of the ratio of the proton contents of the tissue and the wall molecules, the ratio of the molecular weights of the gas and the wall material, and the ratio of the molecular stopping powers of the wall material and the gas.

Stopping powers of the hydrogenous materials in question may be calculated by recourse to the stopping power curves given by Livingston and Bethe, which give the dependence of proton stopping powers on their energy. These stopping powers also depend on the atomic composition of the materials. Typical values for such stopping powers relative to air are listed in Table XII for amber, Bakelite, and Aerion chamber walls. Corresponding values of k_n are given in Table XIII. Since the proton energies involved do not exceed 4 Mev, it appears that values of k_n applicable to the reduction of chamber readings such as those given in Table VIII to tissue effects are approximately 4/3, 2, and 3 for amber, Bakelite, and Aerion, respectively.

If studies are being made of physiological effects at considerable depths within the tissue, consideration must be given to the softening effect of successive neutron collisions and the

TABLE XII. Dependence on proton energy of stopping-powers of hydrogenous walls.

Wall material \ Proton velocities in 10^9 cm/sec. / Proton energies in Mev	1.0 0.52	1.5 1.17	2.0 2.09	2.5 3.26	3.0 4.70	4.0 8.36
Amber	3.67	3.50	3.41	3.35	3.32	3.26
Bakelite	5.41	5.22	5.12	5.05	5.00	4.95
Aerion	7.71	7.68	7.55	7.44	7.37	7.30

TABLE XIII. Dependence of k_n for monochromatic neutrons on proton energy and chamber walls.

Wall material \ Proton energies in Mev	0.52	1.17	2.09	3.26	4.70	8.36
Amber	1.48	1.40	1.36	1.34	1.33	1.31
Bakelite	2.16	2.09	2.04	2.01	2.00	1.98
Aerion	3.13	3.03	3.00	2.95	2.92	2.90

consequent increase of neutron cross sections. In such cases larger values of k_n than those listed in Table XIII must be selected. By choosing a value of 2.5 for the reduction factor, which reduces Victoreen Bakelite chamber readings (called n units when used for measuring fast neutrons) to tissue dosage, the staff of the Crocker Laboratory at Berkeley has recognized the effect of such soft neutrons within the tissue, and also the ionization which results from the heavier nucleus recoils and the accompanying gamma-rays.

It is believed that biological effects result from the action of the highly energized ions produced from the water of tissue on the protein molecules. Therefore, $I_{T(p),T}$ rather than $Q_{T(p)}$ should be calculated. This can be done through Eqs. (17) and (18). The evaluation can be completed only if W_G/W_T is known. Although the values of the W's must vary with proton energies, relative values must be nearly constant. Moreover W_G/W_T must approximate W_G/W_{H_2O}. Although W_{H_2O} has not been measured, it may be assumed to be about 26 ev, twice the ionizing energy for H_2O. It is not proper to estimate W_{tissue}, as frequently suggested, from the average energy required to produce ion pairs in a gas mixture with atomic constituents those of tissue, since the ionization potentials of large hydrocarbons are larger than those of the smaller molecules of the mixture.

Relative Effectiveness of Neutron and X-Irradiation of Tissue

In many biological studies it is not necessary to evaluate W_T, for frequently the relative ionizations produced in the medium by the two types of radiation are adequate. Ionization effects produced by x-rays are caused by recoiling electrons, the energy absorbed being proportional to the number of electrons per unit mass or volume of the substance and to the conversion coefficient of photon energy to kinetic energy of electrons. This coefficient is the sum of the respective coefficients for photoelectrons, Compton recoils, and electron pairs. Using primed letters to represent x-ray effects we have

$$I'_{T(e)}=I'_{A(e),G}\frac{Q'_{T(e)}W'_{G(e)}S'_A}{Q'_{A(e)}W'_{T(e)}S_G'}$$

or

$$I'_{T(e)}=I'_{A(e),G}\frac{Z_TN_Tk_{e,T}W'_{G(e)}}{Z_GN_Gk_{e,A}W'_{T(e)}} \tag{20}$$

since

$$\frac{Q'_{T(e)}}{Q'_{A(e)}}=\frac{Z_TN_T}{Z_AN_A}\frac{k_{e,T}}{k_{e,A}};\quad\text{and}\quad\frac{S_A'}{S_G}=\frac{Z_AN_A}{Z_GN_G}.$$

where Z is the number of electrons per molecule, N is the number of molecules per gram, and k_e is the fraction of photon energy converted per electron to kinetic energy of secondary electrons. Consequently, the energy absorbed per gram of tissue is

$$Q'_{T(e)\text{per gram}}=W'_{T(e)}I'_{T(e),T\text{per gram}}$$

$$=k_zW'_{G(e)}I'_{A(e),G\text{per gram}} \tag{21}$$

where

$$k_z=\frac{Z_TM_Gk_{e,T}}{Z_GM_Tk_{e,A}}. \tag{22}$$

Values of the conversion coefficients (k_e) at various x-ray energies have been calculated by Mayneord[27] for tissue, air, nitrogen, and oxygen. These are nearly the same for the gases and practically the same for tissue. Even for soft radiations the tissue value is hardly 10 percent less than that for air. Hence the energy absorption per gram in tissue must be nearly that in these gases and the value of k_z is very close to unity.

Finally, the ratios of the energies absorbed and of the resulting ionizations produced by x-rays

[27] W. V. Mayneord, Brit. J. Radiol. 8, 235 (1940).

and neutron beams is given by

$$\frac{Q'_{T(e)}}{Q_{T(p)}}=\frac{I'_{T(e),T}}{I_{T(p),T}}=\frac{k_x}{k_n}\frac{I'_{A(e),G}}{I_{A(p),G}}=K\cdot r/n \quad (23)$$

where $K=k_x/k_n$, and r and n are the exposures of the x-ray and neutron beams measured in roentgens and n units, respectively. This equation holds for measurements made per unit volume or per unit gram of the materials. Since k_x is approximately unity, K is the inverse of k_n, whose value was discussed in the preceding section.

If, after the relative ionizing energies of x-ray and neutron beams have been so determined, disproportionate biological actions occur, they must result from the strikingly opposite character of the ionic distribution resulting from the two agents, i.e., the widely spread and relatively weak ionization along the paths of the electrons scattered by x-rays, and the concentrated and dense ionizations along the paths of nuclei recoiling from neutrons. As reported by Aebersold and Lawrence, inequalities in biological sensitivities have been observed in most investigations, the relative sensitivities apparently resulting from the physiological condition of the irradiated material.

The authors gratefully express their appreciation of the interest and valuable assistance given them by members of the Radiation Laboratory, particularly Dr. K. McKenzie, and thank Professor E. O. Lawrence and the staff of the Laboratory for their cooperation in making available long periods of cyclotron time. The work was made possible by the generous support of the Rockefeller Foundation and the Josiah Macy, Jr. Foundation. One author was enabled to participate in the research through a fellowship awarded by the Finney-Howell Foundation, the other through a grant from the Trustees of Smith College.

PHYSICAL REVIEW VOLUME 69, NUMBERS 1 AND 2 JANUARY 1 AND 15, 1946

Activity of N^{16} and He^6

H. S. SOMMERS, JR.* AND R. SHERR*
Jefferson Physical Laboratory, Harvard University, Cambridge, Massachusetts

(Received August 28, 1945)

An interrupted flow method of handling short lived gases is described. By use of the method, pure N^{16} and pure He^6 are readily produced. Geiger counter measurements on the N^{16} give a period of 7.3±0.3 sec. Presence of gamma-rays having energy greater than 5 Mev is demonstrated with a cloud chamber and absorption measurements. A lower limit to the end point of the N^{16} spectrum is derived from absorption curves, and an upper limit fixed by excitation measurements. By taking into account the barrier of N^{16} against emission of a proton, and excluding the electron self-energy, the maximum electron energy of the decay may be set at 10±0.5 Mev. The electron absorption curves show the beta-spectrum to be complex with a softer component having an end point at approximately 4 Mev corresponding to decay to an excited state of O^{16} in the region of 6 Mev. The He^6 period found is 0.85±0.05 sec., and its end point 3.5±0.6 Mev, in agreement with Bjerge and Bröstrum.

Part I. N^{16}

A. INTRODUCTION

N^{16} WAS reported in 1934 by Fermi[1] and his co-workers and also by Livingston, Henderson, and Lawrence.[2] Both groups found a negative electron emitter with lifetime of nine or ten seconds formed by the bombardment of fluorine with neutrons, and both assigned it to the reaction $F^{19}(n|\alpha)N^{16}$. In 1936 Fowler, Del-

* Now at the Radiation Laboratory, Massachusetts Institute Institute of Technology, Cambridge, Massachusetts. This work was completed in 1942.

[1] Fermi, Amaldi, d'Agnostino, Rasetti, and Segrè, Proc. Roy. Soc. A146, 483 (1934).

[2] Livingston, Henderson, and Lawrence, Phys. Rev. 46, 325 (1934).

sasso, and Lauritsen[3] produced the same activity by bombarding nitrogen with deuterons, assigning it to $N^{15}(D|P)N^{16}$. From 110 cloud-chamber tracks consisting mainly of positrons from Na^{24} mixed up with a few electrons from N^{16}, they concluded the nitrogen spectrum extended to 6 Mev. Concurrently, two other measurements on this same activity were published. Nahmias and Walen[4] reported both $F^{19}(n|\alpha)N^{16}$ and $F^{19}(n|P)O^{19}$ and showed that the former reaction proceeded with slower neutrons than did the latter, in agreement with the existing assignments. Their nitrogen period was 8.4 ± 0.1 sec. Naidu and Siday[5] produced the nitrogen activity by neutrons on fluorine and obtained a cloud-chamber histogram of some 250 tracks. The inspection end point was 6.5–7.0 Mev; a high energy tail extending to between 10 and 13 Mev they attributed to systematic errors in curvatures which result because the magnetic field was only 1000 gauss.

In 1937 Chang, Goldhaber, and Sagane[6] discovered the reaction $O^{16}(n|P)N^{16}$ (period 8 sec.). They found a good yield with neutrons from 450-kev deuterons on lithium, a detectable amount from the deuterons on boron, but nothing from the deuterons on beryllium, showing fast neutrons were required for the reaction. No positive chemical identification of N^{16} has been made because of its short lifetime,[7] but the various reactions producing an inert gas make the assignment seem unquestionable.

Livingston and Bethe[8] give the mass of N^{16} as 16.011 mass units with an uncertainty of ±0.002. This value apparently comes from the work of Harkins, Gans, and Newson[9] who, with a cloud chamber, measured thirteen recoil pairs which they attributed to the reaction $F^{19}(n|\alpha)N^{16}$. Q's computed from each pair ranged from $+0.7$ to -10.3 Mev, with most of the tracks yielding values between -2 and -5 Mev. Choosing only the latter group of tracks, one gets the mass of N^{16} listed by Livingston and Bethe. This mass indicates that the energy of the transition $N^{16}-O^{16}$ should be 10.2 Mev, while direct measurements have given a value of approximately 6 Mev for the disintegration electrons, with no gamma-ray reported. Since one of us (H.S.S.) was interested in studying the shape of beta-ray disintegration curves with a cloud chamber, it was considered advisable to resolve this 4-Mev discrepancy.

B. TREATMENT OF SAMPLE

(1) Gas System

Because of the difficulty of performing chemical separations before the disappearance of the activity, it seemed best to handle the radioactive nitrogen in the gaseous form, in order to achieve an immediate quantitative separation from all solid impurities. This also permitted ready transportation of the sample to a considerable distance from the cyclotron. The conventional continuous-flow method of transporting the gas proved rather unsatisfactory because of the difficulty of determining just what the cyclotron was doing when the gas sample at the measuring end of the line was bombarded. As all the measurements were made in the control room 120 feet from the cyclotron, the beam had to be interrupted during the measurements to remove the γ-ray background. Under such conditions of short bombardment, the ion current was usually quite unsteady. This fact, coupled with the inconvenience of measuring flow velocities and the large amounts of carrier gas wasted, made some other system desirable.

Following a suggestion of Dr. E. M. Purcell, a discontinuous flow method was used. In this scheme, the target is bombarded in a closed container filled with a quiescent gas at any desired pressure. At the end of the bombardment, a valve is opened permitting the gas to escape down an evacuated flow line to the receiving chamber at the other end; here it is confined by another valve, compressed to the pressure desired, and the measurements taken. To complete the cycle, the receiving chamber and line are evacuated and the target container refilled with the carrier gas. To permit remote

[3] Fowler, Delsasso, and Lauritsen, Phys. Rev. **49**, 561 (1936).
[4] Nahmias and Walen, Comptes rendus **203**, 71 (1936).
[5] Naidu and Siday, Proc. Phys. Soc. **48**, 332 (1936).
[6] Chang, Goldhaber, and Sagane, Nature **139**, 962 (1937).
[7] See, however, Polessitsky, Physik. Zeits. Sowjetunion **12**, 339 (1937), for attempts at identification by elimination.
[8] S. M. Livingston and H. A. Bethe, Rev. Mod. Phys. **9**, 373 (1937). See also the computed value of 16.0114 by W. H. Barkas, Phys. Rev. **55**, 696 (1939).
[9] Harkins, Gans, and Newson, Phys. Rev. **47**, 52 (1935).

control, the valves were made in the form of solenoid-operated hose pinchers. The compressor was a flattened spheroid with a port on each end and a rubber disaphragm stretched diametrically across the center; the pressure of the carrier gas in the one cell thus was determined by the air pressure applied to the other cell.

A target chamber of 20 cu. in. volume containing hydrogen at 25 lb. per sq. in. gauge pressure, a $\frac{1}{16}$ inch I.D. flow line 120 feet long, and a receiving chamber with a volume of 10 cu. in. were used. Gas at a pressure of one atmosphere could be trapped in the receiver $2\frac{1}{2}$ seconds after the end of the bombardment. With a carrier of nitrogen or oxygen instead of hydrogen, 8 to 10 seconds were required to fill the receiver.

(2) Choice of Target

Direct bombardment of nitrogen with deuterons was not feasible because of the overwhelming quantities of O^{15} produced. In fact, bombarding ordinary tank helium with deuterons produced large amounts of O^{15}, N^{13}, and traces of longer-lived gases. Because of this, we used neutron bombardments. Neutrons directly on oxygen gave a moderate activity; however, because of some of the measurements contemplated, a solid target and hydrogen as a carrier were preferred. $Be(OH)_2$ prepared in high emanating form proved very satisfactory.[10]

The $Be(OH)_2$ was precipitated from an ammoniacal solution of $Be(OH)_2$ and repeatedly washed and centrifuged until the ammonium hydroxide content became so small that the precipitate started to go back into solution. It was then spread out into a layer on a sheet of glass, cut into small pieces, and air dried. Finally, each piece was blown clean of any fine particles which might clog the flow line and inserted into the bombardment chamber. About one hundred grams of the compound filled the chamber, volume 350 cc. The material was of such an ashy nature that it seemed expedient to insert a cotton plug in the flow line. With these precautions, no trouble was encountered with clogging of the line.

This target gave copious yields of both N^{16} and He^6 when bombarded with fast neutrons from deuterons on beryllium. With hydrogen gas as the carrier, we had no trouble from other activities; any impurities which may have been produced were of such long life as to be indistinguishable from the control room background. This is in contrast to our experience when silica gel was substituted for the $Be(OH)_2$; the yield of N^{16} dropped to about 10 percent mixed up with an equal activity of a forty-second period.

C. PERIOD

For period and absorption measurements, an alcohol-filled Geiger counter and scale of thirty-two circuit were used. The counter was made of a 5-mil brass cylinder, $\frac{3}{4}$ inch by 3 inches long, waxed into glass ends and filled with argon and alcohol. Thresholds ranged from twelve to fifteen hundred volts, and plateaus were about one hundred volts wide. The scaling circuit was of the type described by Stevenson and Getting,[11] using four tubes per stage. The data were recorded by photographing a Cenco recorder and stop watch with a Ciné Kodak Special. Exposures were about one-fortieth of a second, at eight frames per second. By running the camera in bursts, we could catch the instant at which the Cenco counter moved to within a twentieth of a second, the smallest interval of the stop watch, thus making interpolation in the scaling circuit unnecessary.

To get pure N^{16} the target was bombarded to saturation in a gas whose pressure was adjusted to give an eight-second delivery time. (For optimum concentration, the delivery time should be one half-life.) Measurements were started ten seconds after the cyclotron dee voltage was cut off and continued for two to five minutes, sufficiently long to determine the background.

The usual method of presenting the decay curve by plotting the rate against the time leads to difficulties on short-lived samples. To make all points have the same statistical accuracy, one would like to include the same number of counts in each point, but this very soon makes the counting interval comparable with, or longer than, the half-life, and one cannot assign the

[10] We wish to thank Dr. E. Segrè for some helpful suggestions concerning the method and Dr. H. H. Anderson for assistance in the actual preparation of the $Be(OH)_2$.

[11] E. C. Stevenson and I. A. Getting, Rev. Sci. Inst. **8**, 414 (1937).

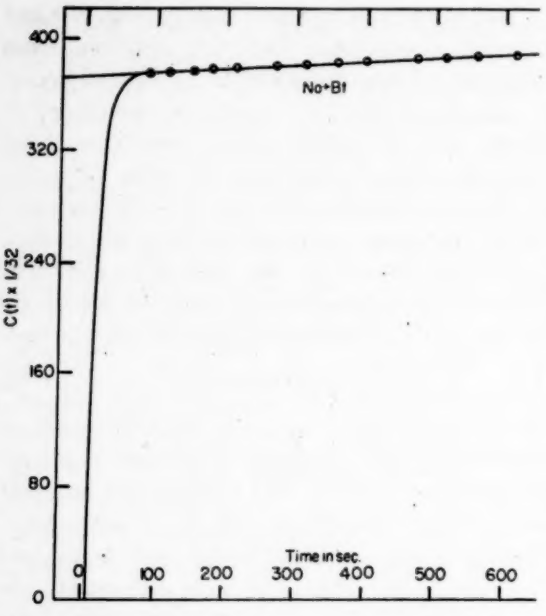

FIG. 1. $C(t)=N_0(1-e^{-\lambda t})+Bt$. Activity of N^{16}.

rate so measured to the midpoint of the interval. Since the camera essentially integrates the decay, it seemed expedient to plot the integrated form of the curve instead of the rate. Thus if $C(t)$ is the counter reading, then:

$$C(t)=N_0(1-e^{-\lambda t})+Bt,$$

where the first term on the right is the true activity and the second the background contribution. A direct plot of $C(t)$ against t gives N_0 and B from the asymptote intercept and slope, and a semi-logarithmic plot of the difference between the asymptote and $C(t)$ against t gives the half-life in the usual manner. Thus the half-life comes from a plot of $N=N_0(e^{-\lambda t})$ instead of from $A=A_0(e^{-\lambda t})$; the advantage is that we get our data from measuring $N(t)$ up to the instant t, which our camera records directly, instead of approximating $A(t)$ (the activity) by its average value over the interval. The precision of either method is of course limited by statistical fluctuations and background uncertainty.[12]

Figure 1 is a sample plot of $C(t)$ against t and shows how constant the background is a short distance (100 feet) from the cyclotron. Figure 2 is the decay curve, which is linear all the way from the initial rate of over 1100 counts per second. Of course, it is fortuitous that the last point lies on the curve, for a slight shift in the estimated asymptote of Fig. 1 will shift this point either up or down, as the rate at the tail is only five counts per second, or twice background.

The question as to the linearity of the counter over such a wide range is a serious one. To check this, we measured several decay curves of N^{16} and, with the same counter, one for Cl^{38}. The Cl^{38} was produced by bombarding NaCl with neutrons from 10.3-Mev deuterons on Be, taken at right angles to the beam, and was separated by precipitation with Ag and repeated washings. The Cl^{38} decay was linear from the starting rate of 160 counts per second, and gave the accepted period of 37 minutes.[13] The background of ten counts per second showed a 15-hour period and was assumed to be Na^{24}. The N^{16} curves agreed with many others we had measured, some with initial activities sufficiently high to block the recorder. Twelve pertinent runs were averaged, and these yielded a period for the N^{16} of 7.3 ± 0.3 sec.

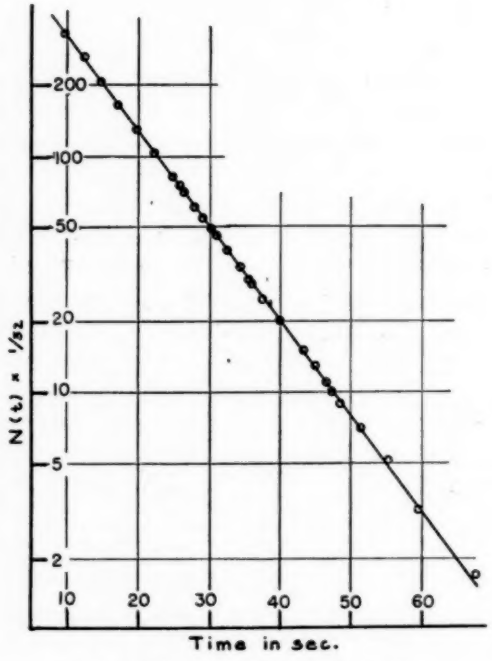

FIG. 2. Decay of N^{16}. $T_{\frac{1}{2}}=7.5$ sec.

[12] We wish to thank Professor S. Goudsmit for bringing this method of presenting the data to our attention.

[13] G. T. Seaborg, Chem. Rev. 27, 199 (1940).

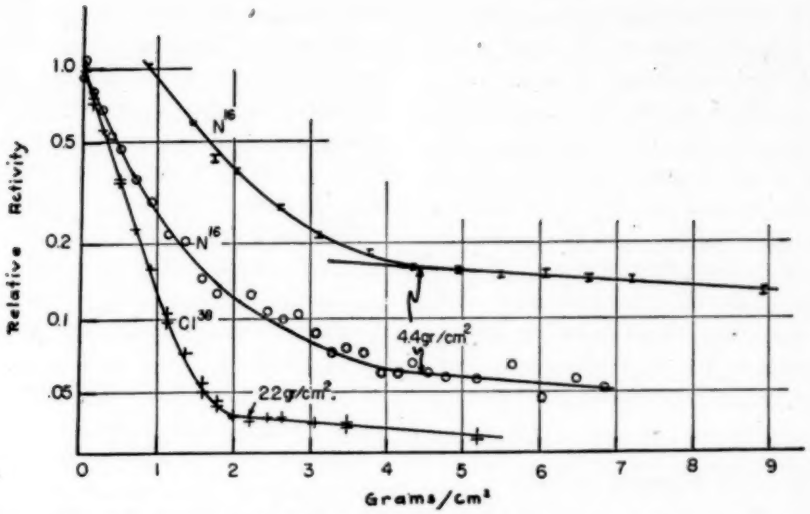

FIG. 3. Absorbtion curves. III N^{16}-cylindrical brass absorbers; ○○○ N^{16} sheet aluminum absorbers; +++ Cl^{38} sheet aluminum absorbers.

D. GAMMA-RAYS

It was possible to explain the discrepancy between the $N^{16}-O^{16}$ disintegration energy computed from mass values and that from beta-decay measurements by the presence of a hitherto unobserved gamma-ray.

The existence of gamma-rays from N^{16} was demonstrated by the presence of tracks inside a cloud chamber with the sample outside the $\frac{1}{4}$-inch glass walls. Insertion of a quarter inch of copper between the gas and the chamber failed to stop the tracks, showing conclusively they were not from high energy primary electrons. A histogram of the recoils from the chamber wall was made by using the field from a Helmholtz coil of $18\frac{3}{4}$-inch mean diameter, radial depth of $4\frac{1}{2}$ inches, axial depth $4\frac{1}{4}$ inches, and coil separation $9\frac{3}{8}$ inches. Calibration of the central field by Dr. G. E. Valley, using a conversion line from zinc in his beta-ray spectrograph, checked with the calculated field strength. Measurements on 125 N^{16} tracks gave a roughly uniform distribution which converged toward an upper energy limit of around 5 to 6 Mev.

A rough statistical analysis of the number of tracks in successive expansions at intervals of twenty seconds indicated the activity had the period expected. Attempts to get recoil pairs from a thin lead sheet inside the cloud chamber proved futile because of the weak intensity of the source; even with the thick chamber wall for the target, only two or three acceptable tracks per expansion were photographed.

The absorption coefficient of the gamma-rays in lead was measured. (See next section for description of the method.) By assuming monochromatic gamma-rays, the value of the coefficient obtained by measuring over a single half-thickness was 0.5/cm Pb. Since this is in the region of the absorption minimum for Pb, the gamma-ray may lie in the range between 2 and 7 Mev. No better measurements than this could be expected because the great thickness of absorbers required greatly reduced the intensity. With cyclotron beams of over 100 μamp., only 80 to 100 counts per bombardment were obtained through the thickest absorbers.

Additional evidence for the existence of a hard gamma-ray is obtained from the complete absorption curve in aluminum, Fig. 3. The gamma-ray intensity is about 7 percent of the total activity at zero absorber. Although there was no simple way of calculating the efficiency of the counter for 6-Mev gamma-rays, the observed intensity could reasonably be attributed to a single hard gamma-ray of this energy.

As another check on the gamma-ray energy, beta-beta coincidence measurements were taken on the gamma-recoil electrons. Various thicknesses of absorbers were inserted between the two coincidence counters to determine the range of these recoil electrons, but the high energy of

the disintegration electron spectrum made our results far less precise than those reported in other cases.[14] It was necessary to interpose a thick absorber in front of the first counter to cut off the primary electrons because their spectrum extended far beyond the gamma-ray energy; hence the source of the gamma-recoil electrons was a thick target and the otherwise sharp coincidence cut-off at maximum electron range was badly smeared. Measurements with five different absorbers, averaging around a dozen bombardments for each absorber, again showed the presence of gamma-rays of greater than 4 Mev.

E. ABSORPTION MEASUREMENTS

An absorption curve of the radiation emitted by N^{16} was taken by using a gas cell, with active volume of $1\times1\frac{1}{4}\times1\frac{1}{4}$ inches and $1\frac{1}{2}$-mil Al windows in front and in back, placed near the counter. A space was left for $1\frac{1}{4}$ inches of absorbers between cell and counter. The whole unit was surrounded by a 2-inch thick lead cylinder 6 inches in diameter. Each reading required a separate bombardment.[15] To provide adequate monitoring, the number of electrons passed through the absorber during the interval from ten to twenty-five seconds after bombardment was compared with the counts recorded during the interval from thirty to forty-five seconds with the absorber removed. Photographic recording again afforded precise reading. Figure 3 shows the curve obtained with sheet Al absorbers; the number of counts obtained during the absorption interval ranged from 2000, with no absorber, to 200 with the thickest, including the background of about fifteen counts as determined from decay curves. The gamma-ray absorption coefficient was measured at the same time.

Because of the surprisingly high activity of the tail, still 5 percent of the total activity after passing through 5 g/cm² of Al, we made a comparison run with Cl^{38}, approximating the same geometry by placing cotton wool soaked in neutron-activated chloroform inside the gas chamber for the source. The Cl^{38} end point agrees well with that reported by Watase and Itoh[16] of 2.3–2.4 g/cm² of Al. Their beta-ray spectrograph measurement gave an upper limit of 5.0 Mev for the chlorine electrons; the nitrogen electron energy must far exceed this. The Cl^{38} comparison run is shown on the same graph with the N^{16}. A third series of measurements made with cylindrical brass absorbers is also included on this graph. These last measurements were made by using a cylindrical shell gas chamber, 2-inches I.D. with $\frac{3}{8}$-inch wall spacing, and a set of telescoping brass absorbers to insert between the inner wall of the gas cell and the outside of the counter. The minimum absorber possible thus was 10 mils of brass for the chamber wall plus 5 mils for the counter; nevertheless the intensity was greatly increased. The curve for cylindrical absorbers gives the best indication of the end point; the lower limit to the spectrum end point is 4.4 g/cm², or 9.6 Mev, from the relation from Curran, Dee, and Petrzilka:[17]

$$E=2.19R,$$

where R is the range in g/cm².

A comparison of the N^{16} absorption curve taken with the Al absorbers against the similarly made Cl^{38} curve suggests that the N^{16} spectrum is complex. If one passes a straight line through the points on this N^{16} curve in the region from 2 to 4 g/cm² and subtracts the extrapolation of this line from the plotted points, he can get a very crude estimate of the intensity of the lower energy N^{16} spectrum. A reasonable estimate of the energy of the softer component obtained in this way is 3.5 Mev, and its abundance seems to be about three times that of the harder component.

F. EXCITATION THRESHOLD

As a further check on the disintegration energy, we tried to determine the threshold for the reaction $O^{16}(n|P)N^{16}$. The mass difference

[14] See for example Curran, Dee, and Strothers, Proc. Roy. Soc. **174**, 546 (1940).

[15] It should be born in mind that the best statistical accuracy feasible when taking measurements on short lived samples is necessarily poor. For a given initial activity the total number of disintegration electrons which are recorded decreases proportionately with the decrease in half-life.

[16] Watase and Itoh, Proc. Phys. Math. Soc. Jap. **22**, 626 (1940).

[17] Curran, Dee, and Petrzilka, Proc. Roy. Soc. **169**, 286 (1938).

TABLE I. Yields for various neutron energies.

	Minimum angle	Rate 9 sec. after bombardment He^6	Rate 9 sec. after bombardment N^{16}	$\frac{He^6}{N^{16}}$	E_n	N^{16} corrected to saturation at 50μ amp.
		(A) Neutrons from D on Be				
1.	90°	185/sec.	8.9/sec.	21	11.6 Mev	11/sec.
2.	90°	150	5.9	25	11.6	7.0
3.	90°	150	7.4	20	11.6	9.3
4.	90°	230	15	15	11.6	16
5.	90°	260	12	22	11.6	11
						Average = 11±0.8
6.	70°	130	24	5.4	12.5	40
7.	70°	150	26	5.8	12.5	34
8.	70°	215	26	8.1	12.5	30
						Average = 35± 2
		(B) Neutrons from D on brass				
1.	90°	29	5.0	5.8	?	7.6
2.	90°	49	5.2	9.4	?	5.2
						Average = 6.4± 1
3.	70°	17	11	1.5	?	11

$N^{16}-O^{16}$ is given by

$$N^{16}-O^{16}=E_n'+(n-P),$$

where E_n' is the minimum neutron energy (in C. of G. coordinates) which will produce the reaction. Since $n-P$ is 0.78 Mev and $E_n'=(16/17)E_n$, the mass difference becomes

$$N^{16}—O^{16}=\frac{16}{17}E_n+0.78 \text{ Mev},$$

where E_n is the neutron energy in laboratory coordinates.

We used neutrons given off from the beryllium target at various angles to the incident deuteron beam and secured an energy range from 14.7 Mev for straight ahead neutrons to 11.6 Mev for neutrons at right angles. As a monitor we took the activity of the He^6 produced in the same bombardment, for since its Q value is about 0.4 Mev,[18] its yield is roughly independent of the neutron energy over the narrow range of energies employed here. Hence its strength gives some indication of the neutron intensity.

Our target was the usual cylinder of $Be(OH)_2$, 3 inches in diameter by 3 inches long, placed as near the beryllium plate serving as the neutron source as was consistent with keeping a constant distance for all the desired angles. The target was bombarded for 30 seconds at a uniform beam and a decay curve taken starting seven seconds after the cyclotron was cut off. Analysis gave the N^{16} and He^6 decay curves. Table I (*A*) gives the results for neutron energies in the neighborhood of the threshold. The first column is the minimum angle between the deuteron beam and the beryllium target, the second and third columns the helium and nitrogen activities, respectively, nine seconds after bombardment. (Their periods were taken as 0.9 and 7.5 seconds for this work.) The fourth column gives the ratio He^6/N^{16}, likewise nine seconds after bombardment; the fifth column the maximum energy of any neutron which could hit any part of the $Be(OH)_2$; and the last column is the nitrogen yield corrected to saturation bombardment with a beam of 50μ amp of deuterons.

Table I (*B*) gives the same information for some runs made with a brass plate for the source of neutrons instead of the beryllium to check whether the neutrons responsible for the N^{16} really came from the beryllium plate. These data show that at a minimum angle of 90° a large part of the N^{16} may have come from stray neutrons, for here the Be source gave an average yield of 11 counts/second against an average with the brass of 6.4/sec. At a minimum angle of 70°, however, there is a big contribution from the beryllium, for here the latter gives an N^{16} activity of 35/sec. against 11/sec. for the brass. A further comparison of the bombardments at 90° shows that the neutrons from the brass, though less intense, have a slightly higher maximum energy than those from the beryllium since the N^{16}/He^6 ratio is three times as large for the brass as for the beryllium.

These excitation measurements show N^{16} was produced by neutrons emitted at an angle of at least 70° with the deuterons incident on the beryllium target. Since the deuterons had a range in air of 72 cm, including the Al foil, their energy was 10.3 Mev, and taking the Q value for the reaction $Be^9(D|n)B^{10}$ to be 4.2 Mev,[19] the neutrons producing the N^{16} had an energy less

[18] Bjerge and Bröstrum, Kgl. Danske Vid. Sels. Math.-Fys. Medd. 16, No. 8 (1938).

[19] S. M. Livingston and H. A. Bethe, Rev. Mod. Phys. 9, 332 (1937).

than 12.6 Mev. This neutron energy gives a value $\leqslant$12.6 Mev for the mass difference $N^{16}-O^{16}$. If one takes into account the potential barrier of N^{16} for the emitted proton, this mass difference is lowered since at low proton energies the small probability of penetrating the barrier would greatly reduce the N^{16} yield even though the neutron energies were somewhat above the reaction threshold. The potential barrier of N^{16} for protons is given by

$$E=Ze^2/r_0A^{\frac{1}{3}}.$$

Taking $Z=7$, $A=16$, and $r_0=1.35\times10^{-13}$ cm, one finds $E=3.0$ Mev. This consideration would place the value of $N^{16}-O^{16}$ in the neighborhood of 10 Mev.

G. DISCUSSION

The absorption curve of the N^{16} disintegration electrons indicates a lower limit of 9.6 Mev for the maximum beta-ray energy. The excitation data give an upper limit of 12.6 Mev. Consideration of the potential barrier for the $n-P$ reaction suggests that this upper limit is probably too high by several Mev. We can conclude that $E_0=10\pm0.5$ Mev, in agreement with the value of 10.2 given by Livingston and Bethe and that a direct transition from N^{16} to the ground state of O^{16} occurs in about 25 percent of the disintegrations.

Our gamma-ray measurements showed the presence of photons with energies greater than 5 Mev coming from excited O^{16} nuclei. Studies of the reaction $F^{19}(H|\alpha)O^{16}$,[20] which also leads to excited states of O^{16}, have given sufficient information about the oxygen nucleus to permit us to make rather plausible postulates about our gamma-rays. There is an O^{16} level at 6.0 Mev which decays by pair emission[21] and another at 6.2 Mev which emits all its energy in a single photon. No lower levels are known, and their existence seems highly doubtful because of the great stability of the O^{16} ground state. We can reasonably assume our gamma-radiation consisted mainly, if not completely, of the known 6.2-Mev quanta.

A gamma-ray of this energy implies the beta-spectrum is complex, being composed of a spectrum with a maximum energy of 10 Mev corresponding to a direct transition to the ground state of O^{16} and another with a 4-Mev end point. Such an energy level scheme was suggested above in the interpretation of the absorption curve. The lower energy spectrum seems to be the more abundant, perhaps accounting for three-fourths of the transitions. Then the 7.2-sec. N^{16} decay is composed of a 4-Mev spectrum, period 10 sec., and a 10-Mev spectrum, period 30 sec., with a relative abundance of 3/1. If one takes He^6, 0.85 sec., $E_0=3.7$ Mev, as an example of an allowed transition inside a supermultiplet, then the 10-sec. decay should be an allowed transition with change of supermultiplet for it has roughly the same energy as the helium but is 1/12 as fast. The high-energy group is then strongly forbidden, for it is 1/35 as fast as the He^6 while its energy is 2.7 times as great.

Incomplete as our data are, it is interesting to speculate on what conclusions the data permit about the states of the nuclear levels. The ground state of O^{16} is known to have zero spin and even parity. N^{16} probably has a high spin, then, for the strong selection rule against the direct transition from it to the ground state of O^{16} seems to imply a large change of angular momentum. A large spin for N^{16} is also consistent with the non-appearance of transitions from it to the pair-emitting level of O^{16}. This conclusion of high spin for N^{16} also implies a non-zero spin for the gamma-emitting level of O^{16}, for otherwise the transition between the two could not be the non-forbidden one observed.

The direct transition from N^{16} to the ground state of O^{16} seems to belong to the second of the forbidden types considered by Critchfield and Wigner,[22] the group comprised of transitions in which the finite size of the nucleus is important. Assigning the transition to this group may seem paradoxical in view of the lightness of the nucleus involved, but the shortness of the wavelengths of these extremely energetic emitted

[20] See Streib, Fowler, and Lauritsen, Phys. Rev. 59, 253 (1941), for a summary and discussion of the radiations from the fluorine reactions.

[21] We tried to find positrons by passing the electrons through a magnetic field, but found that less than one-fourth of the electrons could be positive; the cloud-chamber work of Nahmias and Walen showed actually far fewer positrons than this were emitted, but could not rule out their presence.

[22] C. L. Critchfield and E. P. Wigner, Phys. Rev. 60, 412 (1941).

particles far more than compensates for the small size of the nucleus. The interesting aspect of this group, from an experimental point of view, is that the Kurie plots should be concave toward the axis at the end corresponding to high electron energies. Although the total spectrum of N^{16} is double, measurement of the Kurie plot for the transition to the ground state of O^{16} should be possible because of the great difference of energies of the two spectra. Such a measurement should give telling evidence regarding the theory of Critchfield and Wigner.

Further work along this line has been postponed.

Part II. He^6

A. INTRODUCTION

In 1936, Bjerge,[23] and later Bjerge and Bröstrum,[18,24] reported a short-lived gas emitting negative electrons formed by the bombardment of beryllium hydroxide with neutrons. The period, found by flowing the gas in a carrier past the recorder and measuring the activity as a function of flow rate, was 0.8 ± 0.1 sec.; a cloud-chamber histogram gave the upper limit of the spectrum as 3.7 ± 0.5 Mev. They assigned the activity to He^6 as the only gas with this disintegration energy which could be so formed. Several other workers[25] have reported the same activity from neutrons on beryllium, but no attempt has been made to improve the precision of these measurements.

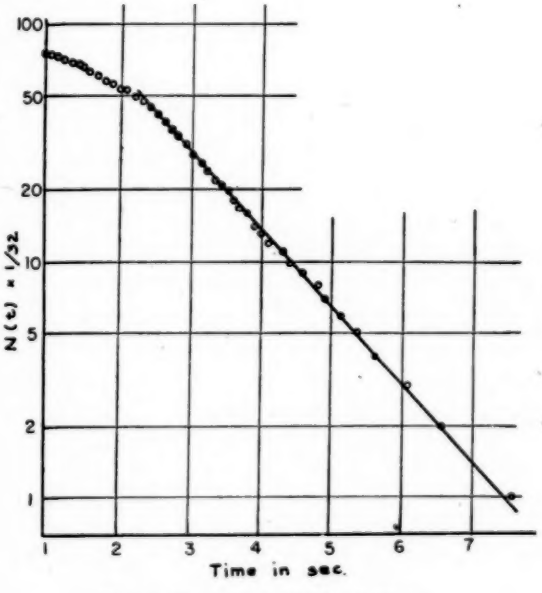

FIG. 4. Decay of He^6. $T_{\frac{1}{2}}=0.90$ sec.

[23] T. Bjerge, Nature 137, 865 (1936).
[24] T. Bjerge and K. J. Bröstrom, Nature 139, 400 (1936).
[25] G. T. Seaborg, reference 11, for complete bibliography.

He^6 is of considerable theoretical interest.[26] It is a member of the group of nuclei containing $4n+2$ primary particles, whose decay rates are so anomalous. Two transitions in this group, He^6-Li^6 and $C^{10}-B^{10}$, are allowed and exceedingly rapid, while the transitions $Be^{10}-B^{10}$ and $C^{14}-N^{14}$ are highly forbidden, contrary to theoretical expectations. Moreover, the He^6-Li^6 transition itself is more allowed than any other known transition and seems almost to lie in a group by itself.

B. PERIOD

Our methods of producing, transporting, and measuring the He^6 activity were the same as those already described in the sections on N^{16}. The pressure of the carrier gas in the target chamber was 25 lb./in.^{2}, and counting was started two seconds after bombardment, the minimum time possible with the rather slow acting valves and compressor in the gas line. The period was measured with the Geiger counter calibrated against the Cl^{38} decay. No subtraction was necessary to eliminate the N^{16} activity since the beryllium neutrons at right angles to the deuteron beam were used. These were too slow to produce N^{16}. Checks to determine that the activity came from the beryllium were substitution of a target of silica gel for the $Be(OH)_2$ (this gave no gas of period shorter than N^{16}) and direct bombardment of beryllium with deuterons, which gave a weak gaseous activity of roughly one second period.

Another check on the identification was to filter the activated carrier gas through a Jena 3G3 sintered glass filter; this showed conclusively

[26] J. R. Oppenheimer, Phys. Rev. 59, 908L, (1941). See reference 22 for a list of theoretical calculations on β-transitions in light nuclei.

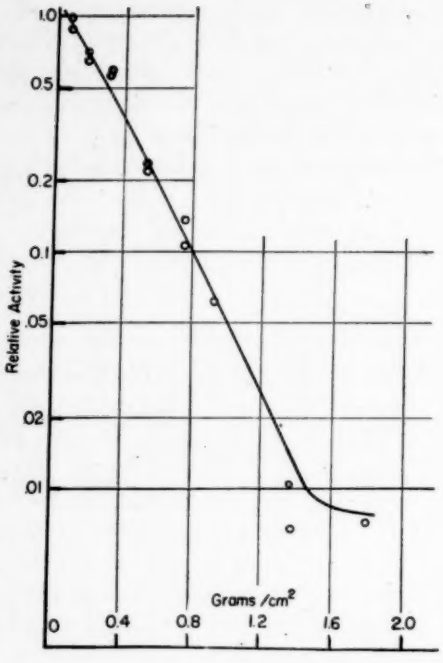

FIG. 5. He^6 absorbtion in aluminum.

the activity was not carried by fine particles of $Be(OH)_2$ dust, for the filter spacings of 20–30 microns passed the activity undiminished.

Figure 4 is a typical decay curve of pure He^6, again recorded photographically. The initial part of the curve, up to 2 sec., shows the build up as the gas flows over; the section from 2–2½ sec. shows the blocking of the counter when the gas is compressed; and the rest of the curve illustrates the rapid recovery of the counter and the purity of the decay. This curve was taken with the scale of 32 circuit. The statistics are actually worse than the graph would lead one to expect. Though the initial rate is high, 750 counts/sec. at 3 sec., the total number of counts recorded over the whole decay time from then on is only about $31 \times 32 = 1000$, as shown by the ordinate. Because of this difficulty, various decay curves differ amongst each other; our period, taken from an average of sixteen runs, is 0.85 ± 0.05 sec.

C. ABSORPTION

We ran an absorption curve on He^6 (Fig. 5) using the flat aluminum absorbers and the same geometry described in the work on nitrogen. The counts recorded in the interval from 2.2–4.0 sec. after bombardment with absorber interposed were compared with those from 4.5–6.0 sec. with no absorber. Again the neutron energy was too low to produce any N^{16} impurity. The estimated end point is 1.6 g/cm², giving a maximum energy of 3.5 ± 0.6 Mev. Because of insufficient data for this absorption curve, the existence of a gamma-ray cannot definitely be excluded. Judging by the concavity toward the axis of the absorption curve and the small intensity for the next to the last points, one would guess there are no gamma-rays. The high point at 1.8 g/cm², which might suggest a gamma-ray, is rather uncertain.

D. CONCLUSIONS

Our results are in substantial agreement with those of Bjerge and Bröstrum. A short lived gas emitting negative electrons is formed by medium energy neutrons on beryllium. Its period is 0.85 ± 0.05 sec., and its maximum energy found by absorption is 3.5 ± 0.6 Mev.

It is a pleasure to thank Professor K. T. Bainbridge for starting us on this work, and Dr. C. L. Critchfield for many valuable discussions. The extensive cooperation of Dr. Curtis, Mr. Bender, and Mr. Harpell of the Harvard Cyclotron Staff made this work possible. The Milton Fund gave generous grants for the construction of the cloud chamber, magnet, and Geiger counter circuits, and the W.P.A. furnished assistance in reducing the data.

Errata: General Theory of Pressure Broadening of Spectral Lines

ALEXANDER JABŁOŃSKI
Department of Physics, Polish School of Medicine, Edinburgh, Scotland

[Phys. Rev. 68, 78 (1945)]

THE following corrections should be made in the above-named paper which was published in the August issue of this journal.

1. Page 81, line 9 from bottom, instead of: "As shown by Kuhn,[19] Minkowski,[20] and Rühmkorf[21] . . . " should be: "As shown by Kuhn, Minkowski, and Rühmkorf[19] . . ."

2. In Eq. (32) replace in both integrals the lower limit of integration r_0 by r_t.

3. In Eq. (37) replace "$r=r_t$" by "$r=r_c$."

4. Page 90, line 14 the sentence: "Apart from l, α depends on $E_{v'}$ and $E_{v''}$" should be enclosed in parentheses.

5. Equation (42a) the expression in brackets should read $(1-v'(r_c)/E_{v'})^{\frac{1}{2}}$.

6. Equations (47), (48), and (49), the power of $[l(l+1)]$ should read $\frac{3}{5}$ instead of $\frac{3}{2}$. There should be no h^2 in the left side of inequality (48).

7. Page 92, line 1, should be " . . . Δl would become 23 for $l_t=100$. . . . "

8. Table I, first line, last column, replace 2.3 by 2.2.

9. Page 92, line 13 second column, should read " . . . Hg+A at 1000°K (large l's) it reaches 0.17. . . . "

10. Page 92, line 24 second column, instead of "therefore" should be "there."

11. Page 92, line 27 second column, replace "cos $(\alpha+\beta\xi)$" by "cos $(\alpha\pm\beta\xi^2)$."

The author is indebted to Miss A. V. Stuart and to Dr. Robin Schlapp for improving the language of his manuscript and to Professor P. Swings for reading the galley proofs. Most of the corrections of the errata are owing to the mistakes in the manuscript itself, and thus Professor P. Swings is not responsible for them.

Letters to the Editor

PROMPT publication of brief reports of important discoveries in physics may be secured by addressing them to this department. The closing date for this department is the third of the month. Because of the late closing date for the section no proof can be shown to authors. The Board of Editors does not hold itself responsible for the opinions expressed by the correspondents. Communications should not in general exceed 600 words in length.

Auger Transitions

FREDERICK R. HIRSH, JR.
University of Southern California, Los Angeles, California
December 13, 1945

IN 1944, J. N. Cooper published a survey[1] of Auger transitions and the resultant doubly-ionized states. Through some oversight[2] he omitted the transition $L_{\rm I}\rightarrow L_{\rm II}M_{\rm IV,V}$ which originates the $L\beta_1$ satellites in the x-ray spectrum. In all, he had some twenty-six transition groups. The final doubly-ionized state includes the same outer shell in each group, but not the same subshell. Including Cooper's omission, then, there should be twenty-seven transition groups. Of these, fifteen Auger transition groups obey the old x-ray selection rules: $\Delta j=\pm 1,\ 0$; $\Delta k=\pm 1$; Δn is arbitrary. Coster[3] looked for radiation from the transitions $L_{\rm I}\rightarrow L_{\rm II}$ and $L_{\rm I}\rightarrow L_{\rm III}$ which he noted were permitted by selection rules. He later observed extremely faint radiation,[4] i.e., these are "radiationless" transitions. The present writer[5] remarked in 1942, that "selection rules point out where the radiationless transitions are sure to occur." Of these fifteen permissible transitions in Cooper's survey,[1] four groups yield x-ray satellites, in two cases of which it is for two x-ray diagram lines (see Table I). The question properly arises as to the meaning of these circumstances: the selection rules point out and control the occurrence of significant Auger transitions. Of the permitted transitions, relatively few result in the proper initial double (or triple) ionization which gives rise to x-ray satellite groups. This in no way contradicts the Franck-Condon principle: ${}_1E_2\gtrsim h\nu_0$, where ${}_1E_2$ is the energy difference of the Auger transition, and $h\nu_0$ is the energy of ionization of the second (outer) shell in the Auger effect. Let $\nu_1=RZ^2(1/n_1^2)$ and $\nu_2=RZ^2(1/n_2^2)$, then ${}_1E_2=h(\nu_1-\nu_2)=hRZ^2(1/n_1^2-1/n_2^2)$; let $h\nu_0=hRZ^2(1/n_3^2)$. Then for the Auger effect: $(1/n_1^2-1/n_2^2)\gtrsim 1/n_3^2$.[6] This last equation may easily be verified, if one remembers that the initial state of the Auger effect is one of ionization. Inspection of quantum numbers reveals the last equation is verified *only* for the old azimuthal quantum number k. Substituting in the last equation, for $L\alpha_1$, $L\beta_2$ and $L\beta_1$, we have

$$1/(1)^2-1/(2)^2\gtrsim 1/(3)^2 \quad \text{or} \quad 1-\tfrac{1}{4}\gtrsim\tfrac{1}{9}.$$

For $M\alpha_1$ and $M\zeta_{1,2}$,

$$1/(2)^2-1/(3)^2\gtrsim 1/(3)^2.$$

However for $M\beta$,

$$1/(3)^2-1/(3)^2=0\neq 1/(3)^2,$$

there is no verification. Thus for five of the six satellite groups, the azimuthal quantum number, k, verifies the Franck-Condon principle somewhat roughly.

TABLE I.

Auger transition	X-ray satellite group	Parent line transition
$L_{\rm I}\rightarrow L_{\rm II}M_{\rm IV,V}$	$L\beta_1$	$L_{\rm II}M_{\rm IV}$
$\begin{cases}L_{\rm I}\rightarrow L_{\rm III}M_{\rm IV,V}\\ L_{\rm I}\rightarrow L_{\rm III}M_{\rm IV,V}\end{cases}$	$\begin{cases}L\alpha_1\\ L\beta_2\end{cases}$	$\begin{cases}L_{\rm III}M_{\rm V}\\ L_{\rm III}N_{\rm V}\end{cases}$
$M_{\rm III}\rightarrow M_{\rm IV}N_{\rm IV,V}$	$M\beta$	$M_{\rm IV}N_{\rm VI}$
$\begin{cases}M_{\rm III}\rightarrow M_{\rm V}N_{\rm IV,V}\\ M_{\rm III}\rightarrow M_{\rm V}N_{\rm IV,V}\end{cases}$	$\begin{cases}M\alpha_1\\ M\zeta_{1,2}\end{cases}$	$\begin{cases}M_{\rm V}N_{\rm VII}\\ M_{\rm V}N_{\rm II,III}\end{cases}$

[1] J. N. Cooper, Phys. Rev. **65**, 155 (1944).
[2] My oversight as well as his, for I saw the paper in manuscript.
[3] D. Coster, Phil. Mag. **43**, 1089 (1922).
[4] D. Coster and R. DeL. Kronig, Physica **2**, 13 (1935).
[5] F. R. Hirsh, Jr., Phys. Rev. **62**, 137 (1942).
[6] Since ${}_1E_2\gtrsim h\nu_0$, we may divide the close equality by hRZ^2, since for ${}_1E_2$, $Z\sim 50$ and for ν_0, $Z\sim 49.5$, the error in the approximation is 2 percent.

Meteoric Impact Ionization Observed on Radar Oscilloscopes

OLIVER PERRY FERRELL
Atlantic City, New Jersey
September 29, 1945

THE short duration scattering of radio signals about 40,000 kc/sec. has been observed for fifteen years.[1] During 1940–41 it was observed and recorded by the author in frequency-modulation broadcast wave propagation tests.[2] This scattering was subsequently attributed to reflection from high density "*D*" and "*E*" region clouds ionized by high velocity meteoric impact.[3] This has been the basis of further study in the radio effects and the ionization dissipation of meteors. Of this, six objectives have been defined;

a. Determination of the virtual heights of the reflecting boundaries,
b. Application to the Maris theory of meteors to obtain accurate data for the astronomical study of masses and velocities,[3]
c. Transitions and dispersion of the ions produced by meteoric impact and the light of the night sky,
d. Correlation with the extended low frequency scattering of the Eckersley type,[4]
e. Determination of critical or limiting scatter radio-frequencies, and
f. Measurement of field-intensities and skip distances.

The first four objectives will be covered in a series of papers soon to be published by the author. The latter two represent new developments which have been brought somewhat closer to solution through wartime radio and radar operation.

The frequency of occurrence and the field-intensities[5] observed at 43,000 kc/sec. led to the supposition that the limiting or critical scattering frequency must lie above 100,000 kc/sec. This was substantiated when "echo-

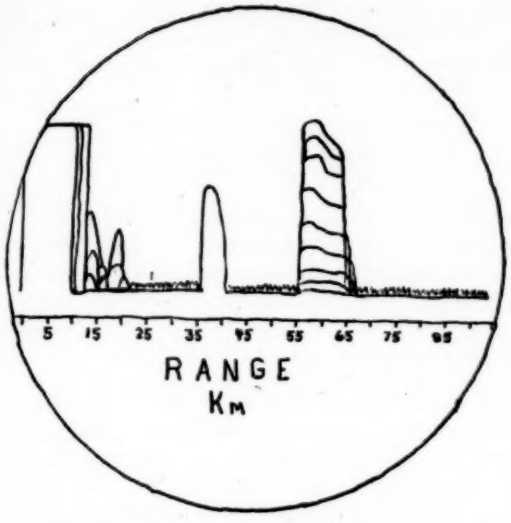

FIG. 1. Typical portion of the range oscilloscope traces on a radar unit showing three types of echo-returns. The rectangular wave form at the extreme left is the transmitter pulse with scattered reflections from hills, trees, large buildings, etc., extending to about 20 km. At 35 km is the echo-return of a single aircraft and at 55 km the multi-return from the ionized columnar meteor train. The sharp leading edge of both of the latter echoes is indicative of reflection from a well-defined boundary. The multi-returns from the meteor train are indicated by the numerous peaks within the echo envelope. The tails of the weaker echoes at about 65 km indicate the slight difference of range which would appear on a slightly different azimuth. The duration of these echoes is between ½ and 3 seconds with constant rapid fluctuations in field-intensity due to the high order of ion-recombination at these frequencies.

returns" coincident with the appearance of bright meteor trains were observed on the oscilloscopes of radar units operating in India. The author, while investigating these peculiar echoes in an unofficial capacity, noted several prominent features, which are reproduced in Fig. 1.

Operating the radar on a frequency of approximately 105,000 kc/sec., echoes were received lasting from ½ to 3 seconds on half-path lengths of 30 to 125 km. This is, naturally, relative to the radar, which for military purposes concentrates a considerable portion of its energy at very low radiation angles and probably, therefore, secures echo-returns from meteor trains passing far from the zenith. The echo rate of occurrence exhibited a random distribution during the early morning hours (0100–0700 hours local standard time) with a strong maximum about 0400 hours. No echoes were observed in the afternoons or early evenings (1300–2100 hours).

The particular character and the steep-sided leading edge of the echo, as illustrated in Fig. 1, are indicative of reflection from a sharply-defined boundary. Movement of the echoes is observed by the superimposition of numerous echoes within or above the original return. Variations in range of the echo radially to the radar, were small probably less than 3 km, although azimuth angles, which were difficult to obtain due to the fluttering signal and return, varied beginning to end points by about 10°.[6] These circumstances are the equivalent of specular reflection as proposed by Pierce for meteoric columnar ionization.[7]

The observation of meteoric impact ionization and the radio effects associated therewith will be greatly aided by the employment of a high angle radiational pattern radar unit operating on frequencies of about 50,000 kc/sec. Undoubtedly, valuable quantatitive information on masses, velocities, and numbers of meteors may be obtained in this fashion.

[1] H. M. Beverage, H. O. Peterson, and C. W. Hansell, Proc. I. R. E. 19, 1313 (1931).
[2] O. P. Ferrell, Radio 258, 9 (1941).
[3] H. B. Maris, Terr. Mag. 34, 309 (1929).
[4] T. L. Eckersley, J. I. E. E. 86, 548 (1940).
[5] The author had observed intensities above 50 microvolts per meter over a path of 390 km (Paxton, Massachusetts to Atlantic City, New Jersey) and intended to expand his meteoric origin hypothesis in the second part of, "Notes on U.H.F. Propagation," (part 1), *Radio*, p. 267 (March, 1942), but was unable to do so before entering the U. S. Army Signal Corps.
[6] Many of these observations were made on SCR270B radar units which introduce considerable inaccuracy in the factor of human judgment and coordination. The exact determination of azimuth is therefore subject to gross extremes.
[7] J. A. Pierce, Proc. I. R. E. 26, 892 (1938).

On the Nuclear Photo-Effect

GLEB WATAGHIN
Department of Physics, University of São Paulo, São Paulo, Brasil
December 8, 1945

THE measurements of the thresholds and yields of the nuclear photo-effect indicate thresholds between 5 and 19 Mev,[1] and cross sections of the order of 10^{-26} cm².[2] Notwithstanding the experimental uncertainty of the latter value, one can easily recognize[3] how important this effect becomes at temperatures for which

$$kT \gtrsim 2\ mc^2 \sim 10^{10}\ \text{e-volts}.$$

Indeed, photons with $h\nu$ above the threshold produce excited nuclei which can undergo several types of processes, e.g., giving rise to a neutron or proton and a β-radioactive nucleus. This source of neutrons gives origin to a great concentration of neutrons at temperatures and nuclear densities indicated below. The neutrons absorbed by other nuclei produce the well-known transformations in which many $\pm\beta$-radioactive nuclei are generated. The emission of neutrinos and antineutrinos in the $\pm\beta$-processes increases very rapidly with temperature, according to formula (1), of this paper and becomes the dominant process above certain critical temperatures depending upon the threshold and the cross section for the photo-effect. These phenomena play an important role in the statistical processes which gave origin to the actual distribution of nuclei in the universe,[4] and possibly in the phenomenon of the stellar collapse.[5]

Let us consider the statistical equilibrium between nuclei, photons, and electrons at $kT \sim 2mc^2$, where m is the mass of an electron. Putting $x_0 = mc^2/kT$, $y = h\nu/kT$, $y_0 = h\nu_0/kT$, where $h\nu_0$ is the threshold for the kind of nuclei under consideration and assuming $y_0 \gg 1$, one obtains directly from the Plank's formula the following value for the number N_{ν_0}, per unit volume, of photons having energy greater than the threshold:

$$N_{\nu_0} = \frac{8\pi}{c^3}\int_{\nu_0}^{\infty}\frac{\nu^2 d\nu}{e^{h\nu/kT}-1} \sim 8\pi\left(\frac{mc}{h}\right)^3 x_0^{-3} y_0^2 e^{-y_0} \sim 1.8 \times 10^{30} \times x_0^{-1} \times \left(\frac{y_0}{x_0}\right)^2 \times e^{-y_0}. \quad (1)$$

Some values obtained from (1) for the mean life of a

TABLE I. Cross section and mean life.

T	x_0	y_0	Cross section for photo-effect	Mean life in sec.
6×10^9	1	20	10^{-28}	30
1.2×10^{10}	0.5	15	10^{-26}	0.1
2.4×10^{10}	0.25	7.5	10^{-26}	3×10^{-5}
6×10^9	1	20	10^{-27}	300
2.4×10^{10}	0.25	7.5	10^{-27}	3×10^{-4}
3×10^9	2	40	10^{-28}	6×10^{11}

nucleus before a transformation by a photo-effect are indicated in the Table I. The assumed values of the cross sections correspond to the approximated ones for photons near the threshold.

The purpose of this remark is to emphasize the role of the photo-effect and of the neutrino emission in the general problem of statistical equilibrium of nuclei, electrons, and photons at $T \sim 10^{10}$ degrees. Similar considerations could be applied to other processes, such as production of excited states of nuclei in non-elastic collisions. G. Gamow pointed out to me that also the evaporation of neutrons and induced fission become important at temperatures considered above. A simple calculation shows that, at temperatures $\sim 10^{11} (kT \sim 10^7$ ev) and nuclear densities $\rho \sim 10^6$, the neutrino emission per cm³ and per sec. becomes larger than the total density of energy of radiation and of electron pairs, and that thermodynamical equilibrium becomes impossible, if light particles and nuclei are present. If the average energy per particle is $>10^8$ ev, then the production of groups of mesons (in collision processes involving nuclei and nucleons) changes even more profoundly the statistical problem. The damping effect of such collisions is caused by the subdivision of primary energy between created particles and to the neutrino emission. The microscopic reversibility of such processes is questionable. The relationship between the postulate of irreversibility of some of these processes and the existence of a finite number of distinguishable states of elementary particles, postulated in the principle of supplementary indeterminacy,[6] will be discussed elsewhere.

[1] G. C. Baldwin and H. W. Koch, Phys. Rev. **67**, 1 (1945).
[2] Bothe and Gentner, Zeits. f. Physik **108** (1939).
[3] G. Wataghin, Phys. Rev. **66**, 154 (1944).
[4] C. F. Weizsäcker, Physik. Zeits. **39**, 633 (1938); Chandrasekhar and Heinrich, Astrophys. J. **95**, 288 (1942); Lattes and Wataghin, in press.
[5] G. Gamov and Schoenberg, Phys. Rev. **59**, 539 (1941).
[6] Comptes rendus **207**, 421 (1938); Nature **142**, 393 (1938).

On the Method of Second Quantization

R. BECKER AND G. LEIBFRIED
Göttingen, Germany
December 29, 1945

IN the quantum theory of wave fields one usually starts with a Hamiltonian function $\mathfrak{H} = \int \psi(x)^+ H_x \psi(x) dx$ from which one derives in the usual manner the equation of motion $(-i/\hbar)\dot{\psi} = H_x \psi$ as a classical wave equation in the three-dimensional space, if the quantities $\psi(x)$ and $i\hbar\psi(x)^+$ are considered as a continuous set of conjugate variables. x is an abbreviation for x, y, z and eventually the spin variable.

The transition to quantum mechanics is obtained by regarding $\mathfrak{H}$ as an operator. The quantities $\psi(x)^+$ and $\psi(x)$ are now operators which in the case of Bose statistics satisfy the commutation rules.

$$\begin{aligned} \psi(x)\psi(x')^+ - \psi(x')^+\psi(x) &= \delta(x-x'), \\ \psi(x)\psi(x') - \psi(x')\psi(x) &= 0, \\ \psi(x)^+\psi(x')^+ - \psi(x')^+\psi(x)^+ &= 0. \end{aligned} \tag{1}$$

We are going to exhibit the elements in Hilbert space on which these operators operate.[1] For this purpose we assume that the operator $A = \int \psi(x)^+\psi(x)dx$ exists. (It follows then by (1) that the operator $\int \psi(x)\psi(x)^+ dx$ does not exist.) We prove first:[2] there exists an element φ_0 with the property that $\psi(x)\varphi_0 = 0$ for all x. Let φ_λ be a normalized eigenvector of A belonging to the eigenvalue λ, that is $A\varphi_\lambda = \lambda\varphi_\lambda$, then it follows from (1), that $\psi(x)^+\varphi_\lambda$ belongs to the eigenvalue $\lambda+1$ and $\psi(x)\varphi_\lambda$ belongs to the eigenvalue $\lambda-1$. In addition to that it follows from $A\varphi_\lambda = \lambda\varphi_\lambda$ that the norm: $\int dx(\psi(x)\varphi_\lambda, \psi(x)\varphi_\lambda) = \lambda \geqq 0$.

In contradiction with that we would obtain a negative eigenvalue if the above mentioned φ_0 would not exist. Starting with φ_0 we construct an element

$$\psi(x_1)^+ \cdots \psi(x_n)^+ \varphi_0 = (n!)^{\frac{1}{2}} \varphi x_1 \ldots x_n, \tag{2}$$

then $\varphi x_1 \ldots x_n$ is normalized to unity if $(\varphi_0, \varphi_0) = 1$ in the sense that:

$$\begin{aligned} (\varphi_x, \varphi_y) &= \delta(x-y), \\ (\varphi' x_1 x_2, \varphi y_1 y_2) &= \tfrac{1}{2}[\delta(x_1-y_1)\delta(x_2-y_2) \\ &\qquad + \delta(x_1-y_2)\delta(x_2-y_1)], \\ (\varphi x_1 \ldots x_n, \varphi y_1 \ldots y_n) &= (n!)^{-1} \Sigma \delta(x_1-y_\alpha)\delta(x_2-y_\beta) \\ &\qquad \cdots \delta(x_n-y_\zeta), \end{aligned} \tag{3}$$

where $\alpha\beta\cdots\zeta$ is a permutation of the numbers 1, 2, $\cdots$, n and the summation extends over all permutations of these numbers. For these vectors, we have then:

$$\begin{aligned} \psi(x_s)^+ \varphi x_1 \ldots x_n &= (n+1)^{\frac{1}{2}} \varphi x_s x_1 \ldots x_n. \\ \psi(x_s)\varphi x_1 \ldots x_n &= n^{-\frac{1}{2}}\{\delta(x_s-x_1)\varphi x_2 \ldots x_n + \cdots \\ &\qquad + \delta(x_s-x_n)\varphi x_1 \ldots x_{n-1}\}. \end{aligned} \tag{4}$$

The most general vector in this Hilbert space is then:

$$\mathfrak{F} = f_0\varphi_0 + \sum_{n=1}^{\infty} \int \cdots \int f_n(x_1, \cdots, x_n)\varphi x_1 \ldots x_n dx_1 \cdots dx_n. \tag{5}$$

On account of (1) these $\varphi x_1 \ldots x_n$ are symmetrical in the $x_1 \cdots x_n$. The same holds true for the coefficients $f_n(x_1, \cdots, x_n)$. The norm of $\mathfrak{F}$ is

$$(\mathfrak{F}, \mathfrak{F}) = |f_0|^2 + \sum_{n=1}^{\infty} \int \cdots \int |f_n(x_1, \cdots, x_n)|^2 dx_1 \cdots dx_n. \tag{6}$$

Now the operation $\mathfrak{H}$, applied on $\mathfrak{F}$ leads directly to the Schrödinger equations for $n = 1, 2, 3, \cdots$ particles which obey the Bose statistics.

One can treat the case of Fermi statistics in an equally simple way by replacing on the left-hand side of Eq. (1) the $-$ sign by a $+$ sign. The Eqs. (2), (5), and (6) remain unchanged. However $\varphi x_1 \ldots x_n$ and $f(x_1, \cdots, x_n)$ are now antisymmetrical in the coefficients.

[1] We obtain in this directly a representation which was obtained by Fock, Zeits. f. Physik **75**, 622 (1932).
[2] This theorem was communicated to us by F. Rellich.

A Particular Type of Cosmic-Ray Stars Observed with Photographic Plate

SARA TAMBURINO
Physical Institute, University of Catania, Catania, Sicily
May 4, 1945

IN the microscopic investigation of photographic plates (Agfa *K*), some of which had been kept at sea level (Catania) while others had been exposed to cosmic rays at 1882 m and at 2942 m above sea level (Mount Etna), 433 "stars" due to cosmic-ray disintegrations were found.

Six of them exhibit a dense track which, after traveling a short distance in the emulsion divides itself into two tracks of lower densities.

We believe that this type of star can be interpreted on the basis of an hypothesis suggested by Ortner.[1] According to this hypothesis, in the disintegration processes produced by cosmic rays nuclear fragments are emitted, which subsequently evaporate generating protons of small energy. The above assumption explains the following facts:

(1) The existence in stars originating from the disintegration of heavy nuclei of protons of low energy (<1 Mev), indeed at an energy smaller than that necessary for passing the Gamow-barrier of the original nucleus.

(2) The position of the maximum of the experimental curve representing the energy distribution of the protons. This maximum occurs for a value of the energy which is about one-half of the predicted value.[2] According to Ortner's hypothesis one can assume that, on the average, every proton leaves the nucleus accompanied by a neutron. Thus the Coulomb energy transferred to each particle is on the average one-half of the energy that a proton leaving the nucleus alone would possess.

The six stars mentioned above are interpreted as showing a nuclear fragment which after a short path in the emulsion (average length 5.6μ) evaporates, giving rise to two (and in one case perhaps three) protons of low energy (from 0.87 to 1.5 Mev; average value 1.15 Mev).

Sketches of the stars showing bifurcations are given in Fig. 1. The characteristic data relative to the various tracks, namely track length (column 2); grain spacing = (length of track)/(number of grains − 1) (column 3); and energy (column 4) are given in Table I. Stars I to VI are those discussed above. Stars VII and VIII differ from the other in that the original track is *less* dense than the two tracks in which it appears to split. These two stars may be interpreted with one of the two following hypotheses:

1. The initial track 2 is caused by a small nuclear fragment (atomic number 2, atomic mass 2 to 4) of high energy (about 15 Mev).

2. Track 2 is caused by a proton and the bifurcation indicates an elastic collision between this proton and a hydrogen nucleus in the gelatine. This explanation, however, does not hold for Star VIII because the sum of the energies of the protons giving rise to the tracks 2′ and 2″ is larger than the energy which corresponds to the spacing of grains in track 2, if this is a proton track.

Among the numerous stars observed, one finds several tracks with grain spacing ~2μ which do not originate from the center of the star but start at distances of 3 to 6μ from the center. In general, this occurrence can be attributed to the statistic fluctuations of the grain spacing. We believe, however, that this is not true for all cases. An extreme example can be found in Star IX of Fig. 1 which contains two tracks (5 and 6) starting 7.5μ from the center of the star. Observation of the direction of tracks 5 and 6 does not support the view that they may have had origin in a disintegration process independent from that which gives origin to the tracks 1–4.

The photographic plates Agfa *K* used (thickness of gelatine 25μ) have been developed with Metol-Hidroquinone Agfa at a temperature of 18° for 5 minutes. The length of the track in the photographic emulsion was determined considering their orientation in space.

For the particles whose path does not end in the emulsion, the total range was determined by means of the range *vs.* spacing curves given by Schopper[3] for *K* plates. (To

TABLE I. Data on stars of Fig. 1.

1	2	3	4		1	2	3	4
Stars	Branches	Length of branches μ	Spacing μ	Energy Mev	Stars	Branches	Length of branches μ	Spacing μ	Energy Mev
I	2	7	1.4		VI	1	5	1.6	
	2′	15	1.8	~1		1′	20	2	1.15
	2″	16	2	1		1″	20	2.2	1.15
II	3	4	1.33		VII	2	7	2.3	
	3′	23	2	1.25		2′	25	1.9	1.32
	3″	18	2	1.05		2″	21	1.9	1.18
III	2	2.5	1.25		VIII	2	5	2.5	
	2′	15	2.1	1		2′	18	1.84	1.05
	2″	18	2	1.05		2″	9	1.8	~1
IV	3	6.4	1.6		IX	1	50	2.5	3.1
	3′	5	2.5	1.5		2	18	2	1.03
	3″	6.5	2.18	1.32		3	32	2.2	1.5
						4	22	2	1.21
V	1	8	1.6			5	25	1.9	1.32
	1′	10	1.6	0.87		6	13	2.6	1.5
	1″	28	2.5	1.5					

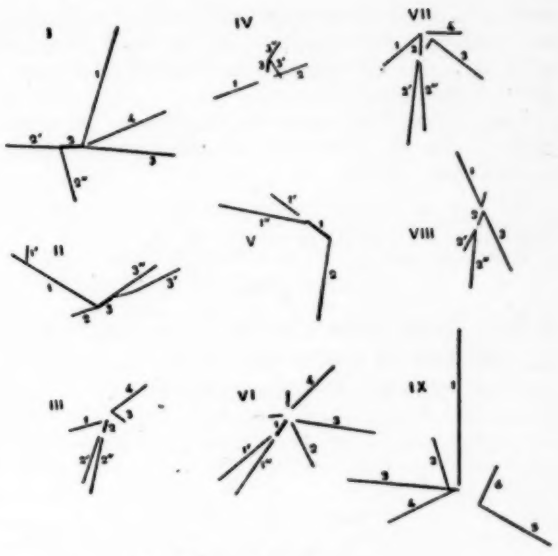

FIG. 1. Stars showing bifurcation.

make sure that these curves could be used for the K plates used by us, we have calibrated some plates with α-particles of Po and with protons emitted from paraffine bombarded with Po α-particles.)

For the energy determination, we have calculated the range in the air and then used the known curves of Livingston and Bethe.

[1] G. Ortner, Mitt. d. Inst. f. Radiumforschg. Wien, No. 436; Wien Ber. 149, 259 (1940).
[2] E. Bagge, Ann. d. Physik 39, 512 (1941).
[3] E. M. and E. Schopper, Physik. Zeits. 40, 22 (1939).

A New Band System in the Green Excited in a Mixture of Xenon and Oxygen and the Energy of Dissociation of CO

CARL KENTY, J. O. AICHER, AND E. B. NOEL
Lamp Development Laboratory, General Electric Company, Nela Park, Cleveland, Ohio
AND
A. PORITSKY AND V. PAOLINO
Cleveland Wire Works, General Electric Company, Cleveland, Ohio
September 20, 1945

A BULB containing pure Xe at about 100-mm pressure, excited by a high frequency discharge, glows with a pale purple color and develops purple streamers. If a little O_2 is present, however, and the discharge is weak and of very high frequency (4.5 megacycles), a beautiful apple-green glow is developed. The spectroscope shows the glow to consist of two lines or narrow bands at about 5677 and 5651A, and a system of bands beginning at about 5556A and shading off to the violet, traceable beyond 5000A. The accompanying spectrogram (Fig. 1) (with Mo arc spectrum included) and densitometer tracing (Fig. 2) show the appearance and wave-lengths of the bands. Some of the bands are shaded toward the red.

FIG. 1. Spectrogram of oxygen and xenon with Mo arc as reference.

The band system was discovered in 1941 by two of us (A. P. and V. P.) in a bulb containing a mixture of Kr and Xe in which some impurity was suspected. It was next observed in the manufacture of flashtubes containing Xe. The conditions under which it was frequently seen suggested it might be associated with one of the constituents of air. Finally it was identified with O_2 by slowly leaking various gases into pure Xe while watching the color of the discharge. Very small amounts of O_2 were found to bring out the glow. In fact, so sensitive to O_2 is Xe at about 100 mm that as little as one part per million can be detected. The most favorable O_2 concentration is of the order of 0.05 percent.

CO_2 gives the bands almost as strongly as O_2. The bands also appear with H_2O vapor, but are much less strong. No bands were found with CO, nor with N_2, H_2, or CH_4.

The bands do not appear under similar circumstances with Kr or A.

This band system is, so far, unreported as far as the writers are aware. It is suggested tentatively that it may be owing to O_2 and that it may result from a resonant energy exchange with metastable Xe atoms. In this case, the excitation energy of the bands would lie well above the dissociation energy of O_2 (5.08 v).

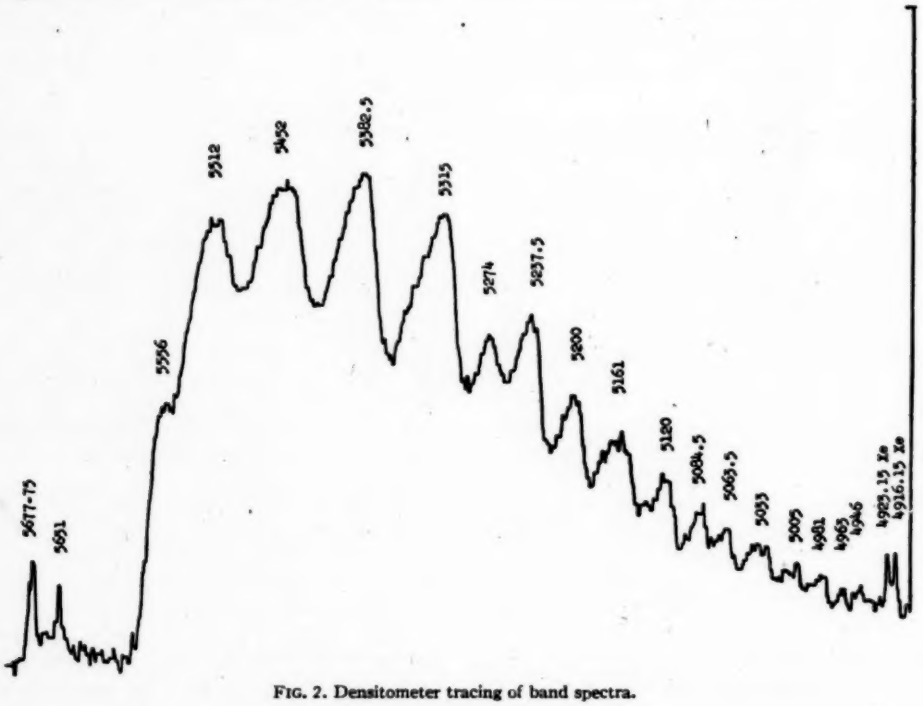

FIG. 2. Densitometer tracing of band spectra.

The suggestion is also made that CO_2 may be strongly dissociated by the metastable Xe atoms (and H_2O somewhat less strongly), thus producing oxygen atoms which combine to form the O_2 molecules; ($D(CO_2)=5.5$ v, $D(H_2O)=5.0$ v). If so, the fact that CO did not yield the bands would indicate that the dissociation energy of CO is greater than the energy of the upper metastable state of Xe, namely 9.4 volts. (Energy of lower metastable state equals 8.3 v.) This appears to be direct evidence in favor of the 9.6-volt value of D(CO) as determined by Hagstrum and Tate[1] from appearance potentials in the mass spectrograph, or for the 11.11 v-value obtained in a recent spectral analysis by Gaydon and Penney,[2] but against the 9.14-volt value determined from certain predissociation data.[3] The higher value appears to be more in accord also with thermochemical data as brought out by Hagstrum and Tate,[1] and also by Asundi and Samuel.[4]

[1] H. D. Hagstrum and J. T. Tate, Phys. Rev. 59, 365 (1941).
[2] A. G. Gaydon and W. G. Penney, Proc. Roy. Soc. A183, 374 (June, 1945).
[3] For a review see G. Hertzberg, *Molecular Spectra and Molecular Structure* (Prentice-Hall, Inc., New York, 1939), Chap. VIII.
[4] R. K. Asundi and R. Samuel, Ind. Acad. Sci. 3A, 562 (1936).

Resonance Absorption by Nuclear Magnetic Moments in a Solid

E. M. PURCELL, H. C. TORREY, AND R. V. POUND*
Radiation Laboratory, Massachusetts Institute of Technology, Cambridge, Massachusetts
December 24, 1945

IN the well-known magnetic resonance method for the determination of nuclear magnetic moments by molecular beams,[1] transitions are induced between energy levels which correspond to different orientations of the nuclear spin in a strong, constant, applied magnetic field. We have observed the absorption of radiofrequency energy, due to such transitions, in a *solid* material (paraffin) containing protons. In this case there are two levels, the separation of which corresponds to a frequency, ν, near 30 megacycles/sec., at the magnetic field strength, H, used in our experiment, according to the relation $h\nu=2\mu H$. Although the difference in population of the two levels is very slight at room temperature ($h\nu/kT\sim10^{-5}$), the number of nuclei taking part is so large that a measurable effect is to be expected providing thermal equilibrium can be established. If one assumes that the only local fields of importance are caused by the moments of neighboring nuclei, one can show that the imaginary part of the magnetic permeability, at resonance, should be of the order $h\nu/kT$. The absence from this expression of the nuclear moment and the internuclear distance is explained by the fact that the influence of these factors upon absorption cross section per nucleus and density of nuclei is just cancelled by their influence on the width of the observed resonance.

A crucial question concerns the time required for the establishment of thermal equilibrium between spins and lattice. A difference in the populations of the two levels is a prerequisite for the observed absorption, because of the relation between absorption and stimulated emission. Moreover, unless the relaxation time is very short the absorption of energy from the radiofrequency field will equalize the population of the levels, more or less rapidly, depending on the strength of this r-f field. In the expectation of a long relaxation time (several hours), we chose to use so weak an oscillating field that the absorption would persist for hours regardless of the relaxation time, once thermal equilibrium had been established.

A resonant cavity was made in the form of a short section of coaxial line loaded heavily by the capacity of an end plate. It was adjusted to resonate at about 30 mc/sec. Input and output coupling loops were provided. The inductive part of the cavity was filled with 850 cm³ of paraffin, which remained at room temperature throughout the experiment. The resonator was placed in the gap of the large cosmic-ray magnet in the Research Laboratory of Physics, at Harvard. Radiofrequency power was introduced into the cavity at a level of about 10^{-11} watts. The radiofrequency magnetic field in the cavity was everywhere perpendicular to the steady field. The cavity output was balanced in phase and amplitude against another portion of the signal generator output. Any residual signal, after amplification and detection, was indicated by a microammeter.

With the r-f circuit balanced the strong magnetic field was slowly varied. An extremely sharp resonance absorption was observed. At the peak of the absorption the deflection of the output meter was roughly 20 times the magnitude of fluctuations due to noise, frequency, instability, etc. The absorption reduced the cavity output by 0.4 percent, and as the loaded Q of the cavity was 670, the imaginary part of the permeability of paraffin, at resonance, was about $3\cdot10^{-6}$, as predicted.

Resonance occurred at a field of 7100 oersteds, and a frequency of 29.8 mc/sec., according to our rather rough calibration. We did not attempt a precise calibration of the field and frequency, and the value of the proton magnetic moment inferred from the above numbers, 2.75 nuclear magnetons, agrees satisfactorily with the accepted value, 2.7896, established by the molecular beam method.

The full width of the resonance, at half value, is about 10 oersteds, which may be caused in part by inhomogeneities in the magnetic field which were known to be of this order. The width due to local fields from neighboring nuclei had been estimated at about 4 oersteds.

The relaxation time was apparently shorter than the time ($\sim$ one minute) required to bring the field up to the resonance value. The types of spin-lattice coupling suggested by I. Waller[2] fail by a factor of several hundred to account for a time so short.

The method can be refined in both sensitivity and precision. In particular, it appears feasible to increase the sensitivity by a factor of several hundred through a change in detection technique. The method seems applicable to the precise measurement of magnetic moments (strictly, gyromagnetic ratios) of most moderately abundant nuclei.

It provides a way to investigate the interesting question of spin-lattice coupling. Incidentally, as the apparatus required is rather simple, the method should be useful for standardization of magnetic fields. An extension of the method in which the r-f field has a rotating component should make possible the determination of the sign of the moment.

The effect here described was sought previously by Gorter and Broer, whose experiments are described in a paper[3] which came to our attention during the course of this work. Actually, they looked for dispersion, rather than absorption, in LiCl and KF. Their negative result is perhaps to be attributed to one of the following circumstances: (a) the applied oscillating field may have been so strong, and the relaxation time so long, that thermal equilibrium was destroyed before the effect could be observed—(b) at the low temperatures required to make the change in permeability easily detectable by their procedure, the relaxation time may have been so long that thermal equilibrium was never established.

* Harvard University, Society of Fellows (on leave).
[1] Rabi, Zacharias, Millmann, and Kusch, Phys. Rev. 53, 318 (1938).
[2] I. Waller, Zeits. f. Physik 79, 370 (1932).
[3] Gorter and Broer, *Physica* 9, 591 (1942).

The γ-Rays of Radium D

TSIEN SAN-TSIANG*
Laboratorie Curie, Institut du Radium, and Laboratoire de Chimie Nucléaire du Collège de France, Paris, France
December 13, 1945

FOR many years RaD was regarded as a radioactive substance which emits nuclear β-rays of very low energy and monochromatic γ-rays of quantum energy 46.7 kev. Just before the war, however, it was shown by Amaldi and Rasetti,[1] using the method of selective absorption, that the radiation is complex, the well-known 46.7 kev line being accompanied by a much weaker component of energy 43 kev. Following the publication of this result, a systematic study of the subject was started in Paris with a very strong source of RaD of about 100 mC, extracted previously by Professors Irène Joliot-Curie and F. Joliot. The following is a brief summary of the main experimental results, obtained in the Curie Laboratory and in the Laboratory of Nuclear Chemistry in the difficult conditions which prevailed from 1942–1945. The results deal with the detailed structure of the γ-radiation, the absolute intensity of the different lines, and the nature of γ-rays of quantum energy 46.7 kev.

In the region between 25 and 100 kev, the analysis made by the methods of selective absorption[2] and crystal diffraction[3] leads to the conclusion that RaD emits in this region four γ-lines (*A*, *B*, *C*, *D*) and two lines of x-rays of K-83, the corresponding energy and intensity being given in Table I.

The existence of these six different radiations is confirmed by another series of experiments in which the corresponding quantum energies are determined by measuring the true range of the photoelectrons which they project in a Wilson chamber.[4,5] This method also suggested the existence of an additional weak line at about 65 kev (x) and relatively intense radiations below 25 kev.

TABLE I. γ-rays from RaD.

γ-ray line	*E* (kev)	*I* (quanta per 100 disintegrations)	Reference
(*X*)	(65±5)	(<0.2)	(5)
A	46.7±0.1	2.8±0.6	(1, 2, 3, 5, 8)
B	43±1	0.2±0.1	(1, 2, 3, 5)
C	37±1	0.2±0.1	(2, 3, 5)
D	32±1	0.4±0.2	(2, 3, 5, 6)
E	23.2±0.6	1.0±0.5	(5, 6)
F	7.3±0.7	~10	(6, 7)

In order to study the region below 25 kev, experiments were made with a Wilson chamber operating at suitable low pressure.[6] It was thus found that in addition to the *L* spectrum of element 83, there is a new γ-ray line (*E*) of 23.2±0.6 kev. This line has thus almost exactly half the quantum energy of the principle line (*A*) and would be confused in diffraction spectrum experiments with the second-order image of the (*A*) line. Another very intense γ-ray line (*F*) of 7.3±0.7 kev has been observed in the energy region below the *L* levels of element 83.[6a] This radiation has been observed previously by Droste[7] who classified it as one of the components of the *L* spectrum of element 83. From the energy determinations in our present experiments, it seems more reasonable to regard it as a new γ-ray line.

In order to investigate the nature of the principle line (*A*) we have determined the intensity of the conversion electrons of this radiation by the usual methods of magnetic β-ray spectrography and obtained the value 2.9 for the internal conversion coefficient, N_e/N_γ in the L_1 level.[5,8] The comparison with the theoretical calculation of Fisk[9] indicates that the 46.7 kev line is most probably a quadripole radiation. For other γ-rays there is no information available about their conversion electrons[10] to permit similar deduction about their nature to be made.

I should like to thank Professors I. Joliot-Curie and F. Joliot for their continuous interest and help, and Drs. Frilley, Surugue, and Ouang, and Mr. Marty for their important contributions and friendly collaboration in the course of these investigations.

* Now temporarily at H. H. Wills Physics Laboratory, Bristol, England.
[1] E. Amaldi and F. Rasetti, Ricerca Scient. 10, 111 (1939).
[2] Tsien San-Tsiang, Comptes rendus 216, 765 (1943); 218, 503 (1944).
[3] M. Frilley, Comptes rendus 218, 505 (1944).
[4] Tsien San-Tsiang, Ann. d. Physik 19, 327 (1944).
[5] Tsien San-Tsiang and C. Marty, Comptes rendus, Seance of 7th May 1945 (in press).
[6] Tsien San-Tsiang and C. Marty, Comptes rendus, Seance of 30th July, 1945 (in press).
[6a] M. Frilley and Tsien San-Tsiang, Comptes rendus (Jan., 1945).
[7] G. von Droste, Zeits. f. Physik 84, 17 (1933).
[8] Ouang Te-Tchao, J. Surugue, and Tsien San-Tsiang, Comptes rendus 217, 535 (1943).
[9] J. S. Fisk, Proc. Roy. Soc. 143, 674 (1934).
[10] H. O. W. Richardson and A. Leigh-Smith, Proc. Roy. Soc. 160, 454 (1937).

Fine Structure of the α-Rays from Protactinium

TSIEN SAN-TSIANG*
Laboratoire de Chimie Nucléaire du Collège de France, Paris, France
M. BACHELET, AND G. BOUISSIÈRES
Laboratoire Curie de l'Institut de Radium, Paris, France
December 13, 1945

THE range of the α-particles from protoactinium, Pa, was first determined by Geiger[1] in 1922, the observations leading to a value of the mean range of 3.63 cm, in air at 15°C and 760 mm of Hg. Recently, Ringo,[2] using a 60°-magnetic α-ray spectrograph has obtained a value 5.053 Mev for the energy of the particles, the corresponding value of the mean range being 3.57 cm. In order to examine this disparity and to detect any fine structure in the α-particle spectrum, we have made experiments with a differential ionization chamber and linear amplifier.[3]

The apparatus employed has already been described in an account of the determination of the range of the α-particles from ionium by Professor I. Joliot-Curie and one of us.[4] For the present experiments the Pa was deposited electrolytically on a sheet of nickel, the active deposit containing more than 50 percent Pa mixed with La. Two sources, each of area 0.12 cm², and emitting approximately

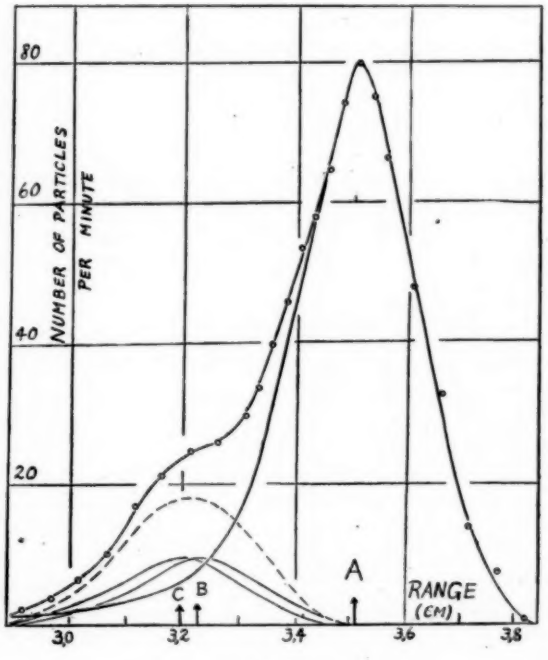

FIG. 1.

3000 and 14,000 particles per second, respectively, were used in succession.

The mean range of the Pa α-particles was determined by comparison with those from Po. Four determinations made with the weaker source gave very concordant results, the mean range being 3.511±0.010 cm at 760 mm, 15°C, the corresponding value for Po being taken as 3.843±0.006 cm.[5]

The frequency range curves have a half-width of 2.1 mm for a very thin polonium source and 2.2 mm for Pa, the latter value being in good agreement with that to be expected from the known thickness of the active layer. Whereas, however, the distribution in range of the Po α-particles shows an almost symmetrical distribution about the mean value, the corresponding result for Pa shows a marked asymmetry corresponding to the presence of particles of lower energy, such as would indicate a fine structure in the α-rays. With the weaker source the number of particles counted was too small to allow any definite conclusions to be drawn and experiments were therefore made with the stronger source.

TABLE I. Energy of gamma-rays.

Groups of α-rays	Mean range (cm)	E_α (Mev)	Energy of disintegration (Mev)	E_γ (kev) from fine structure	E_γ (kev) from β-ray magnetic analysis
A	3.511±0.010	5.00	5.09		
				290±10	287
B	3.23	4.72	4.80		
				320±10	323
C	3.20	4.69	4.77		

The second series of experiments were made at four different values of the gas pressure and definitely establish the existence of an α-group of range about 3.2 cm with an intensity about 15–20 percent of that of the main group (see Fig. 1).

If the frequency-range distribution shown in the figure is resolved into two components, as indicated by the dotted lines, it is found that the main group has a half-width of 2.5 mm, concordant with the value to be expected from the known thickness of the active deposit, whereas the smaller group has a half-width of 2.8 mm. The observations are consistent with the assumption that the weak group is complex and made up of two components of nearly equal intensity and mean range 3.20 and 3.23 cm, respectively, each component having a half-width of 2.5 mm.

The energies of the two γ-rays to be expected from such a fine structure in the α-spectrum are given in Table I and agree, within the limits of the experimental error (10 kev), with the values deduced from the magnetic β-ray spectrum which they produce (E_γ=287 and 323 kev).[6]

A detailed report of the work will be published shortly in the *Journal de Physique et le Radium*.

* Now temporarily at H. H. Wills Physics Laboratory, Bristol, England.

[1] H. Geiger, Zeits. f. Physik **8**, 45 (1922).
[2] R. Ringo, Phys. Rev. **58**, 942 (1940).
[3] E. Rutherford, F. A. B. Ward, and C. E. Wynn-Williams, Proc. Roy. Soc. **129**, 211 (1930).
[4] I. Curie and Tsien San-Tsiang, J. de phys. et rad. **6**, 162 (1945).
[5] M. G. Holloway and M. S. Livingstone, Phys. Rev. **54**, 18 (1938).
[6] L. Meitner, Zeits. f. Physik **50**, 15 (1928).

Reciprocal Electric Force

F. W. WARBURTON
University of Kentucky, Lexington, Kentucky
December 20, 1945

THE force of one electrical charge on another may be obtained from an assumed potential energy W expressed in ascending powers of $1/c$ and the relative velocity $\mathbf{u}=\mathbf{v}-\mathbf{v}'$ of the charges e and e',

$$W=\frac{ee'}{r}\left[1+A\frac{u^2}{c^2}+B\frac{(\mathbf{u}\cdot\mathbf{r})^2}{c^2r^2}+C\frac{u^2(\mathbf{u}\cdot\mathbf{r})}{c^2r}+D\frac{(\mathbf{u}\cdot\mathbf{r})^3}{c^2r^3}+\cdots\right], \quad (1)$$

with coefficients A, B, C, D, $\cdots$ to be determined by experiment. When W is inserted in the Lagrangian equation of motion, the reciprocal force of e' on e is readily found to be

$$\begin{aligned}\mathbf{F}=ee'\Big[&\frac{\mathbf{r}}{r^3}+(1-A)\frac{\mathbf{r}u^2}{c^2r^3}-3(\tfrac{1}{2}-A)\frac{\mathbf{r}(\mathbf{u}\cdot\mathbf{r})^2}{c^2r^5}\\&-2A\frac{\mathbf{u}(\mathbf{u}\cdot\mathbf{r})}{c^2r^3}+2(\tfrac{1}{2}-A)\frac{\mathbf{r}(\mathbf{g}\cdot\mathbf{r})}{c^2r^3}+2A\frac{\mathbf{g}}{c^2r}\\&+2C\left\{\frac{\mathbf{u}u^2}{c^3r^2}-2\frac{\mathbf{u}(\mathbf{u}\cdot\mathbf{r})^2}{c^3r^4}+\frac{\mathbf{u}(\mathbf{g}\cdot\mathbf{r})}{c^3r^2}+\frac{\mathbf{g}(\mathbf{u}\cdot\mathbf{r})}{c^3r^2}+\frac{\mathbf{r}(\mathbf{u}\cdot\mathbf{g})}{c^3r^2}\right\}\\&+2D\left\{3\frac{\mathbf{r}u^2(\mathbf{u}\cdot\mathbf{r})}{c^3r^4}-4\frac{\mathbf{r}(\mathbf{u}\cdot\mathbf{r})^3}{c^3r^6}+3\frac{\mathbf{r}(\mathbf{u}\cdot\mathbf{r})(\mathbf{g}\cdot\mathbf{r})}{c^3r^4}\right\}+\cdots\Big], \quad (2)\end{aligned}$$

where $\mathbf{g}=\mathbf{f}-\mathbf{f}'$ is the relative acceleration of the charges e and e', and B has been determined in terms of A by applying the equation to the pairs of charges making up dipole elements of two currents and integrating for closed circuits.

Neglecting terms in $1/c^3$, we find Eq. (2) reduces to the Weber force if $A=0$, reduces to the Riemann force if $A=\frac{1}{2}$, omits an undesirable term in u^2 if $A=1$, and except for the acceleration terms gives the Ritz formula which is based on ballistic emission. For relative velocity $\mathbf{u}$ and relative acceleration $\mathbf{g}$ directed along r, it reduces to

$$F=ee'\left[\frac{1}{r^2}-\frac{u^2}{2c^2r^2}+\frac{g}{c^2r}+\cdots\right]. \quad (3)$$

As ee'/c^2r is small compared to the mass m of the electron e, Eq. (3) becomes approximately $F=(ee'/r^2)(1-u^2/c^2)^{\frac{1}{2}}=mg$, and the "apparent" force $F'=ee'/r^2=mg/(1-u^2/c^2)^{\frac{1}{2}}$ gives the apparent increase in mass, $m'=m/(1-u^2/c^2)^{\frac{1}{2}}$. The acceleration term, $F_g=ee'g/c^2r=W_eg/c^2=m_eg$ yields an electrostatic mass-energy relation $W_e=m_ec^2$ for the group of charges comprising a body, to which an external charge gives an average acceleration g transmitted from one charge to another in the group by their mutual electrostatic forces. And there is the possibility that nuclear attractions may be expressed as a type of electrostatic van der Waal or resonance force, whence nuclear energy may be expected to fall into this type of mass-energy equivalence.

Equation (2) may be used to describe the change in magnetization of a rod by the passage of longitudinal current through the rod. For the idealized case of a long filament of current i' acting on a circular electronic orbit of radius ρ, let the z axis be parallel to the filament and pass through the center of any orbit, and let the magnetic axis of the orbit lie in the xz plane making an angle α with z. Let β be the angle between the x axis and b, the distance from the orbit to the current filament, and let ϕ give the angular position of the electron e in the orbit. The factor $n'e'v'/c$ is replaced by $i'dz$ and each term of Eq. (2) integrated over the long filament. The term expressing the resulting large periodic force proportional to the central acceleration v^2/ρ of the orbital electron

$$\begin{aligned}-(2C+3D)\frac{ei'v^2\pi}{c^2\rho}[&\mathbf{i}\cos\phi\sin\alpha\cos\beta+\mathbf{j}\cos\phi\sin\alpha\sin\beta\\&-\mathbf{k}(\cos\phi\cos\alpha\cos\beta+\sin\phi\sin\beta)]\end{aligned}$$

can evidently account for the change in magnetization in the rod known as "shock effect." Also the average torque of the conduction current i' on the orbit in the direction of increasing α, becomes

$$\begin{aligned}L_\alpha=&\frac{ev}{c}\frac{2i'\rho}{b}\cos\alpha\sin\beta\\&+(C+3D/2)\frac{ev^2i'\pi}{c^2}(\cos^2\alpha-\sin^2\alpha)\cos\beta\\&+(C+3D/2)\frac{ev}{c^2}\frac{di'}{dt}\frac{\pi}{b}\rho\cos\alpha\sin\beta. \quad (4)\end{aligned}$$

The first term in Eq. (4) gives the standard torque producing circular flux in the rod due to the longitudinal current. $\cos^2\alpha-\sin^2\alpha$ in the large second term is positive for orbital alignment along z or $-z$. Ordinarily $\cos\beta$ vanishes by symmetry. It is suggested that a very slight dissymmetry due to the longitudinal wedge cut in the specimen to reduce the circular flux, would give a minute average value of $\cos\beta$ and account for the effect Perkins[1] observed in nickel which reverses with reversal of current in the rod.

The symmetric reciprocal force provides a direct and unified description of electromagnetism, while the conventional treatment with its necessary relativity corrections built to fitt he classical non-relative, non-reciprocal magnetic force, $ev\times e'\mathbf{v}'\times\mathbf{r}/c^2r^3$, maintains a force, $ev\times\mathbf{H}/c$, which is not complete but which requires "other" quantities of the same magnitude depicted as rate of change in field momentum and as relativistic increase in mass, and which denies action of e' on e proportional to acceleration of e. Equation (2) permits ballistic emission from an oscillating dipole source, whose mix-up-in-phase at angles other than normal to the dipole (where emission speed is c) provides a physical reason for the mathematical expression for the transverse nature of light, which is not present in conventional theory. It conforms to operational theory in that it assigns meaning only at the source and at the absorber where the measurements are made, but it does not preclude description of reaction on the source and action on the absorber by some mechanism which may be developed later to describe transmission from e' to e.

[1] Henry A. Perkins, Phys. Rev. **66**, 21 (1944).

A Mass-Spectrographic Study of the Isotopes of Silicon

EDWARD P. NEY AND JOHN H. MCQUEEN
Rouss Physical Laboratory, University of Virginia, Charlottesville, Virginia
September 23, 1943

THE isotopic constitution of silicon has been studied by Aston[1] and photometrically by McKellar.[2] In the work reported here a Nier[3] type mass spectrometer was used to measure the relative abundance of the silicon isotopes. The vapor studied was SiF_4. Of the positive ions formed by electron impact in SiF_4, the SiF_3^+ group has the greatest intensity. For this reason, measurements were made of the ion peaks at mass numbers 85, 86, and 87. A typical mass spectrum is shown in Fig. 1. The values

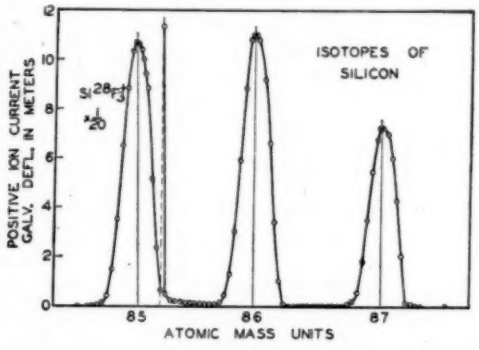

FIG. 1. Mass spectrum of silicon. $Si^{28}F_3$ has been plotted to 1/20 scale. Ion current is in meters deflection at highest sensitivity. One meter corresponds to about 10^{-12} ampere.

obtained for the abundances were: Si^{28} 92.24±0.10; Si^{29} 4.69±0.05; Si^{30} 3.07±0.05. The present values, together with those of McKellar are shown in Table I.

TABLE I. Isotopes of silicon.

Investigator	Percent abundance Si^{28}	Si^{29}	Si^{30}
Present work	92.24	4.69	3.07
McKellar	89.6	6.2	4.2

A search was made for rarer isotopes. None was found, and the following upper limits for the abundances relative to Si^{28} were set: Si^{25}, 1/10,000; Si^{26}, 1/3000; Si^{27}, 1/10,000; Si^{31}, 1/20,000; Si^{32}, 1/50,000; Si^{33}, 1/50,000. Using packing fractions[4] of -4.86×10^{-4} for Si^{28}, -4.54×10^{-4} for Si^{29}, and -5.79×10^{-4} for Si^{30}; and the conversion factor of 1.000275 in going from the physical to the chemical mass scale, we find for silicon the atomic weight 28.087. This is in substantial agreement with 28.06, the chemical atomic weight. The writers take pleasure in acknowledging their indebtedness to Professor A. O. Nier at the University of Minnesota.

[1] Aston, *Mass Spectra and Isotopes* (Edward Arnold and Company, London, 1933).
[2] A. McKellar, Phys. Rev. **50**, 761A (1934).
[3] A. O. Nier, Rev. Sci. Inst. **11**, 212 (1940).
[4] H. E. Duckworth, Phys. Rev. **62**, 19 (1942).

The Occurrence of Superconductivity in a Collective Electron Assembly

WILLIAM BAND
Physics Department, Yenching University, Peiping, China
December 20, 1945

IT was suggested by Frenkel[1] that magnetic interaction between currents might cause the free electrons in a metal to freeze into a rigid lattice, and he gave qualitative reasons for supposing that such an assembly might move through a crystal without loss of energy and so account for superconductivity. Bethe and Frölich,[2] however, showed that there would in fact be no significant decrease of resistance.

Frenkel in fact assumed without proof that the potential

$$\sum_{ij} e^2 u_i u_j / r_{ij} \tag{1}$$

would itself ensure that all the speeds u_i would become equal at sufficiently low T, so that the energy of the electrons would be

$$\sum_{ij} e^2 u^2 / r_{ij}. \tag{2}$$

It is here suggested that a more strategic way of simplifying (1) would be to average the effect of all the other electrons upon any given electron by writing

$$\gamma I = \sum_j e u_j / r_{ij}, \qquad \text{any } i, \tag{3}$$

so that in place of (2) we would have

$$\sum_i \gamma e u_i I, \tag{4}$$

where I is the total current in the specimen. The contribution of a single electron with speed u in the direction of the current would then be γeuI per cm path, and the perturbation to be used in the Boltzmann equation becomes

$$\pm\gamma e u^2 \tau I, \tag{5}$$

where τ is the time of relaxation for the speed u. It can then be shown that in an ideal crystal the Sommerfeld statistical theory leads simply to the result

$$I = \mathrm{E}/(R - \gamma\bar{u}), \tag{6}$$

where E is the e.m.f., R is the ideal resistance, and $\bar{u}$ the electron velocity corresponding to the top of the Fermi limit. The effective resistance thus vanishes when the ideal resistance drops to the value $\gamma\bar{u}$.

This theory, although exceedingly crude, makes superconductivity the analog of ferromagnetism. The current plays the same role as spontaneous magnetization in the Heisenberg theory, and the constant γ takes the place of the simple exchange energy term in the Stoner modification of Heisenberg's theory.

In a paper to appear shortly[3] in the *Proceedings of the Cambridge Philosophical Society*, the writer proposes and examines a model of a superconductor as an aggregation of ideal domains within each of which the above formulae apply, and it is shown that the correct diamagnetic behavior automatically accompanies the superconducting transition and also that the transition temperature depends on the magnetic field in the correct manner.

The theory also leads to the expectation that superconductivity will be found only in those metals in which conducting energy bands are nearly empty; also that the upper limit of the critical magnetic field will be greater for those elements with lower Fermi levels, or more dense band-forms. In fact the "left-hand" group with high H_m are *d*-band conductors, while those with small H_m (the right-hand group) are *p*-band conductors in agreement with the theory.

The theory is consistent with the general principles recently laid down by Mendelssohn in his paper on the "*s*-state."[4]

[1] J. Frenkel, Phys. Rev. **43**, 907 (1933).
[2] Bethe and Frölich, Zeits. f. Physik **85** (1933).
[3] W. Band, "Diamagnetism and superconductivity of a collective electron assembly," Proc. Camb. Phil. Soc. to be published.
[4] Mendelssohn, Proc. Phys. Soc. **57**, 371 (1945).

On Increasing the Effectiveness of a Betatron

THEODORE J. WANG
Ohio State University, Columbus, Ohio
December 29, 1945

BOTH halves of the cycle of an x-ray betatron can be utilized by employing dual injectors and dual targets. The injectors are mounted back to back either outside or inside the equilibrium orbit. One target is located outside the orbit, and the other target is located inside the orbit. Electron beams are sent in opposite directions on successive half-cycles. The particular target which is on the side of the orbit toward the injectors consists of a slight projection from the injector assembly (as used by Kerst). This projection is cleared by each beam on its first revolution following injection. The arrangement is shown in Fig. 1.

For nuclear disintegration studies this scheme doubles the intensity of the output at the position of the intersection of the two x-ray beams. For radiation therapy the crossfire presents advantageous dosage distribution within the body of the patient. For limited applications in radiography the intersection could conceivably serve in the manner of a focal region.

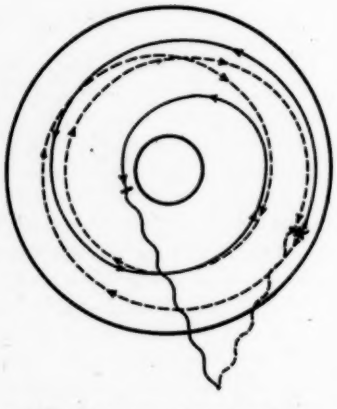

FIG. 1. Dual injector and target arrangement.

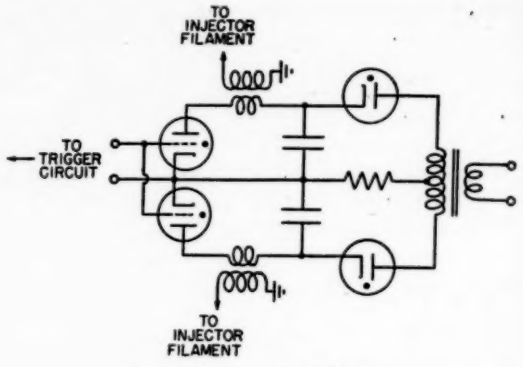

FIG. 2. Injection pulsing system.

For causing the beams to strike their respective targets it is sufficient to use a single pair of orbit-shift coils just inside the orbital radius (one coil above the doughnut and one below) together with a standard pulsing system. It is only necessary to pulse the coils once each half-cycle instead of once each full cycle. Inasmuch as the main flux reverses with each half-cycle while the orbit-shift coils are always pulsed in the same direction, the net result is that the orbit is alternately expanded and contracted on successive half-cycles.

A suitable pulsing system for firing alternate injectors on successive half-cycles is shown in Fig. 2. Both thyratrons are triggered by a single trigger unit; hence a single control adjusts the phase of both injectors.

A Method for Measuring Effective Contact e.m.f. between a Metal and a Semi-conductor[1]

W. E. STEPHENS, B. SERIN, AND W. E. MEYERHOF
Randal Morgan Laboratory of Physics, University of Pennsylvania, Philadelphia, Pennsylvania
December 8, 1945

RECTIFYING action can often be achieved by making a contact of small area between a metal and a semi-conductor. This rectification is interpreted in terms of a potential barrier which is caused by the difference in work functions of the metal and semi-conductor. If the barrier is thin enough, its height can be appreciably lowered by image force and by the quantum-mechanical tunnel effect. The contact e.m.f. also can vary from point to point over the contact area. Consequently, only an effective contact e.m.f. can be readily measured. But this effective contact e.m.f. is one important parameter in the theory and practice of semi-conductor rectifiers.

If the potential barrier acts like a diode in that most electrons (or holes) are stopped by the potential rather than by collisions, then Bethe[2] has shown that the current can be written as

$$j = j_0 \exp\left(-\frac{e\varphi}{kT}\right)\left[\exp\left(\frac{eV}{kT}\right)-1\right],$$

where V is the voltage applied across the contact (taking

account of spreading resistance), φ is the effective contact e.m.f., j_0 is the available current density of electrons.

The resistance of the contact at zero applied voltage can be calculated from the reciprocal of the derivative of j with V, letting $V=0$. Since j_0 is practically independent of temperature at room temperature in impurity semiconductors with excitation energies less than kT, the main temperature effect near room temperature can be written

$$R=R_0\frac{T}{T_0}\exp\left[\frac{e\varphi}{k}\left(\frac{1}{T}-\frac{1}{T_0}\right)\right],$$

where R is the d.c. resistance at $V=0$ and temperature T. The subscript 0 indicates room temperature values.

Consequently, by measuring the zero bias resistance of such a rectifier as a function of temperature, an effective contact e.m.f. may be calculated. This has been done for a few samples (silicon-tungsten) and a typical curve log R/T plotted against $1/T$ is shown in Fig. 1. This plot yields an effective contact e.m.f. of 0.21 ev. By using the observed apparent contact area, an estimate can be made of the barrier lowering due to image force and tunnel effect. Adding this to the effective contact e.m.f. gives the true difference in work function to be about 0.4 ev. The sign of this difference in work function is determined by the direction of rectification. In this case the most current flows when the semi-conductor is positive indicating that hole conduction occurs in the silicon used (aluminum doped), and that in this case its work function is larger than that of the metal. (These work functions are probably not outgassed work functions.) Corrections for variation in contact e.m.f. over the contact area are harder to make. If one spot has appreciably lower contact e.m.f. than the rest, this minimum contact e.m.f. will be measured. Otherwise, some sort of average will obtain.

This effective contact e.m.f. seems to be important to an understanding of small area conductor rectifiers and thermisters, and further work is being done to measure contact e.m.f. by this method.

[1] Based on technical report dated August 17, 1944. This work was done in part under Contract No. OEMsr-388 with the Trustees of the University of Pennsylvania under the auspices of the Office of Scientific Research and Development, which assumes no responsibility for the accuracy of the statements contained herein.
[2] H. A. Bethe, Radiation Laboratory report 317 (April 28, 1943).

Autoradiographic Detection of Aluminum[1]

WILLIAM E. STEPHENS AND MARGARET N. LEWIS
Randal Morgan Laboratory of Physics, University of Pennsylvania, Philadelphia, Pennsylvania
December 13, 1945

IT has been found practical to observe the distribution of small amounts of aluminum in silicon by artificially induced radioactivity. This is of interest in the preparation of silicon crystal rectifier material because in this process small amounts of aluminum are often added to pure silicon in vacuum melts. Slabs of silicon doped with fractions of a percent of aluminum are cut and ground flat. They are then exposed to fast neutrons from a large cyclotron for half a day.[2] These neutrons transmute some of the aluminum to radioactive sodium by the reaction $Al^{27}(n,\alpha)Na^{24}$ (14.8 hr.)

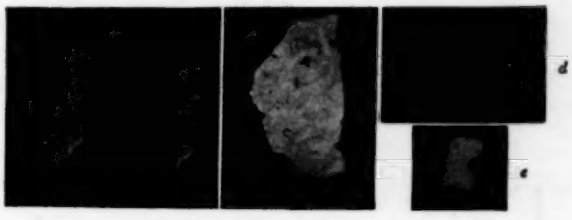

FIG. 1. (*a*) 1-mm thick slab of silicon doped with 0.3 percent aluminum, irradiated with neutrons, placed on x-ray film 24 hours after bombardment, exposed 12 hours; (*b*) Same slab 36 hours after bombardment, exposure 12 hours; (*c*) Optical photograph of same slab, contact face turned up; (*d*) ½-mm thick slabs of aluminum-doped silicon; (*e*) 0.002-cm thick aluminum foil between two slabs of pure silicon ½-mm thick.

FIG. 2. Non-irradiated silicon slabs. (*a*) Lower half ground; (*b*) Exposed to HF; (*c*) Etched with hot NaOH. Exposure 100 hours on Eastman spectroscopic plate.

Since all other induced activities are short-lived, a delay of a day before observation eliminates interfering activities. The slabs are then placed on x-ray film for several hours and the resulting autoradiograph developed. The resolution was about ½ mm, the pattern reproducible and the half-life consistent with the known value of Na^{24}. As shown in Fig. 1, the distribution of aluminum is very non-homogeneous. These streaks of aluminum concentration were not always correlated with grain boundaries. They often extend through thin slabs.

A very disturbing effect was noticed when these silicon surfaces were freshly ground. A uniform darkening of the photographic plate under the slab was found when the slab was ground or etched. This effect was established as the "Russel" effect[3] and seems to be due to a chemical reaction between the silicon surface, water vapor, and possibly air, in which H_2O_2 is produced. This H_2O_2 affects the photographic emulsion so as to make it developable. Pronounced effects of this sort have been reported for Mg, Cd, Zn, Ni, and Al. We have checked its existence in silicon by detecting the production of H_2O_2 by the formation of blue starch-iodide from KI and starch. Figure 2 shows the Russel effects produced by grinding and etching non-irradiated silicon. In autoradiographic exposures of such materials this effect must be avoided.

[1] This work was done in part under Contract No. OEMsr-388 with the Trustees of the University of Pennsylvania under the auspices of the Office of Scientific Research and Development which assumes no responsibility for the accuracy of the statements contained therein. These results were first published in a "classified" technical report dated September 1, 1943. This letter was submitted for clearance on August 30, 1945.
[2] We wish to thank Dr. A. L. Hughes and Mr. Fullbright for their aid in exposing these samples to the Washington University cyclotron.
[3] Colson, Comptes rendus 123, 49 (1896); Russell, Proc. Roy. Soc. 61, 424 (1897); Proc. Roy. Soc. 63, 102 (1898); Proc. Roy. Soc. 64, 409 (1899); Riboul, J. de phys. et rad. [1] 8, 56 (1940).

Proceedings of the American Physical Society

Minutes of the Meeting at St. Louis, November 30–December 1, 1945

THE 268th meeting of the American Physical Society was held in Wayman Crow Hall of Washington University, St. Louis, on Friday, November thirtieth and Saturday, December first, 1945. With this meeting the Society emerged from the difficult years of World War II, with their impediments to travel and their grievous distraction of physicists from the normal life of free interchange of experiences and ideas. The war had indeed ended too lately to permit of the presentation of more than one paper of the category hitherto guarded in secret, but the atmosphere of the meeting and the representation of physicists were already very different from what prevailed at our severely restricted spring meeting. Be it recalled that along with the many limitations of our wartime meetings we are losing also their one attractive feature, the ample leisureliness resulting from the uncongested programmes of which it was often possible for everyone at the meeting to attend most of the papers and discuss them if he so wished. We shall miss this privilege henceforward.

Those who attended this meeting, and the officers of the Society in particular, owe much to Chancellor A. H. Compton who invited us to Washington University and helped in the planning of the x-ray symposium; to the Local Committee, in particular to A. L. Hughes and H. P. Lawther, for making all arrangements; to G. E. M. Jauncey for distributing to all who came a brochure on the "Birth and Early Infancy of X-Rays," of which his speech was a condensation, and to Mrs. A. H. Compton for entertaining the members, guests, and visiting ladies.

The dinner of the Society was held at the Gatesworth Hotel on Friday evening. After-dinner speeches were few and brief, because the Society at the request of some of its members had provided a hall in the Jefferson Hotel for an unofficial discussion of the problems created by the atomic bomb. This discussion was held under the chairmanship of H. H. Goldsmith.

The x-ray symposium mentioned above was held in celebration of the fiftieth anniversary of the discovery. It consisted of twelve papers: the speakers and the titles are given near the end of these Minutes, as also the title of the invited paper by G. A. Boutry of Paris. Following upon these the reader will find the abstracts of the thirty-seven contributed papers.

MEETINGS OF THE COUNCIL

The Council has met twice since the latest preceding issue of these Minutes: in special session at New York on November 10, and in regular session at St. Louis on November 30. At its meeting on November 10 the Council directed that the texts of two suggested amendments to the Constitution of the Society be circulated to the Fellows for inspection; this has been done. G. B. Pegram was renominated to the Governing Board of the American Institute of Physics. E. J. Konopinski, H. H. Nielsen, and E. C. Pollard were nominated to the Board of Editors of the Physical Review, and will be candidates for election for the term 1946–1948.

At the meeting of November 10, four candidates were elected to Fellowship and one hundred and eighty-six to Membership. At the meeting of November 30, seven candidates were elected to Fellowship and sixty-eight to Membership. Their names are appended, as also the names of a number of candidates elected to Membership on May 5, these names having been omitted through inadvertence from the Minutes lately published in *The Physical Review*.

The Society has lost through death the following Fellows and Members of the Society, the letter *F* distinguishing the Fellows: R. S. Bartlett (*F*, Gunnery School); W. H. Dehlinger (Bayside, New York); H. S. Denmark (Battelle); A. S. Fry (General Motors); R. H. Goddard; Wm. James Henderson (National Research Council, Canada); J. L. Hogg (*F*, retired, formerly Bell Telephone Laboratories); D. M. Kabakjian (University of Pennsylvania); I. P. Maizlish (Eastern Kentucky State Teachers College); H. C. Richards (*F*,

University of Pennsylvania); A. V. Ritchie (Beacon, New York); E. C. Wiersma (Delft); P. I. Wold (*F*, Union College); D. L. Zyve (New York).

Elected to Fellowship on November 10, 1945:

Scott Anderson, M. H. Johnson, W. J. Lyons, and N. H. Trytten.

Elected to Fellowship on November 30, 1945:

A. E. Caswell, G. L. Haller, R. C. Herman, J. A. Hipple, Raymond Morgan, Sidney Siegel, and W. E. Shoupp.

Elected to Membership on May 5, 1945 (supplementary list):

Ludwig Adams, N. R. Arthur, G. F. Barnett, T. S. Benedict, T. Benjamin, D. E. Bird, E. C. Blackburn, Marx Brook, Robert Brown, M. J. Buerger, W. E. Burcham, C. E. Cameron, R. E. Carter, H. H. Cary, J. M. Cassels, Madison Cawein, J. H. Coon, P. P. Debye, S. M. Dodds, J. G. E. DuBois, J. A. H. Duffie, E. C. Farmer, Samuel Fine, Edward Fisher, G. N. Fishman, C. M. Fogel, Sholom Friedland, H. M. Froslie, Herman Glaser, L. J. Goodman, Jr., L. L. Green, Mark Gurevitch, W. H. Hannah, A. J. Hartzler, J. M. Hastings, F. L. Hereford, Jr., R. C. Herman, L. C. Hutchinson, Oscar Imalis, Swami Jnanananda, J. A. Karas, R. J. Kennedy, H. B. Klevens, G. M. Koehl, R. J. Kutsky, J. S. Levinger, Bernardo Lombardo, Jr., R. R. Luckey, Donald MacNair, Beatrice S. Magdoff, O. A. Marsh, Paul Miller, Fred Mintz, T. J. Neubert, D. F. O'Brien, R. K. Osborne, J. H. Ramser, J. K. Riess, Reinhold Rüdenberg, J. B. Rust, J. C. Scott, A. H. Smith, S. W. Smith, H. R. Snodgrass, A. C. Spencer, U. M. Staebler, Frieda A. Stahl, E. M. Stubblefield, Sister M. C. Tymann, W. H. Voelker, C. F. Weiher, A. G. Weisner, J. M. West, and G. M. Whetstone, Jr.

Elected to Membership on November 10, 1945:

M. M. Andrew, G. A. Argabrite, R. L. Arnett, R. D. Arnold, Walter Aron, F. H. Averbacher, S. H. Autler, H. F. Balmer, W. C. Barber, W. W. Barna, Milton Becker, T. H. Bedwell, N. A. Begovich, Arthur Bernstein, P. C. Bettler, R. T. Beyer, B. A. Bilby, A. S. Bishop, L. A. Blanchet, Leon Blitzer, Mary Layne Boas, R. O. Bock, B. P. Bogert, G. E. Boyd, Virginia M. Brigham, W. H. Brown, J. O. Buchanan, D. P. Burcham, W. F. Burns, S. B. Burson, Charles Butt, W. I. Caldwell, H. F. Carl, H. A. Carlock, G. R. Carlson, J. R. Carr, R. E. Clapp, P. A. Cole, R. I. Condit, M. C. Cottom, W. J. Cotton, J. L. Dalke, W. T. Davies, Thomas Davis, A. J. deBethune, F. W. Decker, J. W. Dibrell, W. A. Douglas, R. D. Dragsdorf, A. S. Dunbar, Eric Durand, R. L. Ely, Jr., H. J. Evans, G. R. Feaster, W. H. Fenn, J. H. Ferry, Jr., W. B. Fretter, Marjorie Friedman, R. P. Ghelardi, P. R. Girardot, W. W. Gold, W. F. Goodell, Jr., M. H. Greenblatt, T. A. O. Gross, N. N. D. Gupta, J. W. Hackett, S. P. Haddad, C. E. Hall, D. B. Hall, Jane H. Hall, C. N. Hamtil, Gladys I. Heinlein, J. J. Hibbert, Bernard Hildebrand, R. G. Hillger, R. E. Holland, W. D. Hope, R. E. Hopkins, J. A. Hutcheson, H. F. Ivev, H. A. Jarrell, G. W. Johnson, L. G. Jones, J. A. Jungerman, H. E. Kallmann, G. N. Kamm, Ruth E. Kaplan, Samuel Katz, E. J. Kelly, Jr., E. H. Kerner, J. M. Klaasse, J. S. Klein, G. J. Koch, T. M. Lambert, E. L. Langberg, J. M. Lapetina, P. W. Levy, G. E. Liddiard, F. B. Lincoln, Jr., D. P. MacMillan, W. R. Maltby, J. I. Marcum, P. M. Marcus, Fitz-Hugh Marshall, A. N. May, A. O. McCoubrey, W. A. McKinley, E. B. McMillan, F. L. McMillan, Jr., A. W. McReynolds, R. E. Meagher, Alejandro Medina, Jose Medina-Hernandez, J. E. Mekota, Jr., H. E. Metcalf, E. J. Mayer, J. M. Miller, Bernard Miller, W. A. Miller, Johann Mokre, T. I. Monahan, C. L. Moore, H. T. Motz, J. P. Nash, J. R. Niles, Myrtle S. Oberholtzer, A. C. Omberg, N. H. Painter, G. E. Pake, M. L. Polk, W. G. Proctor, F. G. Prohammer, R. C. Raymond, W. O. Reed, B. B. Reynolds, Edwin Richter, S. L. Ridgway, D. B. M. Rosenblatt, J. B. Rothschild, Kalman Rusinow, L. W. Ryan, David Sayre, L. S. Schwartz, H. C. Schweinler, Nathan Shapiro, C. S. Sharp, Nathaniel Shear, Rudolph Sher, F. B. Shull, L. I. Shusset, L. A. Siegel, H. L. Smith, J. B. Smith, O. J. M. Smith, F. S. Stein, R. B. Sutton, W. E. Talvitie, Charles Tanford, R. F. Trimble, C. A. Truesdell, R. E. Trumble, W. Van Roosbroeck, C. E. Vogeley, Jr., Sylvia Vopni, John Wahl, S. E. Walkley, A. W. Waltner, A. G. Ward, B. P. Washburne, Peter Waterman, K. M. Watson, K. H. Weber, J. J. Wedel, Jr., R. T. Weidner, C. E. Weinland, F. O. Werner, C. A. Wert, V. C. Westcott, E. F. Westrum, Jr., E. R. Wicher, R. C. Williams, L T. Winkler, H. E. Wolf, M. L. Yeater, G. J. Yevick, and John Zulon.

Elected to Membership on November 30, 1945:

Sam Adams, A. Arons, W. R. Arnold, J. L. Asmuth, E. C. Barker, Herbert Becker, Raymond BeLair, B. B. Benson, Frances L. Britt, R. N. Close, Ruth A. Cohn, L. J. Cook, E. M. Corson, Samuel Devars, Frederic de Hoffmann, Russell De Waard, J. F. English, Jr., R. T. Harling, Robert Frickel, G. A. Garrett, Dorothy F. Gillette, Marvin Gimprich, Chong Gong, P. L. Gregoire, B. J. W. Grier, R. J. Harrison, J. I. Hoover, Samuel Hopfer, R. N. Hotchkiss, A. G. Hoyem, H. W. Hunter, Franklin Hutchinson, E. D. Jarema, W. B. Jones, P. J. Kaesberg, Norman Knable, Herbert Leaderman, F. E. Martin, P. B. Moon, Rodney Morison, E. V. Murphree, Eldred Nelson, D. C. Peaslee, R. A. Peck, Jr., H. Pomerance, C. A. Randall, Jr., A. F. Reid, H. J. Riblet, J. M. Richardson, G. H. Robillard, B. V. Rollin, B. G. H. Rowley, W. G. Schneider, M. G. Schorr, David Shugar, M. M. Shurman, Miriam Sidran, B. M. Siegel, Martin Siegmann, Thorbjorn Sigurgeirsson, Robert Simha, H. W. B. Skinner, C. A. Stevens, C. J. Swartwout, L. P. Tarasov, A. R. Tobey, E. H. Turner, and S. D. Warshaw.

KARL K. DARROW, *Secretary*
American Physical Society
Columbia University
New York 27, New York

Invited Paper

Notes on the Optics of Organic Glasses. G. A. BOUTRY, *Conservatoire National des Arts et Métiers, Paris.* (35 min.)

Symposium in Celebration of the Fiftieth Anniversary of the Discovery of X-Rays

The Birth and Early Infancy of X-Rays. G. E. M. JAUNCEY, *Washington University.*

The Diffraction of X-Rays by Elements in the Liquid State. N. S. GINGRICH, *University of Missouri.*

Studies of the Structure of Metals by X-Ray Diffraction. C. S. BARRETT, *Carnegie Institute of Technology.*

X-Ray Diffraction Study of the Structure of Glass. B. E. WARREN, *Massachusetts Institute of Technology.*

The Scattering of X-Ray Photons. A. H. COMPTON, *Washington University.*

Evolution of the X-Ray Tube; Powder Metallurgy. A. W. HULL, *General Electric Company.*

An Investigation of Radiography in the Range from 500 to 2500 Kilovolts. R. J. VAN DE GRAAFF, W. W. BUECHNER, H. FESHBACH, A. SPERDUTO, E. A. BURRILL, AND L. R. MCINTOSH, *Massachusetts Institute of Technology.* (To be given by Mr. Van de Graaff.)

X-Ray Therapy. G. FAILLA, *Columbia University.*

Some Problems of Thick and Thin Targets. PAUL KIRKPATRICK, *Stanford University.*

Present Status of the Value of h/e from X-Ray Measurements. J. W. M. DUMOND, *California Institute of Technology.*

Structure in High-Frequency Limit of Continuous X-Ray Spectrum, and Value of h/e. J. A. BEARDEN, *Johns Hopkins University.*

Spectral Fine Structure and its Relation to the Physical State. C. H. SHAW, *Johns Hopkins University.*

Contributed Papers

B1. Decade Counting Circuits. VICTOR H. REGENER, *University of Chicago.*—Pentodes are used in two simple ring-of-ten circuits for high speed counting of pulses from Geiger tubes or for accurate frequency measurements. One circuit uses in one ring ten miniature pentodes type 6AK6, thirty resistors and ten condensers. This circuit is especially suited for the counting of sharp pulses. The other circuit uses in one ring ten twin-pentodes type 12L8-GT, twenty resistors, and no condensers. This circuit is especially suited for frequency measurements of periodic currents of arbitrary wave form and of frequencies from zero to above 10^5 cycles per second. The number of pulses or cycles received by a ring-of-ten is indicated on the screen of a one-inch cathode-ray tube type 913. The spot on the screen has ten possible positions, arranged on a circle, corresponding to the ten states of equilibrium of the ring-of-ten. When counting, the spot moves successively through the ten positions. Several of these ring-of-ten units, each with its cathode-ray tube, can be connected in cascade. Thus, electronic counting with direct indication of the decimal figures is made possible.

B2. Geiger-Muller Counter Technique for High Counting Rates. C. O. MUEHLHAUSE AND H. FRIEDMAN, *U.S. Naval Research Laboratory.*—Counting rates of 100,000 per second have been measured with a self-quenching G-M counter operated at 50 to 100 volts above threshold. The counter was coupled to a video amplifier having linear response to four megacycles per second and a maximum gain between 10^3 and 10^4. The amplified pulses were counted by a scaling circuit capable of responding to uniform pulse rates up to two megacycles per second. The triggered sweep oscilloscope method, devised by Stever* to measure "dead-time," was applied to the present combination of counter and amplifier. At amplifications under ten, a dead-time interval of 3×10^{-4} second was observed, in agreement with Stever's results. At higher amplifications the dead-time pattern persisted but pulses were observed within the dead-time interval. These latter pulses arise from impact ionization in the reduced fields that exist immediately following the formation of a positive ion sheath, and make possible the high counting rates observed.

* H. G. Stever, Phys. Rev. 61, 38 (1942).

B3. Recurrences of Small Bursts of Cosmic Rays. JAMES W. BROXON, *University of Colorado.*—Upon analysis by Chree's method of superposed epochs, the writer[1] found pulses at about 28-day intervals in the intensity of cosmic radiation measured by Long and Whaley[2] at Boulder during 18 months in 1938–39. In the same investigation, they found indications of both diurnal and seasonal variations in frequency of the smallest bursts they recorded. These bursts corresponded to about 3×10^6 ion pairs in the heavily shielded, spherical chamber of 13.8 liters. Application of Chree's method to the frequency of these small bursts over the n-day range, $-45\leqslant n\leqslant 45$, shows irregular but apparently significant loops. Both preceding and subsequent difference curves indicate pulses with peaks

at about 27 days before and after the selected days of high or low frequency of the small bursts. The combination of difference curves formed by the average of frequencies for positive and negative day numbers of the same magnitude agree with the individual difference curves. The secondary pulses correspond to variations of some 3 or 4 percent from the average frequency of 36 small bursts per day.

[1] J. W. Broxon, Phys. Rev. **59**, 773 (1941).
[2] V. A. Long and R. M. Whaley, Phys. Rev. **59**, 470A (1941).

B4. Experiments on the Elastic Single Scattering of Electrons by Nuclei. R. J. VAN DE GRAAFF, W. W. BUECHNER, AND H. FESHBACH, *Massachusetts Institute of Technology.*—Experiments completed in July, 1941 on the elastic single scattering of electrons by nuclei are described. Observations were made at voltages from 1.27 to 2.27 Mev and at angles from 20° to 50°. The scattering foils were aluminum, copper, silver, platinum, and gold. The use of an accurately focused homogeneous beam of electrons from an electrostatic generator made possible a clear-cut control of experimental variables, the method being designed to minimize the effect of x-ray background, etc. The present results are in close agreement with the Mott theory over the entire range of the experimental variables except for the case of 2.27 Mev electrons striking aluminum. Excepting only this case, the average of all the ratios of experimental result to theoretical prediction is 1.01 with a standard deviation of 0.07. This is in contrast with the wide divergence in most previous work in this field. The results of this paper extend the range of validity of the Coulomb law of attraction between electron and nucleus in close to the surface of the nucleus. The scattering of 2.27 Mev electrons by aluminum will be repeated as these results now indicate for the larger angles an interesting divergence from theory.

B5. The Lifetimes of Metastable States. MARCELLUS L. WIEDENBECK, *University of Notre Dame.*—Estimates of the lifetime of metastable states of isomeric nuclei against γ-emission have been given by Bethe[1] and Hebb and Uhlenbeck.[2] The latter authors have also proposed a correction for Bethe's lifetimes in order to take into account the additive decay probability brought about by internal conversion. Available data on forty metastable states of nuclei (stable and unstable) have been plotted and compared with the present theories. With only four exceptions, all points lie near two parallel lines when $\log \lambda(\text{sec.}^{-1})$ is plotted against $\log E$ (Mev). These empirical lines are in the region of, and intersect those obtained from Bethe's formula for spin changes of four and five units. The agreement is greatly improved if the correction for internal conversion is taken into account. In the range considered, the agreement with the relationship given by Hebb and Uhlenbeck is less close. Experimental verification of these spin changes can be obtained by measuring the conversion coefficients or, if a sufficient quantity of active material is available, the spin of the isomer may be measured directly.

[1] H. A. Bethe, Rev. Mod. Phys. **9**, 226 (1937).
[2] M. H. Hebb and G. E. Uhlenbeck, Physica **5**, 605 (1938).

B6. Wide and Sharp Neutron Groups. A. A. YALOW* AND M. GOLDHABER, *University of Illinois.*—We have continued our studies of wide and sharp neutron groups. For nuclei of odd charge and odd mass number, of which we have investigated a fairly representative sample, it appears that sharp levels cluster around low neutron energies. The "double filter method" [1] has been extended to further cases (Rh, In, Ir, and Au). In Ir (19*h*) the activity induced by D neutrons can be effectively eliminated by an In filter. The remaining activity, 30 percent in our arrangement, is due to a group with an energy of approximately 50 ev. The absorption in B with and without "self-filtration" has been measured for several wide groups (Br (18 min.), I (25 min.) and As (26.8h)). The absorption decreases with self-filtration, as was known previously for I. It seems plausible that this effect is due to the preferential removal by the filter of the oblique neutron rays from the non-parallel beam. For the remaining "straightened" beam the effective boron thickness is thus decreased.

* Now at the Federal Telephone and Radio Laboratories, New York, New York.
[1] A. A. Yalow and M. Goldhaber, Phys. Rev. **68**, 99A (1945).

B7. Resonance Scattering of Group Neutrons. M. GOLDHABER AND A. A. YALOW,* *University of Illinois.*—In the course of an investigation of the absorption in B and Mn of the R neutrons activating a Mn detector, and in experiments in which Mn absorbers were used with different detectors, we noticed some anomalies which it seemed possible to explain by assuming that Mn is activated by neutrons from two regions: a broad low energy region (strong absorption in B, weak absorption in Mn) and a resonance region with an energy >50 ev (weak absorption in B, strong absorption in Mn), where strong resonance scattering also takes place. This assumption was tested by a series of experiments in which the primary R neutrons were reflected from Mn, C, and other scatterers, and the secondary neutrons recorded by various group detectors responding to different neutron energies. Mn and Br (18 min.) proved the most sensitive detectors for the secondary neutrons from a Mn reflector. The absorption of the primary R neutron component which is reflected by Mn, was studied in a number of absorbers and was found to be particularly strong in Mn. The resonance character of the scattering in Mn seems thus established.

* Now at the Federal Telephone and Radio Laboratories, New York New York.

B8. Nuclear Processes by Polarization Scattering of Deuterons. EUGENE GUTH, *University of Notre Dame.*—The deuteron, because of its low binding energy, may be polarized by the field of a nucleus that it strikes. In this way the neutron may come close enough to the nucleus to enable an energy transfer from the deuteron to the nucleus without the necessity of a (d,d) reaction or even excitation by the Coulomb field of the deuteron. This new process by "polarization scattering" is somewhat similar to the well-known Oppenheimer-Phillips process, but differs from it essentially in that the outgoing particle is not a proton but

a deuteron. This difference makes it possible to distinguish between the two processes even when the conditions for the O-P-process are fulfilled (kinetic energy of the deuteron larger than its binding energy; medium and heavy nuclei); the same holds for excitation of the nucleus by a deuteron disintegrated by the Coulomb field of the nucleus, and for the ordinary (d,d) reaction mentioned before. As an example for the new process, In^{115} should be excitable by deuterons; this prediction was actually verified by M. L. Wiedenbeck (personal communication), thus proving the existence of polarization scattering. Observation of the inelastically scattered deuterons seems to be a promising method for studying nuclear spectroscopy. Polarization scattering may be used, among other things, to liberate neutrons from Be^9 and D, etc.

C1. The Photomultiplier X-Ray Detector. FITZ-HUGH MARSHALL AND L. P. HUNTER, *Westinghouse Research Laboratories. (Introduced by J. W. Coltman.)*—To the conventional list of x-ray detectors—photographic film, fluorescent screen, ionization chamber, and Geiger or proportional counter—a new instrument has been added in recent years. It consists of a photo-multiplier tube measuring the light from a fluorescent screen. It has high practical sensitivity, and it is extremely fast, the response time being of the order of microseconds. While it does not show drift of the type usually observed in d.c. amplification of ionization chamber currents, it is sensitive to changes of potential applied to the photo-multiplier tube and is subject to various fatigue effects. The present work has been devoted to studying the characteristics of the photo-multiplier x-ray detector and comparing them with those of the ionization chamber and other x-ray detectors. Particular attention has been given to speed of response and limitation of sensitivity by noise. Fatigue effects have been found to arise in the later stages of secondary emission amplification in the photo-multiplier tube.

C2. Fluorescent Yield of Calcium Tungstate Excited by X-Rays. E. G. EBBIGHAUSEN AND J. W. COLTMAN, *Westinghouse Research Laboratories.*—The fluorescent energy yield from a calcium tungstate screen and its spectral distribution were determined by comparison with the spectrum of a standard tungsten lamp. The energy distribution of the lamp was calculated on the basis of the temperature, the spectral emissivity of tungsten and the transmission of the quartz lamp window. A quartz spectrograph was used, and reciprocity law failure was avoided by appropriate reduction of the light from the lamp. Exposure times varied from twenty minutes to one hour depending on the region of the spectrum. The combined results from seven plates gave a spectral curve extending from 3500A to 6200A with a maximum at 4150A. The total light energy out (after correcting for the angular distribution from the screen) was 14.8 ergs/cm² per r-unit incident at 80 kv constant potential with 1 mm aluminum and ½ mm copper filter. Using curves[1] of the energy distribution of the x-rays, the relation between the r-unit and energy for various wave-lengths, and the absorption coefficient of calcium tungstate, the energy absorbed was calculated and an over-all conversion efficiency of 2.8 percent was obtained.

[1] Terry and Ulrey, *X-Ray Technology.*

C3. The X-Ray K Absorption Edge of Silicon. VOLA P. BARTON, *Goucher College,* AND GEO. A. LINDSAY, *University of Michigan.*—Very few measurements of the K absorption edge of silicon have been made. In 1925 Lindh found 6731 x.u. for the wave-length in silicon metal and about 6707 x.u. for silicon in the compounds SiO_2, Na_2SiO_3, and K_2SiO_3. In 1931 Deodhar found for silicon in quartz 6706 x.u. by using quartz as the reflecting crystal. For these wave-lengths it is difficult to prepare screens which are thin enough and still capable of being handled. In the present work reflecting crystals of quartz and of four different micas were used, and in addition silicon and Na_2SiO_3 in a finely powdered form were put on the face of a gypsum crystal. The reference lines were in higher orders, thus necessitating a correction for refraction. By applying the correction for refraction the wave-length of the absorption edge of silicon in all the compounds examined was found to be practically the same—about 6700 x.u., while that of silicon metal was 6716 x.u. If the refraction correction is not made the wave-lengths for the various compounds differ much more among themselves.

C4. X-Ray Energy Level Widths of Tungsten. JOHN N. COOPER, *University of Oklahoma.*—Data on the widths of K^1, L^2, and M^3 series lines of tungsten enable one to estimate the widths of certain energy levels on the assumption that the energy width of any line is the sum of the level widths involved in the transition. If mutually self-consistent widths are assigned to the K, L, and M levels, very large differences arise in the widths of the N_{II} and N_{III} levels as calculated from the breadths of lines involving these states. The differences are far too great to be explained by reasonable experimental errors or by the uncertainties in the corrections applied for crystal diffraction patterns. [The reported width of $M\zeta_1(M_VN_{III})$ is ten times the sum of the widths of $M\alpha_2(M_VN_{VI})$ and $M\delta(M_{IV}N_{III})$. As MBS[3] have observed, this is utterly inconsistent with the above assumption.] Accordingly, it appears that the Weisskopf-Wigner theory of line widths is not adequate to explain the observed breadths in all cases.

[1] Richtmyer and Barnes, Phys. Rev. **46**, 352 (1934).
[2] John N. Cooper, Phys. Rev. **61**, 234 (1942).
[3] Munier, Bearden, and Shaw, Phys. Rev. **58**, 537 (1940).

C5. The Curved Crystal Spectrograph Applied to Determine the Complete Spectrum of All Orders Obtained when the Camera Is Rotated about a Proper Pivot. JOHN W. FARNHAM, J. E. EDWARDS, AND F. C. BLAKE, *Ohio State University.*—Using Larsson's value for the index of refraction of α-quartz the attempt is made to compare the Bragg angles for the several orders of Faces 100 and 110 as measured by the powder method and by the curved crystal spectrograph method. The second order of 130 and

310, however, does not appear since, for this order, the oxygen and silicon atoms practically neutralize one another.

C6. On the Proper Indexing of the Crystal Faces of α-Quartz by the Powder Method and the Calculation of Their Structure Factors for Both Right-Handed and Left-Handed α-Quartz. F. C. BLAKE, *Ohio State University.*—On account of the importance of α-quartz in thin sections in the curved crystal spectrograph[1] tables will be presented for all possible faces of α-quartz as determined by the powder method using the molybdenum $K\alpha$-doublet at 40 kilovolts. Comparison is also made with Bradley and Jay's determinations[2] made with Cu $K\alpha_1$, all of the unindexed lines in their work being properly indexed. Tables of the unreduced structure factors for both right-handed and left-handed quartz will be shown. Comment will be made on the matters of twinning and interpenetration of twins.

[1] E.g., Edwards, Pool, and Blake, Phys. Rev. **67**, 150 (1945).
[2] Phys. Soc. London **45**, 507 (1933).

C7. Characteristic X-Rays Excited by Beta-Particles. J. E. EDWARDS AND M. L. POOL, *Ohio State University.*—X-ray photographs of 12.8-hour Cu^{64} taken with a curved crystal spectrograph[1] show x-ray lines characteristic of Cu and Ni. Since there is no other evidence for the existence of a genetically related isomeric pair in Cu^{64}, the characteristic Cu x-rays are probably excited by the strong β-activity also present in the 12.8-hour period. Further evidence to support this view was obtained by photographing a piece of inactive Cu foil while it was being bombarded by P^{32} β-particles whose maximum energy is 1.7 Mev. With a P^{32} β-activity comparable with the β-activity in the deuteron activated Cu, x-rays characteristic of Cu were observed. Similar photographs of characteristic x-rays excited by P^{32} β-particles in other elements were obtained. The characteristic x-rays and general x-radiation excited by P^{32} β-particles in Al, Cu, Ag, Sn, and Pb were also studied by absorption of the radiation in Al, Cu, and Pb. The ratio of the intensity of the characteristic radiation to the average intensity of the general radiation is rather high. Thus the appearance of characteristic x-rays in the presence of a strong β-activity does not always indicate K-capture or internal conversion.

[1] J. E. Edwards, M. L. Pool, and F. C. Blake, Phys. Rev. **67**, 150 (1945).

C8. X-Rays from Radioactive Te. M. L. POOL AND J. E. EDWARDS, *Ohio State University.*—A radioactive isomer has been found in Te^{121} with the aid of a curved crystal x-ray spectrograph. The pair consists of a new 17 ± 1 day activity produced by the reactions $Sb(d, 2n)$ and $Sb(p, n)$ and a previously assigned activity evaluated here as 143 ± 5 days. X-ray photographs of characteristic radiation from Te^{121} were taken during various phases of decay extending over a period of 235 days. Sb and Te x-rays, a 0.61-Mev gamma-ray, a 0.223-Mev gamma-ray, and conversion electrons are associated with the long period. Sb x-rays and a 0.61-Mev gamma-ray are associated with the short period. The observations are simply explained by the isomeric transition. No evidence of the "fast" gamma transition[1] was found. Satellite x-ray lines were not observed near the strong characteristic lines.

[1] R. D. O'Neal and Gertrud Scharff-Goldhaber, Phys. Rev. **62**, 83 (1942).

C9. Thickness Measurements of Thin Coatings by X-Ray Absorption. L. S. BIRKS AND H. FRIEDMAN, *U.S. Naval Research Laboratory.*—An x-ray absorption method was applied to the measurement of thin films on thick crystalline or polycrystalline backings. Characteristic x-rays were reflected from the base material at one of the Bragg diffraction angles, and the diffracted intensity measured by a Geiger counter system. When the base material was covered with a thin coating, the x-rays were reduced in intensity according to the exponential absorption law for the coating material. From the measured ratio of intensities for the coated and uncoated backing, the geometry of the arrangement, and the known absorption coefficient for the coating, it was possible to compute the thickness of the coating. Measurements were made with a powder diffraction spectrometer[1] utilizing the focusing principle. The area of specimen covered by the x-ray beam was varied between one square centimeter and one square millimeter. Metal plating thicknesses were determined in the range 10^{-5} to 10^{-2} centimeters. The method is generally applicable to coatings of any material or combination of materials whose x-ray absorption coefficients are known.

[1] H. Friedman, Electronics **18**, 132 (April, 1945).

C10. X-Ray Measurement of the Thickness of Silver Plating. R. B. GRAY, *Erie Resistor Corporation.*—The thickness of a plated metal layer can be determined by comparing the intensities of the back-reflection lines of the base metal and the plated metal. The intensity ratio is

$$\frac{i_p}{i_B}=\frac{k_p}{k_B}\cdot\frac{\mu_B(1+\sec\theta_B)}{\mu_p(1+\sec\theta_p}\cdot[\exp(-\mu_p(1+\sec\theta_B)\rho)-\exp(-\mu_p(\sec\theta_B-\sec\theta_p)\rho)].$$

A photograph of silver plated brass was made using Fe $K\alpha$ radiation. The 311 planes were found to be most suitable for comparison. The x-ray method indicated a thickness of 2.2 microns. Chemical stripping of the whole piece indicated a thickness of 3.3 microns. This difference is due to the extra build-up which occurs at the corners of plated pieces.

D1. Note on Accelerational-Velocital Magnetic Forces. F. W. WARBURTON, *University of Kentucky.*—Additional symmetric $1/c^3$ terms in the mutual force of two charges, obtained with the general Lagrangian equation and relative potential energy, give zero average force and torque of a conduction electron on a circular electronic orbit, when local variations in force are neglected. This periodic disturbance of the electron in the orbit—which disappears for alignment of orbital axes parallel and antiparallel to current in the rod—is of the order of one to ten percent of the applied magnetizing force in the experiments showing the "shock effect." The factor containing velocity of one charge and acceleration of the other suggests that local variation of this force on non-circular orbits may account

for the change in magnetization in nickel, found by Perkins, which reverses with the velocity or acceleration of the conduction electrons. As another argument for the more general basic force formula for charges, the restriction in the $1/c^3$ terms imposed by classical propagation of the non-reciprocal magnetic force in $1/c^2$, is compared with restrictions in $1/c^3$ magnetic terms which would be imposed by propagation of the electrostatic force alone.

D2. A Study of Stationary Electromagnetic Modes for Region Between Parallel Perfectly Conducting Planes and Application to Electron Accelerator. E. S. AKELEY, *Purdue University.*—The fundamental stationary *TM* modes possessing circular symmetry relative to axis perpendicular to planes are found. The relative intensity of modes are fixed by perfectly conducting surface of revolution $y(z)$ connecting planes; y is radius of one surface and z distance from one plane. There are three types of modes $\lambda_0<\lambda_1$, $\lambda_0=\lambda_1$, $\lambda_0>\lambda_1$ where λ_0 is wave-length in absence of planes and λ wave-length on axis between planes. Simultaneous excitation of modes $\lambda=\lambda_0$ and $\lambda=\lambda_0/2n+1$ is treated. Requirement *y finite* fixes relative intensity for given $y(0)$ and makes surface meet planes at right angles. If $y(0)>Y$ (Y depending only on n), surface deviates only slightly from that for one mode $\lambda=\lambda_0$ except in neighborhood of planes. If $y(0)<Y$ surface has $2n$ cusps. Numerical integration is used to determine shapes of surfaces and their relative dissipation of energy—an important consideration in design of electron accelerator. In accelerator only the mode $\lambda=\lambda_0$ causes acceleration of electron, the other mode is required to keep size of cavity finite.

D3. A Comparison of the High Frequency Accelerator and Betatron as a Source of High Energy Electrons. J. R. WOODYARD, *Purdue University.*—A cavity resonator consisting of a long cylinder oscillating in a high order longitudinal electric mode may be used as a linear accelerator of electrons, provided electrical loading is added to give the nodes the required spacing. Typical methods of loading are compared. The average power requirements can be brought down to reasonable values by driving the resonator in short bursts instead of continuously, as is well known in ionosphere work. By making the resonator sufficiently long, any energy can be obtained, at least in principle. The total cost should vary directly as the length and therefore as the electron energy for such an accelerator. With a betatron, on the other hand, the weight and cost vary approximately as the cube of the energy. Therefore, above some value of electon voltage, the linear accelerator would be preferable from the standpoint of cost. More or less crude estimates place the cross-over point around 100 megavolts. In addition, the linear accelerator excels in ease of bringing out a beam of electrons, in case internal target bombardment is not desired. Approximate numbers are given for the amount of power required in terms of electron voltage and tube length.

D4. Effect of Transverse Pressure on the Steady-State Electrical Conductivity of Rocksalt. CHARLES N. HAMTIL,* *St. Louis University.*—The effect of transverse pressure on the steady-state electrical conductivity of rocksalt was investigated in the temperature range 300–317 deg. C. The change in resistivity of the crystal when subjected to pressure was determined from the change in deflection of a high-sensitivity galvanometer in the crystal circuit. The e.m.f. applied to the crystal was 100 volts d.c. Pressure was applied to the crystal in a direction normal to the straight line joining the two electrodes, by means of flat steel plates insulated from the crystal. It was found that when transverse pressure of 33 kg/cm^2 is applied to a crystal, there results an increase in conductivity whose magnitude is approximately 7 percent of the steady-state conductivity of the unloaded crystal. The effect is attributed to a lowering by pressure of the counter-e.m.f. of polarization. It is suggested that the application of pressure causes some ions in the "polarization layers" to return to normal lattice positions.

* Now at Rockhurst College, Kansas City, Missouri.

D5. Investigation of the Surface Photoelectric Effect of Metallic Films under the Influence of Strong Electrostatic Fields. VINCENT P. JACOBSMEYER, S.J., *St. Louis University.*—This investigation was a preliminary test of the Guth-Mullin[1] theory of the "photoelectric analog of the Schottky effect." The variation of the photoelectric current with strong electrostatic fields (at least to 1.4×10^6 volts/cm) was observed for various conditions of the photoelectric surface and for different cathode-anode geometries. The emission surfaces were Bi films of approximately 900 and 500 atom-layers, respectively, deposited at room temperature by evaporation in high vacuum on a surface of liquid bright Pt, and also a liquid bright Pt surface not covered with Bi. The photoelectric currents for sixteen runs fluctuate about a fixed reference "Schottky line" (the most probable straight line through the experimental points as calculated by the method of least squares). A comparison of the position of the maxima and minima of the curves obtained is made with the experimental thermionic results of Seifert and Phipps[2] and the theoretical derivations for the photoelectric by Guth and Mullin.[1] It is concluded that a real variation of photoelectric current with applied electric field is observed which has the approximately periodic character predicted by Guth and Mullin.[1]

[1] E. Guth and C. J. Mullin, Phys. Rev. 59, 575 (1941).
[2] R. L. E. Seifert and T. E. Phipps, Phys. Rev. 56, 652 (1939).

D6. Initiation of High Frequency Gas Discharges. T. HOLSTEIN, *Westinghouse Research Laboratories.*—A general characteristic of gas discharges in electric fields of microwave frequencies ($\omega>3000$ megacycles/sec.) is that the drift motion of electrons in one period is much smaller than the linear dimensions of the discharge region. Under these conditions the only important cause of electron removal in gases which do not attach electrons is diffusion to the walls. The sparking condition is: rate of ionization >rate of diffusion. In a discharge region contained between two electrodes separated by a distance, d, and in a pressure range such that $\omega\tau_i>1$, $\omega\tau_e<1$, $d^2\gg\lambda_i\lambda_e$ (where τ_e, τ_i, λ_e, and λ_i are the mean times and free paths for elastic and

inelastic collision) the ionization and diffusion rates are the same as those which prevail in a spatially constant d.c. field whose magnitude is equal to the r.m.s. value of the high frequency field. The relation between X, the r.m.s. value of the sparking field, p, the pressure, and d, in terms of the electron temperature, T_e, and Townsend's α, is found to be

$$(pd)^2 = \pi^2 K T_e [(\alpha/p)(X/p)e]^{-1}.$$

This formula has been applied to obtain high frequency sparking fields for a number of different gases.

D7. Extinction of Gaseous Discharges. ERNEST MAYER, *Westinghouse Research Laboratories.*—The role of ambipolar diffusion in the extinction of gaseous discharges has been investigated. On the assumptions of a Maxwellian distribution for electron energies and constant electronic mean free path, the electron temperature T_e decreases, due to elastic collisions with gas atoms, according to the formula

$$T_e = T_g \coth^2 ((T_g/T_0)^{\frac{1}{2}} + At),$$

with T_g the gas temperature, T_0 the initial electron temperature, and A a constant involving gas and electron parameters. For a simplified one-dimensional model of the discharge region the time and space dependence of the electron concentration n is

$$n = n_0 \cos \frac{\pi x}{d} \exp\left[-B\left(\frac{T_0/T_g}{(T_0/T_g)^{\frac{1}{2}} + \coth At} + 2At\right)\right],$$

where d is the electrode separation, B is a constant involving d and the gas and electron parameters. Curves of T_e/T_0 and n/n_0 *vs.* time are calculated for a neon discharge under typical operating conditions.

D8. Heat Conduction Effects with Liquid Crystals and Suspended Particles. G. W. STEWART, *State University of Iowa.*—The transverse orientation of liquid crystals in a heat flow is reviewed, and the cause of the phenomenon is not found in differential temperature expansion, the momentum of high frequency acoustic waves, the anisotropic heat conduction in the liquid crystals and in unavoidable convection currents. The liquid crystals are not immersed in an isotropic liquid, but it is interesting to note that tobacco virus and vanadium pentoxide floating in water do not show an orientation in heat flow.

D9. Rapid and Direct Measurement of Vapor Pressure of Liquid Metals. A. H. WEBER AND M. GONZAGA PLANTENBERG, O.S.B., *St. Louis University.*—Studies of various properties of thin metallic films have led to the development in this laboratory of a rapid direct method for measuring the vapor pressure of the liquid metals evaporated to form these films. The method employs a vacuum microbalance, consisting of a glass bucket hanging from an helical quartz spring,[1] of sensitivity 4.20×10^{-7} g/scale division. From kinetic theory the force F (of impact of a beam of atoms, issuing from an orifice of area dS, upon the bucket bottom which subtends the solid angle $d\omega$ at dS) is related to the vapor pressure p of the evaporating metal by

$$p = 2\pi F/dSd\omega.$$

F is measured directly by observing the decrease in length of the quartz spring when a shutter between the bucket bottom and the orifice dS is opened. The vapor pressure of a metal can be determined in 2–3 minutes compared to the many hours required in the previous method.[2] Preliminary results with Bi are reported and discussed.

[1] Gift of The General Electric Company.
[2] A. H. Weber and S. C. Kirsch, S.J., Phys. Rev. 57, 1042 (1940).

E1. On a Statistical Approach to Biological Effects of Radiations. I. OPATOWSKI, *University of Chicago.*—The paper develops the idea of W. F. G. Swann[1] according to which the living matter undergoes under the effect of radiations a number of successive transitions between certain states 0, 1, $\cdots n$. By a biological mechanism the organism may return spontaneously to its original state 0 through reverse transitions. Irradiation of an aggregate of microorganisms is considered under the assumption that the transition frequencies are constant in time but may be different for each single type of transition. Experiments give the percentage P of microorganisms accomplishing the transition $(0 \rightarrow n)$ within a time of radiation t. It is shown that any process admitting reverse transitions from some or from all states, except from the nth state, gives rise to the same relation $P(t)$ as a suitable process between the same states but without reverse transitions. Consequently, in order to obtain information on the biological reaction of the microorganisms, knowing $P(t)$ for several radiation intensities I, it is necessary to know also the dependence of the transition frequencies on I. The paper will appear in the December, 1945 issue of the *Bulletin of Mathematical Biophysics.*

[1] W. F. G. Swann and C. Del Rosario, J. Frank. Inst. 211, 303–317 (1931).

E2. Specific Heats of Hevea, GR-S and GR-I Polymers. B. A. MROWCA, R. L. ANTHONY. AND W. H. HAMILL, *Notre Dame University.*—A calorimeter, suitable for the rapid determination of specific heats of new polymers, is described. The results obtained have a precision much better than those obtained by simple mixture methods. Specific heat values are reported for Hevea and GR-S gum and tread stocks, for raw butyl (Butyl B-1.45) and for a butyl gum stock. It is shown by direct measurement that specific heats of compounded stocks can be calculated quite accurately by adding the fractional specific heats of the ingredients, and therefore do not need to be measured when the specific heat of the raw rubber is known. The specific heat of a standard carbon black (standard micronex) as it exists in the rubber is found to be 0.18 cal./g/1°C, a value identical with the specific heat of graphite. It is shown that for all rubbers upon which thermodynamic studies have been made the observed dependence of stress upon temperature requires that variations in C_L, the specific heat at constant length, with L be so small as to affect only the 4th significant figure in the specific heat.

E3. Fast Stress-Strain Machine. S. L. DART, R. L. ANTHONY, AND P. E. WACK, *Notre Dame University.*—It is of great importance in the study of rubber to obtain a stress-strain curve with sufficient rapidity that it may be relatively free from time effects. Such a curve may be used to give the stress-temperature relations of rubber and, in conjunction with adiabatic temperature rise measurements, to give the entropy and internal energy components of the stress. A machine which will record a complete stress-strain loop at the rate of about 100 percent a second and is relatively free from inertial effects has been developed in the Rubber Research Laboratory, University of Notre Dame. This machine uses the principle of a mechanical balance and has an accuracy of about 1 percent deviation from the mean. It shows not only the correct S shaped curve but also the correct temperature behavior for natural rubber. By the use of a special type clamp and of properly shaped samples true elongations can be read directly from the recorded clamp separations.

E4. Phase Transitions at Low Temperatures in Natural and Synthetic Rubber. PAUL E. WACK, *Notre Dame University.*—Phase transitions in natural and synthetic gum stocks were studied at low temperatures ranging from +25°C to −75°C. Mechanical changes accompanying the phase transitions were observed, in particular the changes in stress with temperature and time at constant length of the sample, i.e., stress-relaxation, and isometrics, and the changes in length as a function of temperature and time at constant stress, i.e., creep and isotonics. An autographic stress-time-temperature machine was designed so that a maximum movement of the rubber of 0.1 mm would set the automatic balancing mechanism into action. This feature is of the highest importance for the observation of second-order transitions. For Hevea gum, crystallization was observed at low temperatures for only those elongations above 200 percent. The maximum rate of crystallization occurred at −20°C. The stress-strain curve obtained by cross plotting the stress-temperature curves at −50°C for instance shows a "well," due to the decrease of stress upon crystallization, similar to the behavior of a van der Waals gas. Internal energy and entropy curves as a function of elongation were obtained from the stress-temperature curves. The data cover a wider range of variables than any of the data published hitherto.

E5. Mechanism of Natural Oxidation of Aluminum, Iron, and Copper. SCOTT ANDERSON, *Anderson Physical Laboratory.*—The author's theory of electrolytic oxidation of aluminum has been extended to include the natural oxidation of aluminum, iron, and copper. When so applied, it appears that space charges control the rate of growth in the early stages. Equations are devised for the three stages of growth, (1) when the mean free path of the moving particles is large in comparison to the oxide thickness, (2) when the mean free path of the moving particles is small in comparison to the oxide thickness, and (3) when the oxide is so thick that space charges are no longer the controlling factor. These equations predict a third power law of rate of growth for stage 1, a fourth power rate for stage 2, and a quadratic law of growth for stage 3. The equations are compared with data of numerous experimenters and agree quite well with the observed rates.

E6. Forced Vibrations of a Whirling Wire.* A. VICTOR MASKET, *Naval Research Laboratory.*—The method of the Laplace transformation and contour integration has been applied to obtain a series solution for the partial differential equation governing the transverse vibrations of a long thin wire subject to a combined static tension and centrifugal force when the moving end is forced to execute a sinusoidal motion. The novel features of the solution are first, the eigenfunctions are the transcendental Legendre functions and second, the functions are not orthogonal over any interval of the defined range of validity. The associated problem of resonance is solvable by the same technique.

* Published by permission of the U. S. Navy Dept.

E7. Helical Movements of Matter in the Beam of Light and the Magnetic Current. FELIX EHRENHAFT, *New York City.*—Photomicrographs of light-positive and light-negative helical movements of testbodies[1] in the concentrated beam of natural sunlight without and with superimposed homogeneous magnetic or electric field parallel to the propagation of light will be shown. There are up to 150 regular spaced turns per second in gas of atmospheric pressure. The diameter of the helical path is often 100 times larger than the radius of the moving testbody. The red end of the visible solar spectrum causes no noticeable photophoretic movement of smoke particles, whereas the end of visible blue-violet causes their light-negative movement (experiment, R. Whitall, H. W. Zieler). An iron particle, radius about 1.5×10^{-4} cm, describes in the horizontal homogeneous magnetic field of 50 gauss parallel to the concentrated natural beam of sunlight during half a second a helical path, the diameter of which is in average 2.7×10^{-3} cm; the average distance between the seven consecutive turns is 1.4×10^{-3} cm. Its photophoretic velocity without external magnetic field is about 1.1×10^{-2} cm/sec. Therefore the longitudinal magnetic field in this concentrated beam itself is approximately 64 gauss. The electric charge of the particle is about 1×10^{-9} e.s.u. The magnetic charge is about 2.5×10^{-12} m.s.e. The aforesaid movement gives evidence of electric action of magnetic current. The question of balance of energy responsible for these tremendous helical movements arises. The principle of conservation of linear and angular momentum of electrodynamics and the equation of F. Hasenoehrl $E=(4/3)mc^2$ for blackbody radiation, generalized later on by A. Einstein and applied for radioactive radiation, has to be radically modified for natural light.

[1] Science **101**, 676 (1945).

E8. A Quantitative Method for the Spectroscopic Analysis of Potassium-Sodium Solution. WAYNE SCANLON, *Purdue University.*—A rapid and accurate method of quantitative analysis of sodium and potassium was developed which gives direct measurement of concentrations ranging

from 10 mg/100 cc to 200 mg/100 cc. The solution containing the sodium and potassium is sprayed into a flame where the resonance lines of these elements alone are appreciably excited. The resonance lines of sodium at 5890 and 5895A and those of potassium at 7664 and 7699A are separated enough in the spectrum to permit their isolation almost completely by means of color filters. The light from the flame is by this means separated, one color falling on a red sensitive photoelectric cell and the other on a yellow sensitive cell. The photoelectric current is measured by means of a high sensitive galvanometer. The illumination gas and air mixture that gave the most stable conditions was determined. These could be maintained steady enough to permit calibration of the galvanometer scale in terms of concentrations of potassium and sodium. The amount of solution required is small, as little as 1 cc being sufficient. The results obtained on test solutions showed errors not greater than about 3 percent to 5 percent.

E9. A New and Rapid Method for Constructing Quarter-Wave Plates, Half-Wave Plates, Half Shades and Ellipticity Compensators. WILFRIED HELLER, *University of Chicago.*—The traditional method of constructing such devices by splitting mica or by reducing calcite or quartz plates to the optimum or critical thickness, is both expensive and time consuming. For precision measurements at 5890A, for example, a Senarmont compensator must consist of mica 29.45 microns thick. A new and rapid method for obtaining such devices for any wave-length desired resulted from photoelastic investigations on polymer films, conducted in conjunction with Mr. H. Oppenheimer and to be published shortly. Films of certain plastics, such as polyethylene, acquire on stretching a birefringence which does not change on removing of the load. By varying the elongation between 0 and 200 percent, a permanent path difference of any magnitude within the limits of approximately 0A and 4×10^5A per one-mm layer can be obtained. The method can be used for quarter-wave compensators, Laurent half-shades, Bravais half-shades, Chaumont quadruple field analyzers and for producing circularly polarized light from natural light. Noteworthy among the various other possible applications of the films is the substitution of the Johannsen comparator in work with the polarizing microscope by a slide containing a series of polymer films of systematically varied path difference.

E10. On the Self-Diffusion of a Pure Gas Through a Long Capillary when the Mean Free Path Is Comparable to the Capillary Diameter. R. D. PRESENT AND W. G. POLLARD, *SAM Laboratories, New York City.*—Knudsen* showed theoretically and experimentally that the flow of a pure gas through a long capillary of radius r at pressures so low that intermolecular collisions can be neglected is diffusive in character and the diffusion coefficient is $2\vartheta r/3$ where ϑ is the mean speed of the molecules. Mass motion sets in when the mean free path is comparable to r and at higher pressures the flow is laminar. Experimental plots of specific flow $(F/\Delta p)$ *vs.* mean pressure $\bar{p}$ are linear at high pressures ($\lambda \ll r$) but show a minimum in the neighborhood of $\lambda \approx r$. No satisfactory explanation of this minimum has hitherto been given. We have calculated the self-diffusion coefficient for "tagged" molecules diffusing in the absence of a pressure gradient; i.e., for the case of diffusion with no mass motion. The resulting formula is valid at all pressures and reduces to the correct limiting values: $\vartheta\lambda/3$ when $\lambda \ll r$ and $2\vartheta r/3$ when $\lambda \gg r$. Furthermore the theoretical curve of $F/\Delta\bar{p}$ *vs.* $\bar{p}$ has a large negative slope for a long tube at pressures so low that no appreciable mass motion can occur. This explains the minimum found by Knudsen and others. The fact that this minimum is not observed when porous media are substituted for capillary tubes can also be explained.

* M. Knudsen, Ann. d. Physik **28**, 75 (1909).

P1. The Theory of the Herschel-Quincke Tube. G. W. STEWART, *State University of Iowa.**—A former discussion of the theory of the Herschel-Quincke tube is continued and supplemented by the investigation of Professor H. S. Uhler of a more general case. With the areas of the bifurcated conduits different, it is found that the number of frequencies giving zero transmission is again more numerous than determined by the condition of a difference of phase corresponding to that of one-half wave-length in the two branches. In the more general case the former fixed relations between these phase differences no longer hold. They are now connected by the equality,

$$S_2 \sin a_3 = -S_3 \sin a_2,$$

where S_2 and S_3 are the areas and a_2 and a_3 the phase differences in the corresponding branches. Curiously, there may be zero transmission with branches of different areas.

* To be given after paper D9 if time permits.

P2. A Simple Apparatus for Demonstrating Fluorescence, Light Scattering, and Its Polarization and Depolarization. WILFRIED HELLER, *University of Chicago.**—A small, portable apparatus was constructed for demonstrating all essential features of these phenomena. Minor alterations would make the apparatus applicable to quantitative measurements. Starting with the light source, the essential parts of the apparatus are: collimator, heat filter, light filter, rotatable polaroid, cell containing the light scattering or fluorescent system, second polaroid rotatable around axis normal with respect to primary beam, and telescope. Using only the first of the removable polaroids, the change of Rayleigh radiation with the azimuth of the electric vector can be demonstrated; using only the second polaroid, a separation of light scattering and fluorescence can be effected in systems exhibiting both phenomena. With both polaroids, the four Krishnan components of multipolar radiation can be separated. By removing the telescope, the variation of light scattering with the angle of observation with respect to the primary beam can be followed. The existence of a Mie effect (dissymmetric radiation) in the case of multipolar radiation can be demonstrated. The apparatus is operated with interchangeable round cells of varied size, with square cells or

with cells containing, for accurate work, a Rayleigh horn. Conservative absorption due to light scattering can be studied in the direction of the primary beam.

* To be given after paper E9 if time permits.

T1. On the Deviation of the Biological Effects of Radiations from the Bunsen-Roscoe Law. I. OPATOWSKI, *University of Chicago.*—The effect of a radiation depends often not only on the total energy absorbed but also on its time distribution. To explain this it is assumed that the effect of radiations consists of successive transformations between a certain number of states 0, 1, $\cdots n$ and that these transformations follow a simple probabilistic model, which from a mathematical viewpoint is a generalization of the classical type of radioactive disintegrations. The transitions $(i-1\rightarrow i)$ and $(i+1\rightarrow i)$ are interpreted, respectively, as due to the action of radiation and to the biological reaction of the organism. The frequencies of these transitions are assumed, respectively, to be in a direct proportion to the radiation intensity I and to decrease as I increases. Then the probability that the organism be in the state n after a time t of radiation depends on It only, if t is sufficiently small but not if t is large. The result may be applied also to some types of photochemical processes. The paper is a part of an article to appear in the December, 1945 issue of the *Bulletin of Mathematical Biophysics.*